

Middlesex University Research Repository:

an open access repository of
Middlesex University research

<http://eprints.mdx.ac.uk>

Court, David Gilmore, 1999.
The Formation of Silicon Nitride from
Trisilylamine and Ammonia.
Available from Middlesex University's Research Repository.

Copyright:

Middlesex University Research Repository makes the University's research available electronically.

Copyright and moral rights to this thesis/research project are retained by the author and/or other copyright owners. The work is supplied on the understanding that any use for commercial gain is strictly forbidden. A copy may be downloaded for personal, non-commercial, research or study without prior permission and without charge. Any use of the thesis/research project for private study or research must be properly acknowledged with reference to the work's full bibliographic details.

This thesis/research project may not be reproduced in any format or medium, or extensive quotations taken from it, or its content changed in any way, without first obtaining permission in writing from the copyright holder(s).

If you believe that any material held in the repository infringes copyright law, please contact the Repository Team at Middlesex University via the following email address:
eprints@mdx.ac.uk

The item will be removed from the repository while any claim is being investigated.

The Formation of Silicon Nitride from
Trisilylamine and Ammonia

DAVID GILMORE COURT

A thesis submitted in partial fulfillment of the
requirements of Middlesex University for
the degree of Master of Philosophy

School of Engineering Systems

Middlesex University

June 1999

ABSTRACT

Silane gas has been used for three decades as a precursor for plasma enhanced chemical vapour deposition processes but is unsustainable in the longer term due to the extremely hazardous nature of the compound. Alternative precursor materials have been proposed but have proved to be largely incompatible with the chemistry of the deposition process or the requirements of semiconductor process technology. One compound with the chemical and technological potential as a precursor for silicon nitride deposition is trisilylamine.

Calculation of the Gibbs free energy change for the formation of silicon nitride from the reaction of trisilylamine and ammonia demonstrates that the reaction is thermodynamically feasible as is the reaction involving silane with ammonia. The standard molar enthalpy of formation for trisilylamine was obtained from a semi-empirical molecular orbital calculation while the standard molar entropy of formation was determined from spectroscopic data in the absence of a calorimetric value.

Thermodynamic properties have been calculated for a range of aminated species using semi-empirical methods and entropy vs. molecular weight equations. These species are potential intermediates in a plasma discharge of trisilylamine and ammonia, with their successive combination leading to the deposition of a film of silicon nitride. Thermodynamic values for reactions involving the formation, propagation and termination of radical species of trisilylamine and ammonia have been determined and a mechanism is proposed for the deposition of silicon nitride films by plasma enhanced chemical vapour deposition. These results indicate that there is no thermodynamic barrier to the use of trisilylamine as a precursor with ammonia gas for the plasma enhanced deposition of silicon nitride films.

ACKNOWLEDGEMENTS

I would like to thank Middlesex University for the opportunity to undertake this programme of research and for the allowance of time to complete the work.

I am indebted to my supervision team who supported and encouraged me when times got very hard and progress was very slow. My initial choice of Dr. John Spears as Director of Studies proved to be absolutely correct and his kind but forthright manner was exactly what any research student needs to stay on the straight and narrow. After he retired and became an advisor to the project the mantle was assumed by Dr. Michael Censlive who guided the project through to its conclusion. It is essential to have a balanced team and in Professor Bernard Aylett and Dr. Peter Revell I could not have had two better external supervisors. Both provided the technical expertise and personal support that has ultimately allowed me to complete this project.

I would like to acknowledge the contribution of specific members of staff at Middlesex University. Professors John Butcher and George Goldspink for their support and encouragement while Heads of the Microelectronics Centre. Dr. Michael Censlive for his help with the calculation of rotational entropy, Keith Pitt for his advice on layout and content and Dr. Dick Warn for his initial assessment of the entropy of trisilylamine which provided my initial target to aim for. I am also grateful for the support given to me by all my colleagues from the Microelectronics Centre, the School of Engineering Systems and the demised Faculty of Technology.

I acknowledge the contribution of CambridgeSoft who provided a copy of their latest version of the semi-empirical modeling software programme Chem3D in return for a product review which currently resides on their Web page. Without this software it would have been extremely difficult to complete this programme of work.

Finally, this programme of research would not have come to fruition without the support of my darling wife Gerry, who has never wavered in her support of my academic aspirations.

CONTENTS	
	Page
ABSTRACT	i
ACKNOWLEDGEMENTS	ii
CONTENTS	iii
LIST OF TABLES	viii
LIST OF ILLUSTRATIONS	xi
CHAPTER 1 INTRODUCTION	1
1.1 Semiconductor Devices	3
1.2 PECVD Silicon Nitride	6
1.3 Safety In CVD	8
1.4 Trisilylamine	10
1.5 Aims of the Research Programme	11
CHAPTER 2 LITERATURE REVIEW	13
2.1 Plasma Enhanced Deposition Techniques	14
2.2 Plasma Enhanced Deposition Parameters	17
2.2.1 Uniformity	17
2.2.2 Carrier Gas	18
2.2.3 RF Frequency	19
2.2.4 RF Power	20

CONTENTS (CONT...)

	Page
2.2.5 Deposition Temperature	20
2.2.6 Silane/Ammonia Ratio	20
2.2.7 Pressure	20
2.3 Deposited Film Characteristics	22
2.3.1 Stress	22
2.3.2 Hydrogen Content	24
2.3.3 Refractive Index	24
2.3.4 Deposition Rate	25
2.3.5 Annealing Effects	26
2.3.6 Etching Effects	26
2.3.7 Analytical Techniques	27
2.4 Deposition and Film Structure	30
2.5 Deposition with Inorganic Silanes	33
2.6 Deposition with Organosilanes	35
2.7 Trisilylamine	37
2.7.1 Structure and Bonding	37
2.7.2 Application to Chemical Vapour Deposition	39
2.7.3 Comparison of Properties	41
2.7.4 Substituted Trisilylamine	42
CHAPTER 3 ATOMIC AND MOLECULAR ORBITALS	45
3.1 Schrödinger Wave Equations	46
3.1.1 One Electron Atom	46
3.1.2 One-Electron Orbitals	48
3.1.3 Many Electron Atom	49

CONTENTS (CONT...)

	Page
3.1.4 Many Electron and Many Nuclei Systems	51
3.2 One Electron Spin Orbitals	52
3.3 Hartree-Fock (HF) Method	54
3.4 Linear Combination of Atomic Orbitals (LCAO)	56
3.5 Basis Sets	58
3.6 Semi-empirical Methods	62
CHAPTER 4 THERMODYNAMIC CALCULATIONS	63
4.1 Standard Molar Enthalpy Change (ΔH_m°) for the Formation of Si_3N_4	65
4.2 Standard Molar Entropy of Formation (S°) for Trisilylamine	67
4.2.1 Translational Entropy	67
4.2.2 Rotational Entropy	67
4.2.3 Vibrational Entropy	69
4.3 Gibbs Free Energy Change (ΔG_m°) for the Formation of Si_3N_4	73
4.4 The Accuracy of the Standard Molar Entropy of Formation (S°) Calculation for Trisilylamine	74
4.5 Standard Equilibrium Constant	76
CHAPTER 5 SEMI-EMPIRICAL CALCULATIONS	77
5.1 Software	78

CONTENTS (CONT...)

	Page
5.2 Standard Molar Enthalpy of Formation(ΔH_f°) for Trisilylamine	81
5.2.1 Standard Molar Enthalpy of Formation	81
5.2.2 Molecular Geometry and Atomic Charges	84
5.2.3 Molecular Geometry and Atomic Charges	85
5.3 The Effect of Hydrogen Removal	93
5.4 An Estimation of the Si-N and Si-H Bond Strength	95
5.5 The Formation of Aminosilanes	98
CHAPTER 6 PLASMA ENHANCED DEPOSITION OF SILICON NITRIDE	105
6.1 The Characteristics of a Plasma	107
6.2 Mean Free Path for Trisilylamine	111
6.3 Thermodynamics of Reactions	113
6.4 Initiation of the Plasma Reaction	118
6.5 Propagation Reactions	121
6.6 Termination Reactions	124
6.7 The Use of ΔH_m° in Place of ΔG_m° in Reaction Analysis	125
CHAPTER 7 DISCUSSION	129
7.1 Semi-empirical Calculations	131

CONTENTS (CONT...)

	Page
7.1.1 Limitations of the Models	131
7.1.2 Molecular Structure of Trisilylamine	133
7.1.3 Atomic and Electron Charge Distribution	135
7.2 Hydrogen Removal and the Estimation of Si-N and Si-H Bond Strength	136
7.3 Thermodynamic Values	137
7.3.1 Standard Molar Enthalpy of Formation (ΔH_f°) for Trisilylamine	137
7.3.2 Standard Molar Entropy of Formation for Trisilylamine	138
7.3.3 Gibbs Free Energy Change (ΔG_m°) for the Formation of Si_3N_4	141
7.4 Reaction of Trisilylamine and Ammonia	142
7.4.1 Feasibility of Reaction	143
7.4.2 Formation of Products	145
7.4.3 Radical Reactions	146
CONCLUSIONS AND RECOMMENDATIONS FOR FUTURE WORK	148
GLOSSARY OF TERMS	153
REFERENCES	156
APPENDIX 1 THERMODYNAMIC VALUES FOR MOLECULES	i
APPENDIX 2 PARAMETERS USED IN SPARTAN SEMI-EMPIRICAL MO MODELS	iii
APPENDIX 3 EXAMPLE OF A HYPERCHEM LOG FILE FOR A SEMI-EMPIRICAL CALCULATION	xv
APPENDIX 4 FORMATION OF SILICON DIOXIDE FILMS	xxi

LIST OF TABLES

	Page
1.1 Some Industrial Applications of Silicon Nitride	2
1.2 Comparison of Properties of Thermal CVD and PECVD Silicon Nitride Films	6
2.1 Variation of PECVD Deposition Parameters for Silicon Nitride Films	17
2.2 Variation of Properties of Silicon Nitride Films As-deposited in Argon, Helium and Nitrogen Gases	19
2.3 Thermal Expansion Coefficients of Materials Used in the Manufacture of Semiconductor Devices	23
2.4 Conditions for the Deposition of Silicon Nitride Films	27
2.5 Assignment of Infrared Bond Frequencies for PECVD Silicon Nitride Films	29
2.6 Structures of Heavy Atom Portions of some $X(YH_3)_3$ Molecules	37
2.7 Comparison of Total Energy Values for Trisilylamine	38
2.8 Comparison of Experimentally Determined and Calculated Geometry Data	39
2.9 Comparison of Physical Properties of Silane (S), Disilane (D), Trisilane (TS) and Trisilylamine (TSA)	42
2.10 Table of Physical Properties of Trisilylamine (TSA) Compared to Silane (S) and Trichlorosilane (TCS)	43
2.11 Comparison of Percentage Elemental Composition for Potential Source Materials for PECVD Si_3N_4 Deposition	44
3.1 Ground State Electronic Configuration for H, N and Si	49
3.2 Configuration for Semi-empirical Models	60
3.3 Configuration for Ab Initio Models	60
3.4 Performance of the Computational Models	61
4.1 Calculation of the Vibrational Entropy Component of Trisilylamine	70
4.2 Comparison of Entropy Values of TSA and BCl_3	75

LIST OF TABLES (CONT...)

	Page
5.1 Values of ΔH_f° for Silane and Ammonia from Geometric Optimisation Calculations	79
5.2 Values of ΔH_f° for Trisilylamine from Geometric Optimisation Calculations	81
5.3 Calculation of Standard Deviation of ΔH_f° for Trisilylamine	82
5.4 Repeatability of ΔH_f° Value for MNDO/d, AM1 and PM3 Semi-empirical Methods from Energy Minimisation Calculations using Chem3D	83
5.5 Comparison of Bonding Data for Trisilylamine from Energy Minimisation Calculations using Chem3D	84
5.6 Comparison of Atomic Charge Data for Trisilylamine from Energy Minimisation Calculations using Chem3D	85
5.7 Values of Dipole Moment for Trisilylamine from Energy Minimisation Calculations using Chem3D	86
5.8 Values of ΔH_f° of Dehydrogenated Trisilylamines from Energy Minimisation Calculations using Chem3D	93
5.9 Values of ΔH_f° of Substituted Trisilylamines from Geometric Optimisation Calculations using Chem3D	100
5.10 Values of ΔH_f° of Substituted Trisilylamines from Geometric Optimisation Calculations using Hyperchem 5.1	102
5.11 Comparison of ΔH_f° Values for Substituted Trisilylamines from Chem3D and Hyperchem 5.1 Semi-empirical Models	102
5.12 Normalisation Factor Derived from Values of ΔH_f° and Molecular Weight	103
6.1 Values of ΔH_f° for Silylamine, Triaminosilane and Tetraaminosilane from Chem3D	113
6.2 Values of ΔH_m° for Substituted Trisilylamines Using AM1 and PM3 Models	126
6.3 Results of Entropy Calculations for Substituted Trisilylamines	126
6.4 Values of ΔS_m° for Substituted Trisilylamines	127

LIST OF TABLES (CONT...)

	Page
6.5 Values of ΔG_m° for Substituted Trisilylamines Using AM1 and PM3 Models	128
7.1 Quality of Agreement between Electron Diffraction and Semi-empirical Bonding Data for Trisilylamine	134
7.2 Trends in Values of ΔH_m° and ΔG_m° for AM1 and PM3 Semi-empirical Models	144
7.3 Values of ΔH_f° for Addition of Amino Groups to Trisilylamine using AM1 and PM3 Semi-empirical Models	145

LIST OF ILLUSTRATIONS

	Page
1.1 Example of a Silicon Nitride Ceramic Turbine Rotor Blade	1
3.1 Graphical Representation of the 1s and 2p Atomic Orbitals	50
3.2 Graphical Representation of Split Level Basis Set	59
5.1 Newman Projection of Trisilylamine from Semi-empirical Models	88
5.2 Total Charge Density of Trisilylamine from Various Semi-empirical Models	89
5.3 HOMO and LUMO of Trisilylamine from AM1 Semi-empirical Model	90
5.4 HOMO and LUMO of Trisilylamine from PM3 Semi-empirical Model	91
5.5 HOMO and LUMO of Trisilylamine from MNDOD/d Semi-empirical Model	92
5.6 Formation of Molecules by Amination of Trisilylamine	98/99
5.7 Graph of Standard Molar Enthalpy of Formation vs. Number of NH ₂ Groups for MNDO/d, AM1 and PM3 Semi-empirical Models	101
5.8 Graph of Normalisation Factor vs. Number of NH ₂ Groups	104
6.1 Characterisation of a Plasma by Electron Density and Energy	107
6.2 Radial Flow Parallel Plate Reactor	108
6.3 Structure of N(SiH ₃) ₂ SiH(NH ₂) ₂ from PM3 Semi-empirical Model	122
6.4 Structure of N(SiH ₃) ₂ SiH ₂ NHSiH ₂ (SiH ₃) ₂ N from PM3 Semi-empirical Model	122
7.1 Bimolecular Reaction of Silane and Ammonia	143

1 INTRODUCTION

The silicon nitride of the text book is a white powder whose production was first reported in 1910 by Weiss and Engelhardt (Turkdogan et al., 1958). In practice, the silicon nitride supplied to chemists is invariably a grey powder contaminated with the presence of unreacted or excess silicon. The annual world production of silicon nitride is estimated at around 500 tons (Hrsak et al., 1998).

Depending on the method of formation there are two modifications available. One modification is denoted the α form, composed of SiN_4 tetrahedra in a hexagonal unit cell, and produced by the direct heating of silicon in nitrogen gas at temperatures between 1300°C - 1380°C (Sidgwick, 1952). Alternatively there is a β form, with a phenacite structure, formed by the action of ammonia gas on silicon at 1500°C (Trotman-Dickenson et al., 1973).

In chemical terms, silicon nitride is very stable having a melting point of 1900°C and with excellent resistance to acids and alkalis. As a pure material silicon nitride has good dielectric properties which are similar to those of silicon dioxide. These properties, coupled with its stability in air up to temperatures of 1650°C , make silicon nitride the material of choice for many commercial applications. As an engineering material, the predominant uses are in the form of a sintered powder casting or as a deposited layer. The areas of commercial application have changed over the years to encompass high technology areas such as the turbine and automotive industries. One example of a modern application is the silicon nitride ceramic turbine rotor blade shown in figure 1.1.

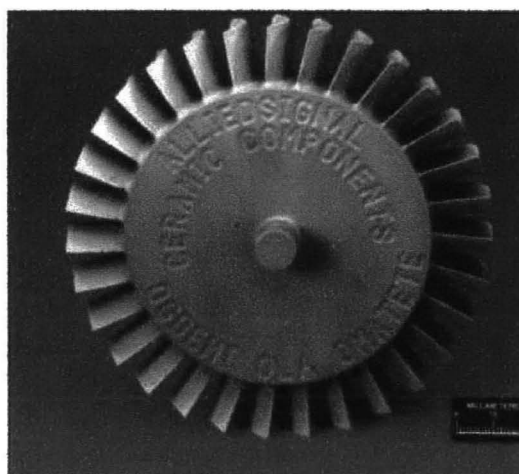


Figure 1.1

Example of a Silicon Nitride Ceramic Turbine Rotor Blade

These new application areas are in addition to the traditional uses in thermal and electrical insulation and high temperature applications. Some examples of the commercial uses of silicon nitride are given in table 1.1.

Table 1.1

Some Industrial Applications of Silicon Nitride

Area of Technology	Application
Semiconductor	Dielectric and passivation layers
Electronics	Component packaging
Optical	Lens coatings, phase shift masks
Aerospace	Jet engine components, rocket nozzles
Measurement	AFM tips, sensor diaphragms, flow and pressure sensors
Automotive	Diesel engine glow plugs
Industrial	Thermometer sheathing, electrical insulators, cutting tools
Mechanical	Coatings for tool bits, wear resistant seals
Metallurgical	Crucibles for crystal pulling equipment

One of the major application areas for silicon nitride has been in the fabrication of semiconductor devices where thin film dielectric and passivation layers are important requirements of integrated circuit technology. In semiconductor fabrication the silicon nitride films are deposited on silicon substrates or compound semiconductor materials such as gallium arsenide using silane and ammonia gases as precursors.

1.1 SEMICONDUCTOR DEVICES

The semiconductor devices used in digital computer microprocessor and memory applications are based on the metal-oxide-semiconductor (MOS) device structure. Many advances have been made since MOS technology was developed in the 1960's culminating in the complimentary MOS (CMOS) devices in current production. The inherent advantages of CMOS technology include lower power consumption, high noise margins and the ability to integrate complex functionality. The complexity of the integrated circuits has increased as the feature size has decreased to the current levels of device integration designated as very large scale integration (VLSI) and ultra large scale integration (ULSI).

Whatever the complexity of the device structure the fundamental material requirements are for:

(a) Silicon (or Compound Semiconductor) Substrate

Can be obtained in sizes up to twelve inches in diameter for production quantities, with high or low resistivity in either n-type or p-type doping.

(b) Insulating Layer(s)

Undoped silicon dioxide, doped silicon dioxide, polyimide, low dielectric constant polymers or silicon nitride for use as interlayer dielectrics, final passivation and barrier layers.

(c) Conducting Layers

Polysilicon or refractory silicides for gate electrodes, titanium and platinum silicides for barrier layers and aluminium or copper for global interconnect. The insulating layers used on silicon substrates are formed by gas phase deposition and are extremely thin (generally $\ll 1 \mu\text{m}$).

A typical, state of the art silicon gate CMOS process will require in excess of 100 process stages beginning with wafer cleaning and ending with wafer probing. This may include 10 or more chemical vapour deposition (CVD) stages but the actual number of CVD steps will be process and technology dependent. The remaining processing stages

include thermal processing, ion implantation, photolithography, plasma etching and metal deposition (I.C.E Corp., 1990).

Invariably, the CVD process does not occur in isolation and will be an integral part of a sequence of steps. An example is the local oxidation of silicon (LOCOS) process where a thin layer of silicon nitride is used as a mask for selective oxidation of the silicon surface. This process involves not only the silicon nitride film deposition and silicon oxidation processes but also photolithographic processes to define the windows in the nitride film and plasma etching to etch the windows and remove post oxidation films.

All CVD processes require the precursors to receive an input of energy sufficient to initiate a chemical reaction resulting in film deposition. The main sources of energy are thermal energy and energy from a glow discharge. Deposition may also occur at a range of pressures and the choice will be process dependent. The major CVD process technologies for the deposition of silicon nitride are as follows:

(a) Atmospheric Pressure CVD (APCVD)

Film deposition occurs at atmospheric pressure at temperatures in the range 700 - 1100°C.

(b) Low Pressure CVD (LPCVD)

Films are deposited around 67 Pa (500 mTorr) pressure and at temperatures in the range 750 - 850°C. In general the reaction of dichlorosilane and ammonia is preferred to silane and ammonia on the grounds of better uniformity and higher deposition rate (see Schlote et al., 1995; Sherman, 1987).

(c) Plasma Enhanced CVD (PECVD)

In an RF glow discharge at 67 Pa (500 mTorr) pressure, silicon nitride films can be deposited from silane and ammonia at temperatures between 25 - 400°C.

(see Lee et al., 1993; Martineau et al., 1989).

Film quality is generally better with LPCVD films due to lack of particulation and lower hydrogen content in the films. With horizontal tube reactors the temperature profile along the length of the tube has to be adjusted with a lower temperature at the input end and a higher temperature at the exit end to compensate for depletion of precursor material. One essential requirement is that the deposition temperature of

dielectric and passivation films is lower than the onset temperature of solid state diffusion of dopants (boron, phosphorus or arsenic) in silicon ($\sim 900^{\circ}\text{C}$). For this reason the favoured CVD techniques for VLSI technologies are LPCVD and PECVD.

1.2 PECVD SILICON NITRIDE

The versatility of plasma deposited silicon nitride films is evident in the variety of applications that have been reported. Some examples include X-ray lithography masks (Suzuki et al., 1982), solar cell technology (Aberle et al., 1997; Winderbaum et al., 1997), metal-nitride-oxide-semiconductor (MNOS) capacitors (Khaliq et al., 1988), passivating layers (Cai, et al., 1998; Donzelli et al., 1987), encapsulants for III-V materials (Valco et al., 1989 & 1987), micro-mechanical applications (Leclerc et al., 1998), non-volatile memory applications (Wang et al., 1995) and gate dielectrics for thin film transistors (Kuo, 1995; Jones, 1985). In table 1.2 a comparison is given of the properties of silicon nitride films deposited from thermal and plasma CVD techniques.

Table 1.2

Comparison of Properties of LPCVD and PECVD Silicon Nitride Films

(from Sze, 1988)

Property	LPCVD	PECVD
Deposition Temperature ($^{\circ}\text{C}$)	700-800 $^{\circ}\text{C}$	250 - 350
Composition	$\text{Si}_3\text{N}_4(\text{H})$	SiN_xH_y
Si/N ratio	0.75	0.8 - 1.2
Atom % H	4 - 8	20 - 25
Refractive Index	2.01	1.8 - 2.5
Density (g/cm^3)	2.9 - 3.1	2.4 - 2.8
Dielectric Constant	6 - 7	6 - 9
Resistivity ($\Omega\text{-cm}$)	10^{16}	$10^6 - 10^{15}$
Dielectric Strength ($10^6 \text{ V}/\text{cm}$)	10	5
Stress (10^9 Pa)	1 T*	0.2 C* - 0.5 T

* where T = tensile stress and C = compressive stress

For silicon nitride films deposited by plasma enhanced CVD techniques the main precursor materials are silane with ammonia. Silane and nitrogen have been used where a lower hydrogen content in the film is required. The structure and properties of the deposited films vary according to the temperature of deposition and the parameters used during the deposition process. The most significant difference is that silicon nitride

films deposited at elevated temperatures have the correct stoichiometric proportions of silicon and nitrogen whereas at lower deposition temperatures the stoichiometry is variable and includes a significant amount of hydrogen in the films. For this reason the formula of plasma deposited silicon nitride is represented as SiN_x or $\text{Si}_x\text{N}_y\text{H}_z$, rather than Si_3N_4 , to reflect this difference. The properties of the films will be dependent on a wide variety of factors which have been reported and compared by Reinberg (Reinberg, 1979). These factors include reactor geometry, choice of precursors, precursor ratios and flow rate.

The effect of kinetic factors on reactions and reaction rates is the most important consideration for practical CVD and a large number of reactions in the gas phase, including that of silane with ammonia, have no measurable reaction rate at room temperature even though the Gibbs free energy change (ΔG_m°) for the reaction is large and negative and therefore suggests that a reaction should occur. Although it is implicitly understood that kinetic factors may have an overriding influence on reactions an investigation of the kinetics of reaction is beyond the scope of this programme of research.

1.3 SAFETY IN CVD

Safety is a major consideration in all forms of semiconductor processing and is no less important in CVD. A number of hazards reported by Hammond (Hammond, 1980) relate to PECVD such as:

- exposure to electric terminals
- exposure to hot surfaces ($\gg 100^\circ\text{C}$)
- exposure to toxic and/or corrosive exhaust gases
- accumulations of reactive by-products in exhaust systems
- handling of gases with flammable, pyrophoric, toxic or corrosive properties.

Until the 1990's source materials for plasma deposition were gaseous and supplied in individual cylinders of a size concomitant with the production volume. Due to the safety problems involved with issues such as:

- compressed gas cylinders
- the movement of cylinders
- piping of highly toxic and corrosive gases over large tube runs

there has been a movement away from gaseous precursors towards the use of liquid sources. The lower toxicity, greater ease of handling and near-rig location remove many of the problems identified with gaseous sources and silane in particular. Maintenance and upkeep of facilities becomes far easier without long runs of tubing containing pyrophoric and toxic gases.

The major problems associated with silane are well documented (Chowdhury, 1996; Fthenakis, 1990; Tucker, 1985). Silane is an extremely hazardous substance and there have been innumerable reports in the scientific press of silane fires and explosions in processing plants and laboratories (Britton et al., 1991). Most incidents occur during changes to systems and a simple process such as changing cylinders involves considerable risk with 100% silane due to problems such as incomplete flushing of gas lines and gas leakage at disconnected tubing joints and cylinder head connections.

The most dangerous semiconductor gases have been the primary targets for a move to liquid precursor sources. These include silane (Newboe, 1991), where the current

threshold limit value (TLV) is 1 ppm (STEL) and 0.5 ppm (LTEL) (H&SE, 1998), as well as phosphine, diborane and arsine (Tucker, 1989) where the TLV values for these gaseous precursors are even lower. The last three gases are used as dopant sources to introduce impurity atoms into substrate materials and silicon dioxide films. Successful replacements have been found because organo-metallic compounds, for example trimethylphosphite (TMPi), trimethylphosphate (TMPo), triethylborate (TEB), trimethylborate (TMB), tert-butylphosphine (TBP) and tert-butylarsine (TBA) are available and have been used variously in metallo-organic CVD (MOCVD), compound semiconductor processing and ion implantation (Singer, 1993; Fitzgerald, 1991; Miller, 1989).

Many attempts have been made to find a suitable replacement for silane in the plasma deposition of silicon nitride films but unfortunately most have proved unsuccessful. The main reason is the maturity of silane as a precursor in deposition processes. This inevitably means there is a huge resistance to alter successful manufacturing processes without an overwhelming reason to do so. As no other precursor has demonstrated equal or superior film deposition characteristics the use of silane as a precursor has continued unabated.

The only successful replacement for silane that has obtained wide commercial acceptance is tetraethoxysilane (TEOS) which is used for APCVD deposition of silicon dioxide films. Results published by Pai (Pai et al., 1993) suggest that good quality silicon dioxide films can be obtained by ECR deposition using tetramethylcyclotetrasiloxane ($(\text{SiHCH}_3)_4\text{O}_4$) and oxygen as precursors.

The liquid and gaseous materials used in CVD processes must be used under conditions of proper containment and with suitable attention to good safety practice. With all semiconductor processes it is advisable to isolate the operators and substances as completely as possible by the use of closed extraction systems. Attention must also be paid to the reaction by-products of CVD processes and the removal of harmful substances before emitting waste gases into the general environment.

To this end, there is an ongoing move to replace the most hazardous CVD gases with safer but equally efficient materials because as the cost of implementing increasingly more stringent safety systems escalates it becomes increasingly more cost effective to reduce the nature of the hazard.

1.4 TRISILYLAMINE

Trisilylamine has the chemical formula $N(\text{SiH}_3)_3$ and is of general interest to chemists because it possesses unusual chemical bonding properties. The shape of the molecule is expected to be pyramidal but has been shown by experimental measurements to be trigonal planar. The reasons for this have been the subject of much discussion among structural and computational chemists.

The focus for this investigation is the potential for trisilylamine to be used as a replacement for silane in PECVD deposition of silicon nitride films. As a room temperature liquid precursor the physical properties of trisilylamine make it a suitable material for use within the modern practices of the semiconductor industry (see tables 2.3 and 2.4). The potential advantage of trisilylamine is that it is a convenient precursor having a structure that anticipates the desired structure in the film (Aylett, 1989). As an inorganic amine it is composed entirely of Si, H and N atoms and therefore if pyrolysed directly or in admixture with ammonia or nitrogen may form silicon nitride without extraneous atoms to contaminate the deposited film. At present there are no other precursor compounds containing purely Si, H and N atoms that have been isolated at room temperature.

Conformal coverage of features and filling of trenches with dielectric films has reached a critical point with feature sizes sub $0.25\mu\text{m}$. The ability to coat conformally via CVD techniques is related to molecular size, surface mobility and sticking coefficient (Singer, 1993). There are no sticking coefficient values available in the literature for trisilylamine, although estimates are available (for references see Chiang and Hess, 1990) for the radical species SiH_2 (0.1), SiH_3 (0.04) and $\text{SiH}(\text{NH}_2)_3$ (0.0015). This inverse relationship of sticking coefficient to molecular weight and size indicates that there is every expectation of low values of sticking coefficient if we compare a potential species like $N(\text{SiH}_3)_2\text{Si}(\text{NH}_2)_3$ from trisilylamine/ammonia reaction to $\text{SiH}(\text{NH}_2)_3$ from silane/ammonia reaction.

Although the use of trisilylamine in glow discharge deposition of silicon nitride has been the subject of a number of American and Japanese patents (see Chapter 2) there is no evidence that the feasibility of the reaction of trisilylamine and ammonia to form silicon nitride has been investigated nor is there evidence that the species that might be involved in such a reaction have been identified.

1.5 AIMS OF THE RESEARCH PROGRAMME

The aim of this programme of research is to provide a theoretical background to the formation of thin silicon nitride films by plasma enhanced chemical vapour deposition from the reaction of trisilylamine and ammonia precursors. Additionally, the intention is to demonstrate that from a theoretical standpoint these precursors are a serious alternative to silane and ammonia for the deposition of silicon nitride films for semiconductor and allied applications.

As practical facilities do not exist to test these assertions at Middlesex University a further programme of research will be required to assess how the theory and practice compare. Much of the work in this project has not previously been published in the literature and therefore is put forward as an initial point of reference for other workers to take forward. The assertion that trisilylamine and ammonia precursors have potential for the deposition of silicon nitride films by PECVD will be tested by the following criteria.

- (a) By determine the feasibility of the reaction of trisilylamine and ammonia to form silicon nitride by evaluating the Gibbs free energy change (ΔG_m°) for the reaction.

The reaction of silane and ammonia will be used as an analogy as this is a very mature technology and a considerable body of information, both empirical and theoretical is available for these precursors. To be directly applicable the Gibbs free energy change for the formation of silicon nitride from trisilylamine and ammonia needs to be of the same order as that of silane and ammonia.

- (b) From semi-empirical molecular orbital calculations to obtain bonding and heat of formation (ΔH_f°) information on species that may result from the reaction of trisilylamine and ammonia in a plasma.

Semi-empirical methods will be used to investigate the structure, bonding and energy of a range of aminated species that may result from the reaction of trisilylamine and ammonia. The important factor is the stability of the species relative to trisilylamine, and the requirement will be that they must have a heat of formation value that is large and negative. Without this the species are unlikely to

be formed on thermodynamic grounds and the reaction will proceed via another route.

- (c) Propose a reaction mechanism by which trisilylamine and ammonia may react in the gas phase to form silicon nitride as a deposited film.

At pressures consistent with glow discharge processes the gas phase plasma reaction is likely to proceed via a radical reaction and consideration will need to be given to the mechanism of initiation, propagation and termination of the radical reaction and the species that may be involved in the formation of silicon nitride from trisilylamine and ammonia precursors.

2 LITERATURE REVIEW

The first published work involving plasma deposition in a semiconductor context was the deposition of silicon dioxide films (Alt et al., 1963) using alkoxy-silanes and oxygen as the precursors. In the following year the organo-silane compound TEOS was reported as a potential precursor for silicon dioxide deposition (Ing et al., 1964). The first publication on glow discharge deposition of silicon nitride films was published in the following year (Sterling et al., 1965). Subsequently, silicon dioxide and silicon nitride films have become inextricably linked with the development of both silicon and GaAs technologies for semiconductor applications.

A comprehensive bibliography on silicon nitride films is available up to 1978 (Morosanu, 1980) and for a comprehensive review of electronics applications see Belyi (Belyi et al., 1988). For semiconductor related applications of PECVD silicon nitride the reader is directed to the silicon supplement of Gmelin (Gmelin, 1990).

2.1 PLASMA ENHANCED DEPOSITION TECHNIQUES

The plasma deposition system typical of the mid 60's was the "barrel" type reactor whose design consisted of a quartz tube with external electrodes for inductively coupling the plasma to the gas. These reactors persist to this day but are used almost exclusively for plasma ashing of photoresist materials. A major innovation in reactor design was the patenting of the radial flow reactor (Reinberg, 1974) which subsequently became the industry standard for plasma deposition equipment. This system featured the capacitive coupling of the plasma between two internal parallel electrodes at relatively high gas pressures and low RF powers. A similar radial flow system to that of Reinberg was subsequently developed by Rosler (Rosler et al., 1976) with higher power and lower frequency operation and with the gas flow in the opposing direction.

A PECVD system was developed and patented (Engle, 1978) based on the low pressure chemical LPCVD type horizontal hot wall diffusion system. Information was reported on the high volume throughput of silicon wafers for silicon nitride deposition (Rosler et al., 1981). The system was put into production by Applied Materials Corp. of America. Improvements to the radial flow systems have been proposed. One technique involved addition of an internal gas-flow discharge limiting shield (Sinha et al., 1978a), another a substrate tuning technique consisting of a grounded cylinder of steel mesh (Nishibayashi et al., 1985) surrounding the electrodes with an external variable induction coil connected between the substrate electrode and ground. The former technique was found to increase the variation of deposition conditions and hence allow increased flexibility in tailoring film properties and the latter technique provided a significant increase in deposition rate of around eight fold over a conventional glow discharge. The deposition rate can also be increased by using a magnetic confinement system (Leahy et al., 1987) analogous to magnetron sputtering. However this system has not achieved the commercial acceptance of its sputtering counterpart. High deposition rates have also been reported for silane and nitrogen mixtures (Chang et al., 1988) using radiant lamp heating as commonly seen in rapid thermal annealing and rapid thermal processing equipment.

Many systems for research and development purposes have utilised quartz tubes and custom reaction chambers for film deposition. Typically, an early type of remote PECVD system (Helix et al., 1978) used inductively coupled RF energy for silicon nitride deposition on compound semiconductor materials at temperatures below the

substrate degradation temperature. Deposition with an inductive heating system (Mito et al., 1986) was found to generate a thermal type plasma. Using silane and nitrogen gases two distinct deposition modes were observed, one similar to the standard glow discharge plasma and the other photo-and radical assisted. Film characteristics were similar but the latter had an order of magnitude larger film deposition rate. For deposition of silicon nitride onto InSb substrates (Olcaytug et al., 1980) a deposition rig with dual, 3.7 & 27 MHz RF frequency power supplies has been used.

External plasma excitation of nitrogen was suggested as an alternative to traditional PECVD (Bardos, 1983) and this method has been subsequently commercialised as remote or RPECVD for low hydrogen content films (see Lucovsky, 1986). In this technique nitrogen or ammonia gas are ionised in an external plasma and allowed to diffuse through silane gas to the wafer. The excited or ionised species interact with silane forming active precursors for film deposition. A major advantage of this film deposition technique is the absence of ion bombardment and substrate heating effects. A review of the fundamental differences between PECVD and RPECVD is available from the literature (Lucovsky, 1987).

It is inherent in PECVD that gases enter the deposition chamber at room temperature and are heated in-situ. In the HOMOCVD technique, gases are heated to temperatures of 500-800°C while the substrates are maintained at temperatures between 200-500°C (Scott et al., 1989). This approach provides an extra variable for control of film composition and properties. The film properties were improved by in-situ nitrogen annealing of the films.

More efficient plasma deposition can be obtained using a high power pulsed plasma source rather than the more conventional continuous source (Scarsbrook et al., 1988). One suggested advantage is that film deposition can be achieved at room temperature. Two RF frequency regions are used in PECVD film deposition. Low frequency operation is typically in the region of 50 - 500 kHz and high frequency operation at 13.56 MHz. Ion bombardment of substrates is more apparent at low frequencies due to the ability of ions to follow the applied field. The deposition frequency has a marked effect on film properties and this phenomena will be discussed later.

Modelling of the radio frequency (RF) discharge using typical plasma processing parameters has been performed (Meyyappan et al., 1990) by the application and solution of the Boltzmann transport equations. Attempts have been made to model the PECVD

process (Collins et al., 1994; Brinkmann, 1992) with the latter group using a computational fluid dynamics (CFD) approach for the silane/ammonia/nitrogen system. Electron cyclotron resonance (ECR) excitation at the microwave frequency of 2.45 GHz became popular in 1990's for PECVD deposition. A comparison of silicon nitride deposition by RF and ECR using the N_2 -3% SiH_4 /Argon system (Bardos et al., 1982) concluded that higher frequency deposition was more efficient due to longer lived metastable states in the plasma. For information on ECR see, for example Keqiang (Keqiang et al., 1986).

A review of the fundamental differences between PECVD and RPECVD is available (Lucovsky, 1987). Good reviews exist in the literature covering the early developments of plasma deposition (Burggraaf, 1980) and more recent developments in plasma system technology (Caquineau et al., 1997; Rosler, 1991; Snow, 1987).

2.2 PLASMA ENHANCED DEPOSITION PARAMETERS

Characteristics of deposited silicon nitride films are dependent on both reactor geometry and equipment variables. A selection of parameters and ranges for deposition variables from the literature are shown in table 2.1.

Table 2.1

Variation of PECVD Deposition Parameters for Silicon Nitride Films

Parameters	Range	References
Frequency (MHz)	0.05 - 15	1
Pressure (mT)	100 - 3500	2
Temperature(^o C)	20 - 500	3
RF Power (W)	100 - 300	4
Si ₃ N ₄ /NH ₃ Ratio	0.2 - 2.0	5
Gas Flow (10 ³ sccm)	1.0 - 2.5	4
References	1 Hess, 1984 2 Gereth et al., 1972 3 Sinha et al., 1978b	4 Sinha et al., 1978a 5 Ling et al., 1986

Bohn performed a 2⁴ factorial multi-response study which confirmed that the primary factors affecting film properties were pressure, temperature, active gas ratio and RF power (Bohn et al., 1985). Of these, the latter two parameters appeared to demonstrate the largest overall effect on all deposition parameters. By appropriate variation of the film deposition conditions one can tailor the film properties to perform a specific function within the processed semiconductor device (e.g. passivation or gate dielectric). The variation of film properties with each of these parameters is discussed in the following section.

2.2.1 Uniformity

In common with all other CVD deposition systems the critical factor in radial reactors is that sufficient silane is available over the area of the electrode to ensure uniform deposition at an appropriate rate. This has implications in semiconductor processing for

the yield of the process. Reinberg suggested there is an approximately quadratic relationship between the electrode area and distance across the electrode (Reinberg, 1979). His actual equation is given below:

$$C(r) = C_o - \pi M_{Si} (r_o^2 - r^2) \quad (1)$$

where $C(r)$ is the residual precursor conc., C_o is the initial precursor conc., r is the radius and M_{Si} is the mass of Si per unit time deposited per unit area on upper and lower plates

Analysis of the non-uniformity of film deposition in relation to RF power and pressure has been reported (Egitto, 1980). In this study optimum uniformity was obtained between 30 - 40 watts power and became progressively less uniform up to 90 watts. A useful window of zero non-uniformity was observed at 60 watts power and pressures between 600 - 800 mTorr.

2.2.2 Carrier Gas

The effects of carrier gases on film deposition is an important consideration in film deposition and comparative studies have been made between argon and helium (Allaert et al., 1985) and argon and nitrogen (Shams et al., 1989a). The work of Allaert is mainly based on film variations due to the influence of deposition rate and are shown for 300°C in table 2.2. This work concluded that film uniformity was better with helium but that the hydrogen content was much higher. A study of helium, argon, krypton and xenon carrier gases (Nguyen, 1983) identified a relationship between increasing atomic weight with decreasing thickness and RI uniformity, which confirmed the findings of Allaert. An increasing deposition rate variation was also reported.

All these effects may be attributed to differences in ionisation via the Penning effect. Amorphous silicon nitride films ($a\text{-SiN}_x\text{:H}$) deposited from silane and ammonia (Hsieh et al., 1994) were found to be highly sensitive to the presence and flow rate of argon, helium, hydrogen and nitrogen diluents. This may be attributed to thermal conductivity differences of carrier gases (especially helium). Work with neon is not currently known to the author.

Nitrogen and argon films show little variation other than deposition rate which is thought to be due to nitrogen involvement in the deposition process (Shams et al.,

1989a). Anomalous etching and poor breakdown characteristics have been reported for nitrogen containing films in a survey of film deposition from combinations of silane, ammonia, nitrogen and argon gases (Maeda et al., 1984).

Table 2.2

Variation of Properties of Silicon Nitride Films As-deposited in Argon, Helium and Nitrogen Gases

		Helium	Nitrogen	References
Refractive Index	2.1	2.35		1
	1.8		1.85	2
Deposition Rate (Å/min)	1235	1315		1
	192		226	2
Si/N Ratio	1.3	2.12		1
	0.81		0.79	2
References	1	Allaert et al., 1985	2	Shams et al., 1989a

A direct relationship has been observed (Kaganowicz et al., 1986) between increasing argon addition (0 - 160 sccm) to pure undiluted silane and ammonia mixtures and the refractive index (1.875 - 1.98). The post-deposition ion implantation of argon (Shams et al., 1989b) reportedly improved the memory properties of MNOS devices by altering the Si-H bond concentration.

2.2.3 RF Frequency

Two frequency regions are generally used in plasma deposition. The low energy region extends from approximately 100 kHz to 1 MHz above which the high frequency region commences (Bruce, 1981). In the low frequency region ions traverse the sheaths within the oscillation period and therefore have an energy equal to the maximum plasma energy. Above 4 MHz the oscillation period is greater than the time for ions to traverse the sheaths and therefore the ion energy decreases to a value which is the average of the plasma potential. The ion energy is frequency dependent and can materially affect the film properties. The variation of film properties with RF frequency has been investigated (Hess, 1984) and demonstrated a significant difference in properties

between low and high frequency regions due to the effect of ion energy in the plasma discharge.

2.2.4 RF Power

The degree of dissociation of silane and ammonia has been shown by Kaganowicz (Kaganowicz et al., 1986) to increase exponentially with increasing RF power (0 - 600 watts). The difference in dissociation is marked at low power but settles to a plateau with a constant difference above 200 watts. The greater dissociation of silane over ammonia is directly related to the difference in bond energy between Si-H and N-H.

2.2.5 Deposition Temperature

Most PECVD nitride films are deposited in the range 250 - 350°C but much lower deposition temperatures are feasible. Although for some applications PECVD films are inferior to LPCVD films the flexibility of the technology can be seen in the work of Dange (Dange et al., 1991) who developed a photoresist lift-off technique for GaAs and InP MESFET devices using silicon nitride deposited at 80°C.

2.2.6 Silane/Ammonia Ratio

By controlling the silane to ammonia ratio a measure of film engineering can be obtained. Sequeda (Sequeda et al., 1981) concluded that hydrogen is mainly bonded as N-H at a ratio < 0.5 and with increasing Si-H bonds at a ratio > 0.5 .

2.2.7 Pressure

Deposition pressure determines the collision frequency in the plasma and is therefore inextricably linked with the plasma power (Rand, 1979). The pressure range typically used in PECVD processing is 0.6 - 1.2 Torr, but deposition from 0.3 Torr to 1.8 Torr is not uncommon. Morosanu reported that total system pressures above 1 Torr lead to particulate formation from increased gas phase reaction (Morosanu et al., 1981). The lower pressure limit is set by the ability to strike and sustain a plasma. Decreasing the total pressure increases the plasma electron temperature, which has the same effect as

increasing the RF power (Kato et al., 1983). Increasing pressure at fixed gas flow has been shown by Smith to increase residence time in the plasma and promote amination reactions leading to higher deposition rates (Smith et al., 1990).

2.3 DEPOSITED FILM CHARACTERISTICS

Due to deposition variation effects on deposited film properties it is useful for the process engineer to understand the inter-relationship of film properties as well as the relationship of properties to deposition conditions.

2.3.1 Stress

Stress in thin films on silicon substrates is very important for factors such as dielectric integrity and long term reliability. The main problem with film stress is the cracking of the film as a stress relief mechanism. Osenbach and co-workers (Osenbach et al., 1990) suggested that film stress can be represented by:

$$\text{total stress} = \text{thermal stress} + \text{intrinsic stress} \quad (2)$$

Thermal stress is due to the mismatch in thermal expansion between, in this case, silicon nitride film and the silicon substrate. Intrinsic stress is due to factors such as lattice mismatch between silicon and silicon nitride film. The thermal expansion coefficients have been measured and the match with silicon improves as the films become more silicon rich (Sinha et al., 1978b). However, in interlayer applications the silicon nitride film may be deposited on other semiconductor materials. In table 2.3, the thermal expansion coefficients of various semiconductor materials are compared. It is evident that while PECVD silicon nitride films are compatible with many semiconductor materials there is a potential thermal mismatch with both silicon and aluminium. Stress is found to be relatively independent of pressure in the range 700 - 900 mTorr but increases exponentially at higher pressures (Sinha et al., 1978a). This region would provide a good window of operation for film deposition.

At high frequency operation (13.56 MHz) the film stress is predominantly tensile, however a change to compressive stress can be effected at higher RF powers. In the work of Sinha the change from tensile to compressive stress occurred in the range 250 - 300 watts (Sinha et al., 1978a) while stress also altered at a power density of between 0.8 - 0.95 W/cm² (Maeda et al., 1984).

Table 2.3

Thermal Expansion Coefficients of Materials Used in the Manufacture of
Semiconductor Devices

Material	Coefficient of Linear Expansion ($\times 10^6 \text{ } ^\circ\text{C}^{-1}$)	References
PECVD Si_3N_4	4 - 7	1
Aluminium	25	2
GaAs	6.86	2
Gold	14.2	2
Molybdenum	5	2
Silicon	2.33	2
Tungsten	4.5	2
MoSi_2	8.2	3
TaSi_2	8.8	3
TiSi_2	10.5	3
WSi_2	6.2	3
References	1 Gorowitz et al., 1985 2 Weast, 1974	3 Miller et al., 1980

Similar results were obtained by Claasen but his information was reported in arbitrary units of RF power and therefore cannot be directly extracted. He also plotted the variation of stress with RF power at low discharge frequency and in this case the films were entirely tensile (Claasen, 1987).

Somewhat disparate results are evident when considering the effects of deposition temperature on film stress. Allaert reported films up to 300°C to be in compression (Allaert et al., 1985) while Sinha found the opposite to be the case. Claasen found a variation with films in compression below 200°C and in tension above. It would appear that there is no simple relationship between stress and deposition temperature and that other factors may have a more significant influence.

Film stresses with increasing ammonia/silane ratio reported by Osenbach demonstrate an exponentially decreasing relationship but in all cases films obtained were in compression. Films in compression were observed by Sinha over a narrower range but the results show basically an opposing trend.

2.3.2 Hydrogen Content

Hydrogen bonding configurations have been determined (Maeda et al., 1985) by FTIR via a comparison of as-deposited films with their annealed or ion implanted counterparts. The work provided an insight into the relative stability of various Si-H and N-H bonds. The use of an infrared calibration graph, based on the direct determination of hydrogen content by resonant nuclear analysis, allows for the rapid determination of hydrogen content in the films (Lanford et al., 1978). With deposition temperature Han observed a linear decrease in hydrogen content with a levelling out at temperatures above 330°C to a value around $0.5 \times 10^{22} \text{ cm}^{-3}$ (Han et al., 1991).

2.3.3 Refractive Index

Films have been studied by Rutherford Backscattering Spectrometry (RBS) with a view to finding a relationship between film composition, density and RI. These parameters can be ultimately connected via the Lorentz-Lorentz equation from which a set of empirical curves have been generated (Sinha et al., 1978c). The refractive index has been shown to increase with increasing pressure (Valco et al., 1987; Gereth et al., 1972). This is in direct contradiction to the work of Sinha who recorded a linear decrease in RI with increasing pressure.

The main effect of increasing the silane to ammonia ratio is to increase the refractive index of the films. This is confirmed experimentally by increasing Si/N ratio from the work of Sinha whereas Valco found the refractive index to be almost independent of silane to nitrogen ratio. This refers to the solid phase Si/N ratio and these conflicting results are due to the differences in deposition conditions.

With refractive index proportional to the Si/N ratio (Helix et al., 1978) the films deposited at values of RI above 2.0 (equal to Si/N of 0.75) are found to be silicon rich. Refractive index demonstrates a linear inverse relationship with RF power (Ishii et al., 1984). At higher pressures the relationship breaks down and work by Han shows an observed maximum between 80 - 90 watts power (Han et al., 1991). With increasing substrate temperature refractive index shows a generally linear increase over the normal deposition range for PECVD.

At temperatures above 400°C the RI becomes independent of temperature (Aleksandrov et al., 1988; Gereth et al., 1972). However, in his studies Valco found the RI to be

effectively independent of deposition temperature at all temperatures between 200 - 400°C. No explanation is provided for this apparent anomaly but the differences in deposition conditions have a significant effect on the film properties.

2.3.4 Deposition Rate

The rate of deposition is related to the amount of silane decomposed in the chamber and Reinberg (Reinberg, 1979) proposed the following relationship for the number of moles per minute of silicon deposited in the films:

$$\frac{dn}{dt} = A \cdot \frac{dT}{dt} \cdot \frac{p}{M} K_{Si} \quad (3)$$

where A is total deposition area, dT/dt is rate of film growth (cm/min), p is film density, M is molecular weight and K_{Si} is the number of Si atoms per unit structure

The deposition rate is dependent on the flow rate into the chamber and will reach a plateau whereby excess precursor material will be pumped from the system without taking part in the reaction. The deposition rate is found to increase in a linear fashion with increasing pressure. The molecular weight of the precursors and therefore the momentum of the molecules will have little effect as the deposition rate has been shown to be independent of whether the active gases are silane and ammonia (Sinha et al., 1978a) or silane and nitrogen (Valco et al., 1987).

In general the deposition rate has been found to either decrease with deposition temperature as reported by Reinberg or be independent as reported by Shitova (Shitova et al., 1975). These observations can be rationalised using the concept of surface controlled reactions and the availability of ionic rather than radical species. However, Allaert reported that films deposited from silane/nitrogen in a helium carrier gas showed an increased deposition rate with substrate temperature (Allaert et al., 1985). This result can be attributed to the very high thermal conductivity of helium compared to nitrogen or other noble gases, because an identical experiment with an argon carrier produced an essentially temperature independent result. The thermal conductivity effect may also be responsible for the results of Gereth (Gereth et al., 1972) who found that using silane/nitrogen in a helium carrier gas the deposition rate was independent of gas ratio.

This contradicts other authors who found that using both the silane/ammonia and silane/nitrogen gas systems the deposition rate increases with increasing gas ratio. Osenbach (Osenbach et al., 1990) discovered that the deposition rate reached a maximum value and suggested the phenomena may be due to either silane conversion or surface reaction saturation.

Over a wide range of RF powers the deposition rate has been found to have a linearly increasing relationship. Sinha found that the deposition rate was independent of RF power and Valco reported a maximum at 50 watts under his deposition conditions. An increasing deposition rate to a plateau was observed by Brooks (Brooks et al., 1988) using the organo-metallic liquid hexamethylcyclotrisilazane (HMCTSZN) with ammonia.

Due to the previously stated problems with comparing deposition results between different workers a full listing of the deposition conditions of the authors referenced will be found in table 2.4.

2.3.5 Annealing Effects

Annealing of films deposited with both argon and nitrogen carrier gases has been shown to have the greatest effect when films were deposited using the optimum deposition conditions (Shams et al., 1989). This study used the memory properties as a guide to film quality and annealing effects. Annealing of plasma deposited films above their deposition temperature leads to evolution of hydrogen and rearrangement of the film structure. Values of activation energy from infra red studies of films annealed at different temperatures (Budhani et al., 1988) yields an activation energy far below the bond dissociation energy. The authors conclude that the mechanism for hydrogen evolution involves a film network effect rather than simple bond breaking.

2.3.6 Etching Effects

Etch rate is dependent on the density of the deposited film and is generally inversely proportional to either the deposition temperature or subsequent higher temperature process. Blaauw demonstrated a two order reduction in etch rate over the temperature range 50 - 500°C (Blaauw, 1984). This was also demonstrated with buffered HF by Lee (Lee et al., 1991) with a deposition temperature range between 50 - 350°C and a

subsequent anneal at 800°C in forming gas. Dry etching is usually based on fluorine chemistry such as 92% carbon tetrafluoride + 8% oxygen (Field et al., 1988).

Table 2.4

Conditions for the Deposition of Silicon Nitride Films

Gases	Frequency (MHz)	Temperature (°C)	Pressure (Torr)	Power (W)	Active ratio*	Refs.
10%SiH ₄ /Ar + NH ₃	13.56	300	0.68	200	0.2	1
5%SiH ₄ /Ar + NH ₃ + N ₂	13.56	300	0.7	30		2
SiH ₄ + NH ₃ + N ₂		300	0.98			3
2%SiH ₄ /N ₂ + N ₂	0.5					4
5%SiH ₄ /H ₂ + NH ₃ + N ₂	13.56	300		60	7.1 ^x	5
2%SiH ₄ /Ar + N ₂		300	0.3			6
SiH ₄ + NH ₃	0.4	280	2	36		7
5%SiH ₄ /Ar + NH ₃	13.56	350	1.3			8
SiH ₄ + NH ₃	0.44	360	2	200		9
SiH ₄ + NH ₃	13	400	0.7	0.7	0.5	10
SiH ₄ + N ₂	0.03	200	0.35	80	0.3	11
References	1	Aleksandrov et al., 1988	7	Ishii et al., 1984		
	2	Bartle et al., 1984	8	Maeda et al., 1985		
	3	Claasen, 1987	9	Osenbach et al., 1990		
	4	Gereth et al., 1972	10	Shitova et al., 1975		
	5	Han et al., 1991	11	Valco et al., 1987		
	6	Helix et al., 1978				

* Active Ratio is defined as SiH₄/NH₃ or SiH₄/N₂

^x Partial pressure ratio pSiH₄/pNH₃

2.3.7 Analytical Techniques

A number of analysis techniques have been applied to the characterisation of deposited film structure and properties. Techniques range from fairly basic laboratory instrumentation to highly specialised and sophisticated equipment. In all cases the

results obtained rely on good sample preparation, correct operation of the equipment and informed interpretation of the data.

Laser ellipsometry is the primary technique for the simultaneous determination of film thickness and refractive index and has been reported by numerous authors. The level of sophistication of instruments varies from manual, fixed angle (70°) to fully automated with $0-90^\circ$ angle coverage. For high precision work a prism coupler is preferred and a comparison of techniques is available (Adams et al., 1979). The silicon to nitrogen ratio is important in controlling film properties and one method involves determination of the optical absorption edge by UV/VIS spectrophotometry. Films are deposited onto transparent glass or quartz substrates along with the silicon substrates and this provides a quick and easy method for film control (Rand et al., 1978).

Electrical measurement techniques such as CV and especially DLTS permit an assessment of the level of interface states in the film (Sanjoh et al., 1990). This is related to the Si/N ratio and important where PECVD films are utilised in an electrically active role such as gate dielectrics in memory devices. Macroscopic information on the bonding structure of materials is obtained from an infra red spectrum by FTIR spectrometry. Of primary interest in silicon nitride films are Si-N, Si-H and N-H bonds and the presence or absence of bonds can be correlated with deposition conditions (Dharmadhikari, 1988). The assignment of bonds in infrared spectra have been reported and are collected together in table 2.5.

Amorphous silicon nitride films contain a large quantity of hydrogen, bonded either as Si-H or N-H. Evidence for the presence of NH_2 bonds is seen in the infrared spectrum with peaks due to bending at $\sim 1550 \text{ cm}^{-1}$ and stretching at 3450 cm^{-1} (Narikawa et al., 1985). Maeda (Maeda et al., 1985) observed NH_2 bond stretching at 3280 cm^{-1} and 3345 cm^{-1} . Pradhan (Pradhan et al., 1992) has suggested that NH_2 bonding has greater thermal stability than NH bonding. Maeda et al. used a spectrum differencing technique to identify SiH, SiH_2 and SiH_3 bond bending between $800 - 900 \text{ cm}^{-1}$ and bond stretching at $2100 - 2260 \text{ cm}^{-1}$. Other workers have not detected SiH bonds in silicon nitride films (Smith et al., 1990a).

Stress measurements are important in assessing the integrity of deposited films and can be obtained by many methods including optical imaging (Yang, 1985), wafer curvature (Retajczyk et al., 1980) and X-ray diffraction.

Table 2.5

Assignment of Infrared Bond Frequencies for PECVD Silicon Nitride Films

Assignment	Bonding Unit	Frequency (cm ⁻¹)	Reference
N-H ₂ stretch		3450	1
		3345, 3280	4
N-H stretch	SiNH	3350	2
		3320	4
Si-H stretch		2120	4
		2198	3
Si-H ₂ stretch		2180	4
Si-H ₂ bend		1550	1
N-H bend	SiNH	1200	2
		1180	1
Si-N assym. stretch		890	1
		830	2
Si-N symm. stretch		490	1
Si breathing	Si ₃ N ₄	450	2
References	1 Narikawa et al., 1985	3 Dharmadhikari, 1988	
	2 Lucovsky et al., 1987	4 Maeda et al., 1985	

It is not within the remit of this work to review all the available physical analysis techniques, but for completeness the reader is directed to references on techniques such as Auger electron spectrometry - AES (Madden, 1981), elastic recoil detection analysis - ERDA (Avasthi et al., 1995), electron spin resonance - ESR (Jousse et al., 1988), Rutherford backscattering spectrometry - RBS (Meyer et al., 1971), x-ray photoelectron spectroscopy - XPS (Nguyen et al., 1987), electron energy loss spectroscopy - EELS (Hezel et al., 1982), proton magnetic resonance - PMR (Reimer et al., 1981) and secondary ion mass spectrometry - SIMS (Benninghoven et al., 1975). Analysis of gas plasma generally divides between optical electron spectroscopy (OES) and quadrupole mass spectrometer (QMS) techniques. The latter technique has found application for plasma etching as well as plasma deposition (Brown et al., 1978).

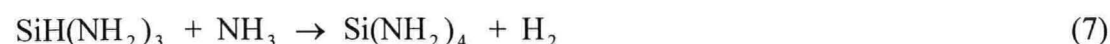
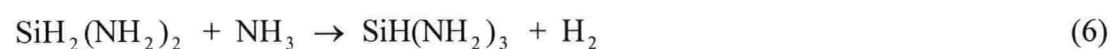
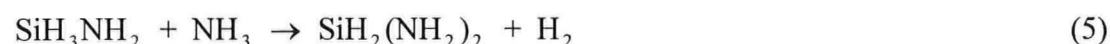
2.4 DEPOSITION AND FILM STRUCTURE

A number of authors have considered the structure of deposited amorphous silicon nitride films. The most important factors determining film deposition and composition are RF power (Yoshimoto et al., 1995), gas flow ratio (R), (Maeda et al., 1991) and reactor design (Osenbach et al., 1990). Information on the processing and characterisation of films deposited by PECVD is available from Zhang (Zhang et al., 1996).

The Si-H bond is easier to break than the N-H bond (3.0 eV compared to 4.0 eV) therefore at low power or when the gas phase ratio (R) of $\text{SiH}_4:\text{NH}_3$ is < 1 , the gas phase formation of disilane is promoted leading to the deposition of silicon rich films with a composition approximating to the general formula $a\text{-Si:H} + \text{N}$. In the intermediate region where $1 < R < 10$, the deposition rate is approximately proportional to the product of the precursor partial pressures and films of the general formula $a\text{-Si} + \text{N}$ are produced. At high pressures or where $R > 10$, the complete decomposition of precursors leads to the deposition of nitrogen rich silicon nitride films. Infrared studies using deuterated precursors have confirmed that the bulk of the hydrogen in the silicon nitride films originates from ammonia and not silane (Hicks et al., 1991; Maeda et al., 1984).

Recent studies of the silane and ammonia deposition process (Smith et al., 1990a) have indicated that the triaminosilane radical is produced at conditions of high RF power and high ammonia to silane ratio and is responsible for silicon nitride film growth by decomposition and condensation on the silicon wafer surface. However, other work (Ishitani et al., 1992 & 1990) suggests that a new gaseous species SiNH_5 is responsible for the deposition of stoichiometric films of SiN_x .

A non-radical mechanism for the formation of tetraaminosilane has been postulated (Tachibane et al., 1993):



in which a sequential process of amination reactions leads to the formation of tetraaminosilane. This mechanism is supported by mass spectral studies of the in-situ plasma reaction of silane and ammonia (Chiang et al., 1990; Smith et al., 1990a). In their paper Smith et al. also reported that the decomposition reaction of tetraaminosilane may proceed to form silicon nitride according to the reaction:



however they do not postulate the individual reaction steps that may occur.

The work of Jasinski (Jasinski et al., 1989) using a single pulse from a 193 nm ArF excimer laser suggests that the deposition of silicon nitride from silane and ammonia under these conditions involves a radical reaction producing a range of aminosilanes including tetraaminosilane. Their work suggests that initiation is via the reaction:



along with hydrogen abstraction reactions involving silane which lead to the formation of silyl radicals:



Their time dependent studies indicate that the initial species are formed simultaneously, rather than sequentially, and they suggest this may parallel the situation in PECVD.

Ab initio studies have been carried out by Tachibane (Tachibane et al., 1992) to determine whether silyl or silylene radicals are the most likely species to be involved in silicon nitride formation from silane as a precursor. They concluded that the silyl radical was more stable than the silylene radical and was therefore the dominant reactive species. Their ab initio calculations also predicted that the reactions involving silyl radicals would be endothermic.

A number of studies have been made of the structure of amorphous silicon nitride, all of which assume a structure based on silicon tetrahedra. Robertson (Robertson, 1983) proposed that the structure of amorphous silicon nitride films is approximated by the β

modification where the nitrogen atom is planar or near planar and the silicon atoms are located in slightly distorted tetrahedral sites. Bonding around the silicon tetrahedra can include the presence of hydrogen atoms and standard configurations can be produced by using a generation probability method (Hasegawa et al., 1991).

The random bonding model of Philipp (Philipp, 1973) considers the structure to be SiN_x with silicon tetrahedra bonded on a statistical basis with no dominant rules of selection and with the assumption that no N-N bonding is present. The structural similarity between planar trisilylamine and crystalline silicon nitride has been noted (Lucovsky et al., 1983) and studies indicate that the "skeletal Si_3N form" persists in the amorphous state. According to Maeda (Maeda et al., 1991) the presence of Si-Si bonding is a prerequisite for amorphous silicon nitride films and this has been corroborated by Yin (Yin et al., 1990).

Experiments have been performed to actively reduce the NH_2 content of silicon nitride films, deposited from silane and ammonia precursors, by the use of hydrogen dilution (Murley et al., 1996). By adjusting the platen temperature and percentage dilution with hydrogen the authors could obtain good control over deposited film stress. The correlation between stress (and other physical properties of deposited films) and film composition is well documented and various physical measurement techniques can be used to infer or determine composition from physical characteristics.

2.5 DEPOSITION WITH INORGANIC SILANES

The most common material used is silane (monosilane) which is reacted in a gas phase plasma with ammonia or nitrogen gas to produce silicon nitride. This has been the standard PECVD reactant for over three decades. The general reaction equations are:



The simple reaction equations give no indication as to the mechanism of reaction or the species involved. Silane and ammonia are generally reacted either as undiluted pure gases or in admixture with a pure diluent gas such as nitrogen, argon or occasionally helium. The reaction of silane with nitrogen produces films with a lower hydrogen content than silane and ammonia, but due to the nitrogen triple bond, the energy requirement is very much greater (Dun et al., 1981).

The chemical homologue disilane (Narikawa et al., 1985) has been assessed for dielectric film deposition and good film deposition was achieved by the PECVD technique (Nallapati et al., 1998). Remote CVD deposition has been performed with an increase in deposition rate but similar bonding modes to silane (Tsu et al., 1986a). Disilane is gaseous like silane but thermodynamically less stable. Its use therefore constitutes a greater safety hazard than that posed by silane. However disilane may have greater applications for amorphous silicon deposition in solar cell technology than in the semiconductor industry.

Trisilane is a liquid precursor with a standard molar enthalpy of formation more positive than either silane or disilane. Due to the hazardous nature of the material there is little information in the literature relating to film deposition via CVD processes. Depositions using hydrogen azide with higher silanes (Kanoh et al., 1991) and tetrasilane (Ishihara et al., 1993) have been reported using chemical vapour deposition techniques at temperatures down to 350°C and 300°C respectively.

The use of silicon tetrafluoride (Fujita et al., 1984a) and silicon difluoride (Fujita et al., 1984b) have been proposed for low hydrogen content films. Silicon difluoride is obtained from the decomposition of silicon tetrafluoride over silicon prior to deposition. Film analysis suggests that fluorinated films are stable and have good electrical and

material properties. To obtain stoichiometric films with $N/Si = 1.3$ (Cicala et al., 1992) hydrogen was added to silicon tetrafluoride diluted with nitrogen. Difluorosilane and ammonia deposition has been reported by Watanabe (Watanabe et al., 1991). The films deposited by this technique demonstrated that low concentrations of fluorine give stable films, however incorporation of oxygen was noted.

Nitrogen trifluoride NF_3 has been suggested as an alternative material for producing fluorinated films by PECVD deposition in admixture with both silane and ammonia gases (Livengood et al., 1987). Remote plasma deposition of silicon nitride films has been demonstrated using silane and nitrogen trifluoride precursors in nitrogen gas (Aleksandrov et al., 1997 & 1996). A bottom anti-reflection (BARL) film has been produced by reaction of nitrogen trifluoride and silane for use in $0.25\mu m$ semiconductor lithographic applications (Jun et al., 1997).

Experiments with the remainder of the silicon halides have been reported in the literature but have little commercial application. Silicon tetrabromide with nitrogen gas was one of the earliest materials investigated (Androshuk et al., 1969; Aboaf, 1969). Silicon tetraiodide has been reacted with microwave activated nitrogen (Shiloh et al., 1977) to give silicon nitride films. However the infrared spectra showed absorbance peaks characteristic of the ammonium ion and ammonium iodide in the films. Silicon tetrachloride has been very widely investigated and reported as a precursor for high temperature silicon epitaxy applications but with little application in PECVD. Ron (Ron et al., 1983) deposited silicon nitride onto Martensitic stainless steel substrates using silicon tetrachloride and ammonia using an RF plasma at temperatures between $300^\circ C$ and $440^\circ C$. The results from energy dispersive x-ray analysis (EDX) analysis showed chlorine present in the film. Hexachlorodisilane Cl_6Si_2 has been successfully reacted with hydrazine N_2H_4 in a CVD reactor at temperatures down to $350^\circ C$ to form amorphous silicon nitride films (Yeh et al., 1996).

2.6 DEPOSITION WITH ORGANOSILANES

Organo-silane compounds have found extensive use in the fields of ceramics, plasma polymerisation and silicon dioxide deposition. TEOS has been a prime replacement for silane in silicon dioxide CVD deposition where, due to the oxidising ambient, the carbon can be removed as gaseous carbon dioxide.

Various authors have reported experimental work with tetrakis(dimethylamido)silane $\text{Si}(\text{NMe}_2)_4$ as a precursor for silicon nitride deposition. While investigating metal nitride deposition Sugiyama (Sugiyama et al., 1975) made an attempt at forming silicon nitride at low temperatures. No deposition was found below 800°C and above this temperature a brown coating consisting mainly of elemental silicon with some silicon carbide, nitride and amide was formed. Subsequent work has led to reports of deposition by APCVD at temperatures between $600 - 750^\circ\text{C}$ (Gordon et al., 1990) and Hoffman (Hoffman et al., 1995 & 1994) reported deposition by PECVD.

One general class of compound to receive attention are the organo-silazanes. From the work of Arkles (Arkles, 1985) the most promising material was a 1,2-dimethylsilazane-1-methylsilazane copolymer. However this could only achieve a conversion to silicon nitride of 80-85% at a temperature of $286-287^\circ\text{C}$ and considerably worse results were obtained with other linear polymers where conversion was in the range 30 - 60%. Mixed products were reported (Mazaev et al., 1983) for thermal decomposition of poly-N-methylcyclosilazane between $200-600^\circ\text{C}$ in an inert atmosphere. The plasma deposition of silicon nitride films onto silicon from a methylsilazane precursor $[\text{CH}_3\text{SiH}_2\text{NH}]_n$ has been achieved using a range of temperatures between 590-1000 K (Moriwaki et al., 1995).

Hexamethyldisilazane (HMDS) has applications in photolithographic processes as an adhesion promoter between photoresists and silicon or silicon dielectric film surfaces. Its use as a potential silicon nitride source has been reported (IBM, 1986; Janca et al., 1983). In the IBM work the HMDS source was held at -29.79°C (using Freon 12 refrigerant) in an apparatus consisting of a rectangular profile quartz tube with external electrodes. A growth rate of 12 nm/min ($120 \text{ \AA}/\text{min}$) was obtained. More recently HMDS has been used to deposit silicon nitride films by RPECVD (Fainer et al., 1997).

One of the most promising materials proposed to date as a precursor (Voronkov et al., 1981) is hexamethylcyclotrisilazane (HMCTS). Belyi (Belyi et al., 1986) deposited onto InSb substrates, and deposition and characterisation of films on silicon substrates

has also been reported (Brooks et al., 1988a & 1988b). Due to the methyl groups in the precursor it was impossible to eliminate entirely carbon from the silicon nitride films. Brooks reported that a carbon content of < 4 at.% was achieved with a hydrogen content of 25 at.% but only with high values of RF power and ammonia to precursor ratio. Deposited by RPECVD from HMCTS, a film of silicon without any carbon bonded in the film has been claimed (Smirnova, 1997).

Brief deposition results have been reported for a silicon nitride film formed from the compound $\text{H}_3\text{Si}(\text{NH}_2)$ diluted with helium gas (Azuma, 1988). Films have been deposited from the precursor monomethylamine CH_3NH_2 in conjunction with silane (Yasui, 1990a) and tetramethylsilane $(\text{CH}_3)_4\text{Si}$ (Yasui, 1990b). Deposition from the compound azidotrimethylsilane has been patented (Nelson, 1979) but evidence of further work is not known at this time.

A number of workers have been involved in the preparation of single component precursors. A range of disilane derivatives have been produced (Schuh et al., 1993) which are liquid at room temperatures and not spontaneously flammable. One of the compounds 1,2-Bis(di-*i*-propylamino)disilane (BIPADS) has been used in a RPECVD system to produce silicon nitride films. The carbon levels were low but high levels of hydrogen were present. Two pentamethylcyclopentadiene substituted silanes, namely $(\text{Me}_5\text{C}_5)\text{SiH}_3$ and $(\text{Me}_5\text{C}_5)_2\text{SiH}_2$ have been reported as being useful for the deposition of silicon nitride films by remote PECVD (Dahlhaus et al., 1993). One stated advantage of these materials is that they are non-hazardous. Mitzel and co-workers (Mitzel et al., 1993) working on single source precursors have identified (hydridosilyl)hydrazines as promising candidates for silicon nitride.

For sub-half micron device technologies tris(dimethylamino)silylazide (TDSA) has been suggested as a precursor for silicon nitride films (Kitoh et al., 1994). Silicon nitride films have also been deposited (Yasui et al., 1994) from the precursor trisdimethylaminosilane (TDMAS) after decomposition by hydrogen radicals from a microwave source. Schlosser (Schlosser et al., 1994) and co-workers have synthesised a range of bicyclic aminosilanes which they suggest have potential as precursors in PECVD deposition of silicon nitride films. Soldner has prepared both isomeric cyclosilazanes (Soldner et al., 1998a) and tetra(alkylamino)silanes (Soldner et al., 1998b) for use as single source precursors for silicon nitride deposition.

2.7 TRISILYLAMINE

Only limited information is available from the literature concerning trisilylamine or its commercial applications, although information is available on specific properties of the material. Trisilylamine is the most thermally stable of the silicon amines but is decomposed on exposure to air. Heslop (Heslop et al., 1976) suggested that silicon dioxide, ammonia and hydrogen are the likely products of reaction. For a full account of the properties of trisilylamine the reader is referred to chapter 5 of Bell (Bell, 1972) and section 3.1.6.2 of Gmelin, Si supplement B4, (Gmelin, 1989).

The original preparation of trisilylamine is credited to Stock (Stock et al., 1921) who reacted monochlorosilane and ammonia in the gas phase in a vacuum apparatus:



Other synthetic methods have been subsequently developed using monobromosilane (Ward, 1970) and monoiodosilane (Varma et al., 1963).

2.7.1 Structure and Bonding

Electron diffraction studies (Beagley et al., 1970 ; Hedberg, 1955) have demonstrated that in the gas phase trisilylamine is a trigonal planar molecule. The planar structure has also been observed in the solid phase (Barrow et al., 1984). These observations are at odds with most of the molecules with the $\text{X}(\text{YH}_3)_3$ structure as shown in table 2.6.

Table 2.6

Structures of Heavy Atom Portions of Some $\text{X}(\text{YH}_3)_3$ Molecules

(from Miller et al., 1974)

X	$(\text{CH}_3)_3\text{X}$	$(\text{SiH}_3)_3\text{X}$	$(\text{GeH}_3)_3\text{X}$
N	Pyramidal	Planar	Planar
P	Pyramidal	Pyramidal	Pyramidal
As	Pyramidal	Pyramidal	Pyramidal
Sb		Pyramidal	Pyramidal

Additional experimental confirmation of the planar structure has been presented from spectroscopic studies (Miller, 1975; Ebsworth et al., 1958) and by electric dipole moment measurements in the gas phase by Varma who obtained a zero dipole moment. The planarity of trisilylamine has been variously attributed by authors to $N(p\pi) \rightarrow Si(d\pi)$ bonding (Thuraisingham, 1979; Perkins, 1967; Sujishi et al., 1954), SiH_3 group non-bonded interactions (Glidewell, 1975), electrostatic repulsion due to the positive charge on the silicon atom (Noodleman et al., 1979) and interactions of SiH (anti bonding) with $N(p)$ orbitals (Cotter, 1996). The shorter than expected length of the Si-N single bonds suggests that the planar trigonal molecular structure possesses some partial double bond character. The extent of the double bond character has been assessed by estimation from the sublimation energy of addition compounds. The resonance energy of trisilylamine was determined to be in excess of 113 kJ mol^{-1} (27 kcal/mol).

Some authors have also published their findings on the structure of trisilylamine using molecular orbital calculations. In table 2.7 the total energy of the molecule is given along with the ab initio molecular orbital model that was used to perform the calculation.

Table 2.7

Comparison of Total Energy Values for Trisilylamine

Molecular orbital model	Total energy (kJ mol^{-1})	Reference
STO-3G	-2.40355×10^6	Livant et al., 1983
STO-3G*	-2.40635×10^6	Livant et al., 1983
3-21G	-2.42079×10^6	Glidewell et al., 1982
6-21G	-2.43299×10^6	Livant et al., 1983
6-31G*	-2.43362×10^6	Julian et al., 1988
6-31G** + MP3	-2.43500×10^6	Tachibana et al., 1993

Converted from 1 hartree = 627.5 kcal/mol (Hehre et al, 1996) = $2.62672 \times 10^3 \text{ kJ mol}^{-1}$

Each successive improvement in the ab initio model provides a better approximation of the wavefunction and therefore the value of the total energy rises with the number of basis sets evaluated by the model. Much of the early ab initio molecular orbital work has less relevance now due to the recent appearance of larger ab initio basis sets which

can more accurately predict the energy and molecular structure of compounds. On this basis there appears little point in determining the bonding and structure of trisilylamine with anything other than the 6-21G, 6-31G* or 6-31G** basis sets.

In table 2.8 a comparison is given between results from experimental studies and the results obtained by calculation using a variety of semi-empirical and ab initio models.

Table 2.8

Comparison of Experimentally Determined and Calculated Geometry Data

	Si - - Si (nm)	Si-N (nm)	Si-H (nm)	∠SiNSi (deg.)	∠HSiN (deg.)	∠HSiH (deg.)	Reference
ED	0.3005	0.1738	0.154	119.6			1
ED	0.2998	0.1736	0.1506	119.4	106.6	112.2	2
ED	0.2997	0.1734	0.1485	119.7	108.1	110.8	2
MNDO	0.3043	0.1757	0.1443	120.0	109.3		3
MNDO		0.1758	0.1443		109.38		4
ab initio ⁺		0.176	0.144		112.00		4
3-21G		0.17673	0.14885	119.99	110.79		5
6-31G*	0.3028	0.1749		119.85			6
Reference	1	Hedberg, 1955			4	Livant et al., 1983	
	2	Beagley et al., 1970			5	Glidewell et al., 1982	
	3	Cuthbertson et al., 1983			6	Julian et al., 1988	

⁺ not specified - sets employed include STO-3G, STO-3G* and 6-21G

2.7.2 Application to Chemical Vapour Deposition

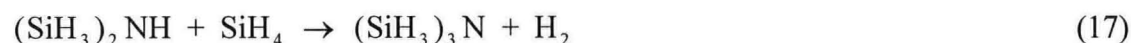
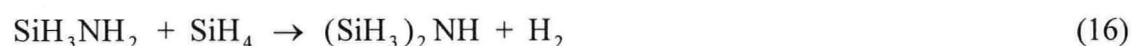
In its application to PECVD, the original patent (Reinberg, 1980) covers the general preparation of silicon nitride films from trisilylamine alone or in admixture with ammonia. However the use of trisilylamine for applications in glow discharge deposition was included in the patent application by Androshuk over 10 years earlier (Androshuk, 1969).

Continuing the work of Reinberg it has been proposed (Hamaya et al., 1986b) that trisilylamine could be used along with nitrogen, ammonia or hydrazine for silicon nitride deposition. Hamaya has further suggested that trisilylamine may be used to

deposit silicon nitride in admixture with silane or one of its homologues such as disilane or trisilane (Hamaya et al., 1986a). The application of silylamines to nitride and oxynitride deposition has been patented by Ishikawa with trisilylamine being the predominantly studied species (Ishikawa, 1994).

It has also been suggested in Research Disclosure (Anonymous, 1987) that disilylamine $(\text{SiH}_3)_2\text{NH}$ and trisilylamine have sufficient chemical stability and vapour pressure for photo-chemical deposition of thin films. The compound in the disclosure is called trisilylamine and has the formula $(\text{SiH}_3)\text{N}$. It is assumed that this is a typographical error and should be $(\text{SiH}_3)_3\text{N}$. In considering the reaction involving silane with excited nitrogen or ammonia, it has been suggested (Tsu et al., 1986a & 1986b) that trisilylamine may be formed as a gas phase precursor which, depending on temperature, may deposit on the substrate as silicon nitride, silicon diimide or a mixture of both substances.

Tachibane et al. (1993) also considered a reaction mechanism for silane/ammonia in which their postulated reaction pathway leads to the deposition of silicon nitride, proceeding via the formation of trisilylamine in the gas phase:



They concluded, however that the formation of tetraaminosilane was the most likely route. A sample of disilazane held at 0°C for 72 hours (Aylett et al., 1969; Aylett et al., 1966) was observed to decompose forming trisilylamine as follows:



The stability of trisilylamine in the absence of air has been investigated and when held at 45°C for 5 days (Scantlin et al., 1972) the initial quantity of trisilylamine was fully retrieved within the limits of experimental error. The reaction with ammonia has been attempted in both liquid and gas phases (Wells et al., 1966). In the liquid phase silane gas was eliminated with a six membered ring compound as the first isolatable product:



In the gas phase no elimination of silane was detected either after 16 hours at room temperature or 1 hour at 100°C.

2.7.3 Comparison of Properties

Silane is the most thermally stable of the silane series being stable indefinitely at room temperature whereas the higher silanes are known to decompose slowly even under inert conditions. The ease of thermal decomposition and reactivity of Si_2H_6 , Si_3H_8 and Si_4H_{10} in air increases with increasing number of Si-Si links. This occurs primarily because:

- The electronegativity of Si (1.8) is lower than hydrogen (2.1) and the δ^+ charge on the silicon atom leaves it vulnerable to nucleophilic attack.
- Charge withdrawal from Si \rightarrow H occurs to the extent that it weakens the Si-Si bond.
- Silicon has low energy d orbitals which are capable of forming intermediate compounds thus lowering the effective activation energy of the process.

In table 2.9 a comparison is given of the physical state, boiling points and heat of formation data of the lower silanes and trisilylamine which emphasises the advantages of trisilylamine, especially in terms of the negative standard molar enthalpy of formation. Table 2.10 compares the physical properties of three materials namely silane gas, trisilylamine and trichlorosilane, showing that trisilylamine may be considered to be closer in its properties to trichlorosilane which is a liquid source used for many years as a precursor in high temperature LPCVD of nitride films in semiconductor applications.

Although safety is an important consideration in CVD deposition processes, other parameters such as reactant purity are also very important. The silane manufacturing process is a very mature process and the equipment for analytical assessment of impurity concentrations is extremely sophisticated (Taylor, 1987). Ultra-pure silane supplies, with a deposited resistivity of 1000 Ωcm , are available world-wide from a number of suppliers.

Table 2.9

Comparison of Physical Properties of Silane (S), Disilane (D), Trisilane (TS) and Trisilylamine (TSA)

Property	S	DS	TS	TSA
Physical form	Gas	Gas	Liquid	Liquid
Molecular weight	32.1	62.2	92.3	107.3
Boiling point (°C)	-112 (2)	-14.5 (2)	52.9 (2)	52 (2)
Melting point (°C)	-185 (2)	-132.5 (2)	-117 (2)	-106 (2)
Heat of formation (kJ/mol ⁻¹)	34.3 (3)	71.6 (3)	108.4 (3)	-131.0 (1)
References	(1) Gmelin, 1989 (2) Weast, 1974		(3) Gmelin, 1982	

This is because silane has been used for many years in CVD deposition of high and low temperature silicon and silicon semiconductor films. Potential precursor materials, like trisilylamine, are frequently not commercially available and therefore must be produced to requirement. Due to the lack of commercial availability of trisilylamine there is no significant body of information on the substance and therefore any comparative study with silane or other commercial precursors must be somewhat limited. A survey of the atomic content of the elements present in each precursor material from the literature is presented in table 2.11 indicating that only three precursors - $N(SiH_3)_3$, $(SiH_3)_2NH$ and $H_3Si(NH_2)$ have no extraneous atoms in their atomic structure.

2.7.4 Substituted Trisilylamine

Fluorinated substances appear to have a beneficial effect on film properties and silicon tetrafluoride has been shown to be the only halogen substituted silane to provide deposited films with good film properties. One may therefore propose by analogy the use of $N(SiF_3)_3$ as an alternative for trisilylamine to reduce the hydrogen content of films and improve film characteristics. The availability of the material is unknown but an attempted preparation of $N(SiF_3)_3$ was reported (Porritt, 1979) using silicon tetrafluoride and trilithium nitride which led to a violently explosive reaction.

Table 2.10

Table of Physical Properties of Trisilylamine (TSA) Compared to Silane (S) and Trichlorosilane (TCS)

Property	S	TCS	TSA
Description	Pyrophoric and toxic	Flammable and corrosive	Spontaneously flammable
Physical Form	Gas	Liquid	Liquid
Molecular Weight	32.12 (2)	135.4 (1)	107.34 (5)
Boiling Point ($^{\circ}\text{C}$)	-112 (2)	31.8 (1)	52 (5)
Melting Point ($^{\circ}\text{C}$)	-185 (3)	-127 (1)	-106 (5)
Vapour Pressure (kg/cm^2)	Gas	0.71 @ 21 $^{\circ}\text{C}$ (2)	0.15 @ 0 $^{\circ}\text{C}$ (4)
Heat of Formation ($\text{kJ}/\text{mol}^{-1}$)	34.3 (7)	-469.3 (2)	-131.0 (4)
Heat of Vaporisation (kcal/mol) ($\text{atm cal}/\text{g}$)	92.2 (2)	47.1 (2)	7 (6)
Critical Temperature ($^{\circ}\text{C}$)	-4 (2)	206 (1)	215 (4)
Critical Pressure (kg/cm^2)	49.4 (2)	40.6 (1)	9.6 (4)
Critical Volume ($\text{cm}^3/\text{gm mol}$)	130 (3)		
Critical Vapour ($\text{cm}^3/\text{gm mol}$)		268 (1)	
Density of Solid (g/cm^3)			1.1 @ -158 $^{\circ}\text{C}$ (4)
Density of Liquid (g/l)	0.68 @ -185 $^{\circ}\text{C}$ (5)	1.342 @ 21 $^{\circ}\text{C}$ (2)	0.895 @ -106 $^{\circ}\text{C}$ (5)
Density of Gas (g/l)	1.34 (2)		
Specific Volume (m^3/kg)	0.75 @ 20 $^{\circ}\text{C}$		
S.G (Gas @ 21.1 $^{\circ}\text{C}$)	1.114 (2)	5.8 (2)	
Heat Capacity (J kg K^{-1})	1375		
TLV (ppm)	0.5		
References	(1) Drews et al., 1973 (2) Taylor, 1989 (3) Borreson et al., 1978 (4) Gmelin, 1989	(5) Weast, 1974 (6) Sujishi et al., 1954 (7) Gmelin, 1982	

Table 2.11

Comparison of Percentage Elemental Composition for Potential Source Materials for PECVD Si₃N₄ Deposition

Source	% Si	% H	% N	% C	% Other	References
SiH ₄	87.5	12.5	-	-	-	
N(SiH ₃) ₃	78.5	8.5	13.0	-	-	1
(SiH ₃) ₂ NH	72.7	9.1	18.2			2
H ₃ Si(NH ₂)	59.6	10.7	29.7	-	-	3
[(CH ₃) ₃ Si] ₂ NH	34.8	11.8	8.7	44.7	-	4
[(CH ₃) ₂ SiNH] ₃	38.4	9.6	19.2	32.8	-	5
(CH ₃) ₃ SiN ₃	24.4	7.9	36.5	31.3	-	6
[(C ₃ H ₇) ₂ NSiH ₂] ₂	21.6	12.4	10.8	55.3	-	7
[(CH ₃) ₂ N] ₃ SiN	16.1	10.4	32.2	41.3	-	8
[(CH ₃) ₂ N] ₃ SiH	17.4	11.9	26.1	44.7	-	9
Si(N(CH ₃) ₂) ₄	13.8	11.8	27.4	47.0	-	10
[(CH ₃) ₅ C ₅]SiH ₃	16.9	10.9	-	72.2	-	11
[(CH ₃) ₅ C ₅] ₂ SiH ₂	9.3	10.6	-	80.1	-	11
SiF ₄	27.0	-	-	-	73.0	12
SiBr ₄	8.1	-	-	-	91.9	13
SiI ₄	5.2	-	-	-	94.8	14
References	1	Reinberg, 1980		8	Kitoh, 1994	
	2	Anonymous, 1987		9	Yasui, 1994	
	3	Azuma, 1988		10	Hoffman, 199	
	4	IBM, 1986		11	Dahlhaus, 1993	
	5	Belyi et al., 1986		12	Fujita et al., 1984	
	6	Nelson, 1979		13	Androshuk et al., 1969	
	7	Schuh et al., 1993		14	Shiloh et al., 1977	

3 ATOMIC AND MOLECULAR ORBITALS

Molecular orbital modeling of molecules is based on the solution of the Schrödinger equation:

$$H\Psi = E\Psi \quad (1)$$

where H is the Hamiltonian operator, E is an eigenvalue and Ψ is a wavefunction

For atoms and molecules the solution can only be exact for the simplest cases, which are the hydrogen atom H and the diatomic molecule H_2^+ . In all other cases the solution of the many-electron Schrödinger equation requires systematic approximations to obtain useful information. These approximations have been refined and improved with time and some of the more sophisticated models can be run in reasonable times with the availability of modern digital computers.

The quantum theory presented in this chapter is not intended to be exhaustive in its content. It is presented as a background to show how the quantum theory used in semi-empirical programmes has developed from the classical Schrödinger equation. Invariably, a number of assumptions must be made and it is interesting to see how these have ultimately provided a set of quantum mechanical calculations that can provide direct molecular and thermodynamic data on molecules with up to 10,000 atoms.

3.1 SCHRÖDINGER WAVE EQUATIONS

The Schrödinger equation is based on the work of Louis de Broglie who proposed that electromagnetic radiation can have a dual nature in that it has momentum like a particle and a wavelength like a wave. This duality is expressed by the relationship:

$$\lambda = \frac{h}{p} \quad (2)$$

where λ = wavelength, p = momentum of the particle and h = Planck's constant

In terms of energy, the wavelength can be expressed as:

$$\lambda = \frac{h}{p} = \frac{h}{(2m(E - V))^{1/2}} \quad (3)$$

where m = mass, E = energy and V = potential energy

3.1.1 One Electron Atom

Schrödinger took the classical 3-dimensional wave equation:

$$\nabla^2 \Psi(x, y, z) = -\left(\frac{2\pi}{\lambda}\right)^2 \Psi(x, y, z) \quad (4)$$

where ∇^2 is the Laplacian operator and Ψ = wavefunction

and inserted the de Broglie wavelength $\lambda = \frac{h}{p}$ in place of the traditional value of λ to make the equation applicable to particle waves. The Schrödinger equation for a one-electron atom is therefore given by:

$$\nabla^2 \Psi = -\left(\frac{2\pi}{\frac{h}{(2m(E - V))^{1/2}}}\right)^2 \Psi \quad (5)$$

rearranging the equation and multiplying through gives:

$$\nabla^2 \Psi = - \left(\frac{8\pi^2 m}{h^2} \right) (E - V) \Psi \quad (6)$$

$$\nabla^2 \Psi = - \left(\frac{8\pi^2 m}{h^2} \right) (E - V) \Psi \quad (7)$$

$$- \left(\frac{h^2}{8\pi^2 m} \right) \nabla^2 \Psi = E\Psi - V\Psi \quad (8)$$

$$\left[- \left(\frac{h^2}{8\pi^2 m} \right) \nabla^2 + V \right] \Psi = E\Psi \quad (9)$$

If we set H to be $\left[- \left(\frac{h^2}{8\pi^2 m} \right) \nabla^2 + V \right]$ then substituting H into equation (9) gives the

familiar form of the Schrödinger equation:

$$H\Psi = E\Psi \quad (10)$$

H is the Hamiltonian operator that contains the important information relating to the energy of the system and E is an eigenvalue. H operates on Ψ which is a wavefunction (eigenfunction) and contains the description of the electrons in the system.

This gives a precise result for the hydrogen atom which has one electron and a nucleus.

3.1.2 One-Electron Orbitals

As we are interested in atoms that contain electrons and nuclei (protons + neutrons) we need to adapt the basic Schrödinger equation to allow for this. For two charged particles whose fields interact there is an associated electrostatic potential energy for each particle which is given by the equation:

$$V = \frac{q_1 q_2}{r_{12}} \quad (11)$$

where q_1, q_2 are the charges on the particles and r is the distance between them

For a nucleus and an electron the charges are opposite and will therefore lead to attraction. We can now rewrite V in terms of the electronic ($-e$) and the nuclear ($+Ze$) charges as:

$$V = \frac{-Ze^2}{r} \quad (12)$$

Substituting for V in equation (9) gives the following relationship:

$$\left[-\left(\frac{h^2}{8\pi^2 m} \right) \nabla^2 - \frac{Ze^2}{r} \right] \Psi = E\Psi \quad (13)$$

We now have a relationship whereby each wavefunction Ψ and its energy correspond to one electron bound to a nucleus. These are one-electron orbitals. Electrons occupying these orbitals are defined by a set of quantum numbers:

a principal quantum number, N , equal to 1, 2, 3, 4, 5,

an azimuthal quantum number, L , equal to $n - 1, n - 2, \dots, 0$

a magnetic quantum number, M , equal to $\pm L$ (including 0)

These one-electron wavefunctions can exist in two spin states (which we can denote as α and β) which are non-overlapping so that no two electrons have all the same quantum

numbers (**Pauli exclusion principle**). The filling of these one-electron orbitals is based on the aufbau principle whereby the total energy is minimised to produce a ground state electronic configuration for the atom. In the case of the three atoms that compose the trisilylamine molecule the ground state electronic configuration for each atom is given in table 3.1.

Table 3.1

Ground State Electronic Configuration for H, N and Si

Elements	1s	2s	2p	3s	3p
H	↑				
N	↑↓	↑↓	↑ ↑ ↑		
Si	↑↓	↑↓	↑↓ ↑↓ ↑↓	↑↓	↑ ↑

Electrons in these one-electron orbitals occupy positions in space governed by the probability density or charge density. This is defined as:

$$\Psi^2 = \Psi \Psi^* \quad (14)$$

where Ψ is a one-electron orbital and Ψ^* is its complex conjugate wave function

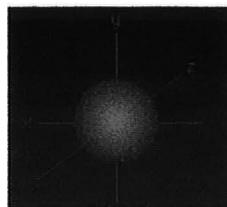
If we sum the probability density over the distance, r , azimuthal angle, Θ , and angle, ϕ , a quantum-mechanical model of the atom can be produced which defines the shape of the atomic orbitals for any set of quantum numbers n , m , and l . Figure 3.1 shows the probability density factor plotted against angle for the 1s and 2p atomic orbitals.

3.1.3 Many Electron Atom

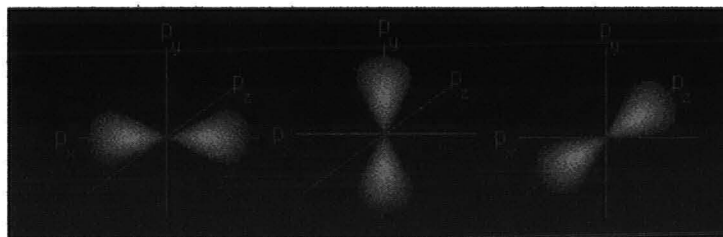
For a many electron atom with a total of k electrons the Schrödinger equation becomes:

$$\left[\left[- \left(\frac{h^2}{8\pi^2 m_e} \right) \sum_{i=1}^{i=k} \nabla_i^2 - \sum_{i=1}^{i=k} \frac{Z}{r_i} \right] + \sum_{i=1}^{i=k-1} \sum_{j=1+1}^{j=k} \frac{1}{r_{ij}} \right] \Psi = E\Psi \quad (15)$$

For a multi-electron system the equation now has to account, not only for electron-nucleus interactions, but also for interactions between all the electrons in the atom.



1s Atomic Orbital



Three 2p Atomic Orbitals

Figure 3.1

Graphical Representation of the 1s and 2p Atomic Orbitals

(Paul R. Young, University of Illinois at Chicago)

In equation (15) the term $-\sum_{i=1}^{i=k} \frac{Z}{r_i}$ accounts for the electron-nucleus interactions while

the final term in the equation $\sum_{i=1}^{i=k-1} \sum_{j=1+1}^{j=k} \frac{1}{r_{ij}}$ is the effect of the electron-electron

interactions on the eigenfunction Ψ . These electron-electron repulsions are generally known as **electron correlation effects** and cannot be completely ignored if the atomic properties of the atoms and molecules are to be correctly predicted. Direct calculation of the electron-electron effects requires information on the position of any two electrons that are interacting at the same time. This is computationally feasible only for very small systems and therefore it is normal to replace this direct term by the effect of the electrons interacting with an average of the nucleus and all the other electrons. This is known as the self consistent field (SCF) **approximation** or the **independent particle approximation** in which the removal of the electron-electron effects effectively leaves an expression for a one-electron system describing a many electron system. One

important property of the SCF approximation is that the solutions satisfy the Variation Theorem so that the energy calculated with an inexact wavefunction is always higher than the actual value of energy calculated with the exact wavefunction. It follows therefore that in optimising the wavefunctions the energy is being minimised and the lowest energy calculated will be obtained from the best approximate wavefunction.

3.1.4 Many Electron and Many Nuclei Systems

When applying the Schrödinger equation to molecules the **Born-Oppenheimer approximation** is applied to simplify the calculation. This states that given the rest mass and energy of the nucleus are significantly larger than that of the electron by a factor of about 10^4 , we can consider the nucleus to be stationary relative to the motion of the electrons. This eliminates the kinetic energy of the nucleus from the Hamiltonian. The Schrödinger equation for a molecule with k electrons and N atoms is therefore:

$$\left[\left[-\left(\frac{\hbar^2}{8\pi^2 m_e} \right) \sum_{i=1}^{i=k} \nabla_i^2 - \sum_{j=1}^{j=N} \sum_{i=1}^{i=k} \frac{Z_j}{r_{ji}} \right] + \sum_{i=1}^{i=k-1} \sum_{l=1+1}^{l=k} \frac{1}{r_{il}} + \sum_{j=1}^{j=N-1} \sum_{m=j+1}^{m=N} \frac{Z_j Z_m}{R_{jm}} \right] \Psi = E\Psi \quad (16)$$

In this equation we now have additional terms to account for interactions involving

additional nuclei. The term $-\sum_{j=1}^{j=N} \sum_{i=1}^{i=k} \frac{Z_j}{r_{ji}}$ describes the electron-nucleus interactions

while the $\sum_{i=1}^{i=k-1} \sum_{l=1+1}^{l=k} \frac{1}{r_{il}}$ term accounts for electron-electron effects. Additionally a final

term $\sum_{j=1}^{j=N-1} \sum_{m=j+1}^{m=N} \frac{Z_j Z_m}{R_{jm}}$ is incorporated for nucleus-nucleus interactions but this term is

generally treated as a constant because the assumption is made that during the calculation the position of the nuclei (in contrast to the electrons) is fixed. This form of the equation using the Born-Oppenheimer approximation is often referred to as the electronic Schrödinger equation.

3.2 ONE ELECTRON SPIN ORBITALS

Most chemists are familiar with the concept of a spin orbital which is the same as the eigenfunction or wavefunction Ψ . If we consider equation (10):

$$H\Psi = E\Psi$$

this can be modified into both separate one electron Hamiltonians, h , and one-electron energies, e , then for a two electron atom the relationship becomes:

$$[h(1) + h(2)]\Psi = (e_i + e_j)\Psi \quad (17)$$

$$\text{where } H = h(1) + h(2) \text{ and } E = e_i + e_j$$

By virtue of the SCF approximation, Ψ is now made up from a combination of one-electron wavefunctions which can be denoted by $\phi_i(1)$ and $\phi_j(2)$.

The spin orbital comprises a space function which is dependent on the position of the electron in space and a spin function which is dependent on the spin of the electron. Space functions are either symmetric or antisymmetric and are derived from the products of the one-electron wavefunctions. To describe the system correctly the wavefunctions must allow for the fact that electrons cannot be distinguished from each other and therefore positional interchange of electrons in a wavefunction must always produce the same wavefunction.

The symmetric and antisymmetric space functions ψ_s and ψ_a can be described respectively by the relationships:

$$\psi_s = \phi_i(1)\phi_j(2) + \phi_i(2)\phi_j(1) \quad (18)$$

$$\psi_a = \phi_i(2)\phi_j(1) - \phi_i(1)\phi_j(2) \quad (19)$$

Interchange of electrons within the wavefunctions produces the relationships:

$$\phi_i(1)\phi_j(2) + \phi_i(2)\phi_j(1) = \phi_i(2)\phi_j(1) + \phi_i(1)\phi_j(2) \quad (20)$$

$$\phi_i(1)\phi_j(2) - \phi_i(2)\phi_j(1) = - \left[\phi_i(2)\phi_j(1) - \phi_i(1)\phi_j(2) \right] \quad (21)$$

Spin functions, like space functions, also have symmetric ω_s and asymmetric ω_a forms and these spin functions mathematically represent the spin states described earlier and designated α and β .

According to the Pauli exclusion principle the wavefunction must change sign when two independent electronic states are interchanged, and therefore only the asymmetric forms of the wavefunctions have any physical meaning. The wavefunction Ψ can now describe a spin orbital when represented by a space function and a spin function:

$$\Psi = \psi_s \omega_a \quad \text{and} \quad \Psi = \psi_a \omega_s \quad (22)$$

Spin orbitals are often approximated by a Slater determinant which is a mathematical function that gives the antisymmetric wavefunction for n indistinguishable particles. Interchanging two electrons corresponds to interchanging two rows and a determinant automatically changes sign if two rows are interchanged. If the two electrons were in the same spin-orbital, then two columns would be the same and a determinant vanishes if it has two rows or columns that are identical. Also the wavefunction automatically obeys the Pauli Principle.

For a two electron system with an α or β spin state the combination of the spin orbitals can be written as:

$$\psi_n = \frac{1}{\sqrt{2}} \left\{ \phi_1(x_1, y_1, z_1, \sigma_1) \phi_2(x_2, y_2, z_2, \sigma_2) \right\} - \left\{ \phi_2(x_1, y_1, z_1, \sigma_1) \phi_1(x_2, y_2, z_2, \sigma_2) \right\} \quad (23)$$

where $\sigma =$ either α or β spin state and x, y, z are electron co-ordinates

If the total wavefunction is to consist of a single Slater determinant then the total energy of this determinant must be equal to the total energy of the Hamiltonian. This requires that the energy be minimised and doing this in relation to the Slater determinant is generally accomplished using the Hartree-Fock approach.

3.3 HARTREE-FOCK (HF) METHOD

The method most used in molecular orbital calculations to solve the molecular wave function is called the Hartree-Fock approach. In place of the Hamiltonian, H , we have an operator that approximates the Hamiltonian. This is known as the Fock operator, F , which uses the SCF approximation for a two electron system by considering the interaction of every electron (test electron) in the average field of all the electrons. The Fock operator is given by the relationship:

$$F_i = -\frac{1}{2} \nabla^2 - \sum_{j=1}^{j=N} \frac{Z_j}{r_{ji}} + \sum_{l=1}^{l=k} (2J_l - K_l) \quad (24)$$

where F_i is the Fock operator, k is the number of electrons, N is the number of atoms, J is the Coulomb integral and K the Exchange integral

The Coulomb integral, J , embodies the average potential of interaction for an electron due to all the other electrons in the system. The Exchange integral, K , represents additional charge factors associated with exchange of same spin electrons. Both J and K are functions of the one electron molecular orbitals and by virtue of this so is the Fock operator F_i .

If we consider equation (14) in terms of a two atom system and apply the SCF approximation, the resultant Hamiltonian is:

$$H \cong -\left(\frac{1}{2}\right)\nabla_1^2 - \frac{2}{r_1} - \left(\frac{1}{2}\right)\nabla_2^2 - \frac{2}{r_2} \quad (25)$$

The first two terms in equation (25) can be equated with the terms seen in equation (24) for the Fock operator. These terms can be replaced by the Fock operator and can be incorporated into the wave equation (17):

$$[h(1) + h(2)]\Psi = (e_i + e_j)\Psi$$

to give the relationship:

$$\left[h_i + B_i \right] \Psi_i = e_i \Psi_i \quad (26)$$

where $h_i = h(1) + h(2)$, B_i is a term containing J and K and e_i is the averaged electron energies (SCF)

This is the basis of the **LCAO approximation** method to obtain a value for the wavefunction Ψ_i . An initial guess is made at a set of wavefunctions Ψ_i and by using the Hartree-Fock method a value can be obtained for B_i from the initial value of Ψ_i . Applying the Fock operator with the value of B_i a new value of Ψ_i is computed. This process is continued iteratively for successive calculations of Ψ_i and B_i until the value of Ψ_i produces a constant minimum value of E .

Two variations of the HF method can be applied. If two electrons are paired and occupy the same spatial orbital with different spins, then this restriction allows the magnetic moments of the electron spin to cancel therefore reducing the computation requirements. This is called a restricted Hartree-Fock (RHF) method. Without this assumption we have the unrestricted Hartree-Fock mode (UHF) of calculation.

3.4 LINEAR COMBINATION OF ATOMIC ORBITALS (LCAO)

The LCAO method is the main method used to build molecular orbitals from one-electron spin orbitals. The molecular orbitals can be described by the equation:

$$\psi_i = \sum_{j=1}^{j=m} c_{ij} \phi_j \quad (27)$$

where ψ is a molecular spin orbital, m is the basis set size (see section 3.5) and c_{ij} is a molecular orbital coefficient

From which equation we need to determine the value of the molecular orbital coefficient c_{ij} .

The Variation Theorem asserts that the calculated molecular energy, E , will always be higher than the true molecular ground state energy E_0 . This is because a trial wavefunction energy (E_i) can only have an energy equal to, or higher than, the ground state energy. By definition the ground state energy is the lowest possible energy of the molecule. We therefore require the trial wavefunction to define the ground state of a system which will have the lowest possible energy and in the limiting case $E_i = E_0$. The best approximation of the wavefunction is when the value of c_{ij} produces the minimum energy for a particular Hamiltonian and basis set. This coefficient determines the contribution of the one-electron wavefunction to each of the molecular orbitals and provides the best approximation to the actual wavefunction. The average energy $\langle E \rangle$ is given by the equation:

$$\langle E \rangle = \frac{\int \psi^* H \psi \, d\tau}{\int \psi^* \psi \, d\tau} \quad (28)$$

where ψ^* is the complex conjugate of the molecular spin orbital, H is the Hamiltonian and $d\tau$ is an infinitesimally small volume of space

If we substitute the LCAO approximation for ψ_i given in equation (27) into the average energy of equation (28) then the minimum energy condition for each molecular orbital

coefficient c_{ij} will occur when the derivative of the average energy is zero. Differentiation of $\langle E \rangle$ leads to two useful integrals known as the Coulomb integral H_{kl} and the Overlap integral S_{kl} given by equations (29) and (30) respectively:

$$H_{kl} \equiv \int \phi_k H \phi_l d\tau \quad (29)$$

$$S_{kl} \equiv \int \phi_k \phi_l d\tau \quad (30)$$

The equations for each ψ_i can be used to obtain a value for the average energy $\langle E \rangle$ by the method of determinants using a secular determinant. This requires that values for the Coulomb and Overlap integrals are available. Once a value of $\langle E \rangle$ has been obtained then a value can be obtained for the molecular orbital coefficient c_{ij} .

The general practice in molecular orbital computer packages is to generate molecular orbitals via a matrix comprising the Hamiltonian, H , Coulomb integral, H_{kl} , Overlap integral, S_{kl} , molecular orbital coefficient, c_{ij} and the average energy $\langle E \rangle$.

There are two modes of calculation available with most molecular orbital programmes. One mode of calculation is known as the **direct SCF** method where the required integrals are calculated dynamically thus making optimal use of the capabilities of modern computer technology. Also available is the **indirect SCF** method where the required integrals are calculated initially, prior to the computation and the results stored and accessed from memory as required.

3.5 BASIS SETS

Basis sets are the one-electron wavefunctions used in the LCAO approximation method to build molecular orbital wavefunctions. They are composed of a mathematical function that approximates the wavefunction, generally with a simplification of the radial term to cut calculation time.

In section 3.2.3 to simplify the calculation of the Schrödinger equation the electron correlation effects (electron-electron interactions) were effectively ignored. However, if we ignore them completely the orbital descriptions will not be correct because the effect of the nucleus on the electrons is to contract the electron density. This can be overcome by introducing factors that reduce the effect of the nucleus. One way is to introduce a screening constant which compensates for the screening effect of electrons on each other from the nuclear charges. A second way is to modify the nuclear constant, Z , by replacing it with an adjustable parameter zeta (ζ) which can be used to compensate for the electron correlation effects. The two most popular are the Slater-type orbitals (STO):

$$\phi(r) = r^{(n-1)} e^{-\left[\frac{(Z-s)r}{n} \right]} \quad (31)$$

where r is the radius, s is a screening constant and Z is the nuclear constant

and the Gaussian-type orbitals (GTO):

$$\phi(r) = e^{-\alpha r^2} \quad (32)$$

where α is a curve fitting constant which approximates an STO

In practice all the standard basis sets use GTO's to approximate an STO because this is much easier from a computational viewpoint. This can be expressed mathematically as:

$$\phi^{\text{STO}} \approx \sum_{v=1}^n k_n \phi_v^{\text{GTO}} \quad (33)$$

The minimal basis set is designated as STO-3G in which spherical symmetry is preserved and only the minimal number of orbitals are used to accommodate the electrons. The basis set is designated as 3G because 3 Gaussian wavefunctions with different values of α (the curve fitting constant) are used to approximate the STO function.

The minimal basis is useful for simple molecules but the limited number of wavefunctions do not describe more complex molecules very accurately. A better option are the split valence basis sets which double the number of wavefunctions associated with the valence orbitals. This is achieved by splitting the orbitals into an inner core (a) and an outer envelope (b) with an area (c) for varying the relative sizes of the orbitals as shown in figure 3.2.

Split valence basis sets are designated as 3-21G, 4-31G and 6-31G this represents the GTO's describing the 1s (3, 4 or 6), 2s, 2p_x etc., (2 or 3) and 2s', 2p_x' (1 in each case) orbitals. Double zeta basis sets are also available which split the core orbitals.

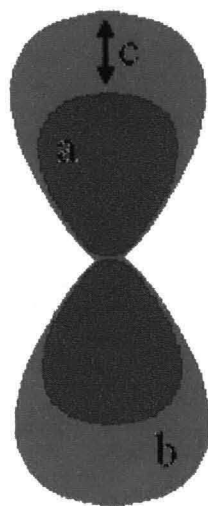


Figure 3.2

Graphical Representation of Split Valence Basis Set

The final basis sets that are generally available are those that feature polarisation. This is achieved by adding d orbital functions into the molecular orbital description for all atoms except for hydrogen. This can be important in the modeling of second row elements. These are recognisable by the addition of an asterisk to the designation, such as 3-21G* and 6-31G*. A further polarisation is available in the 6-31G** basis set

which has a set of p orbital functions that can be applied to add polarisation to the hydrogen atoms.

For calculations on trisilylamine, the number and type of basis sets implemented in a commercial molecular orbital modeling package called SPARTAN from Wavefunction, Inc. is shown in table 3.2 for semi-empirical models and table 3.3 for ab initio models. In each case the shell type is indicated (s, sp, p or d) and the number of each type of shell that makes up the representation of the molecule (e.g. for MNDO there are 13 s shells + 4 p shells = 17 shells). Each shell comprises 1 or more gaussians (up to a maximum of six) and the total number is given in the basis set column. Some models explicitly include d shells (e.g. MNDO/d) represented by either five spherical d orbital functions (5d) or six Cartesian d orbital functions (6d).

Table 3.2

Configuration for Semi-empirical Models

Semi-empirical model	s shells	p shells	5d shells	basis sets	electrons
MNDO	13	4	-	25	26
MNDO/d	13	4	3	40	26
AM1	13	4	-	25	26
PM3	13	4	-	25	26

Table 3.3

Configuration for Ab Initio Models

Ab Initio Models	Shells used in calculation					basis sets	electrons
	s	sp	p	5d	6d		
STO-3G	13	7	-	-	-	41	58
STO-3G*	13	7	-	3	-	56	58
3-21G	22	11	-	-	-	66	58
3-21G*	22	11	-	-	4	90	58
3-21G(*)	22	11	-	-	3	84	58
6-31G	22	11	-	-	-	66	58
6-31G*	22	11	-	-	4	90	58
6-31G**	22	11	9	-	4	117	58

In most applications it is reasonable to assume that the more rigorous the mathematical description of the system implemented in the programme, the more confidence can be placed in the result obtained. In table 3.4 an attempt has been made to assess the various computational methods in terms of their general accuracy of prediction of molecular properties when compared to experimental data. A table has been compiled to compare the performance of the models which have been graded from 1 - 5 with a grade of 1 meaning poor and a grade of 5 meaning excellent.

Table 3.4

Performance of the Computational Models

Computational Model	Equilibrium Geometry	Transition State Geometry	Conformational Energy	Reaction Thermodynamics
molecular mechanics MM2, MM3, etc.	4 - 5	1 - 4	5	1
semi-empirical AM1, PM3	4	1 - 2	1	1 - 4
ab initio - small STO-3G	4	4	1 - 4	4
ab initio - split valence 3-21G*, 6-31G*	4 - 5	4	4 - 5	4 - 5
ab initio - correlated	5	5	4 - 5	5

3.6 SEMI-EMPIRICAL METHODS

Semi-empirical methods are based on the Hartree-Fock SCF method where a matrix is constructed and the integrals calculated to produce molecular wavefunctions. However, computational complexity is reduced via a series of assumptions that increase the speed of the calculation but reduce the quality of the approximation of the wavefunction. The principal assumption is the zero differential overlap (**ZDO**) **approximation** whereby an assumption is made that there is no overlap between different orbitals. The justification for this approach is based on the orthogonalisation of atomic orbitals and leads to a significant reduction in the number of two electron integrals that have to be calculated. Another means of achieving computational simplicity is by considering only the valence electrons directly and utilising a function to account for the core electrons and effects associated with the nucleus.

Further reduction in the computational workload is achieved by replacing as many of the remaining integrals as possible with parameters. These parameters are optimised to provide the best approximation of the molecular properties compared to known experimental data and vary according to the particular semi-empirical model. A set of parameters for the MNDO, MNDO/d, AM1 and PM3 semi-empirical models from the Wavefunction, Inc. Spartan molecular orbital programme can be seen in Appendix 2.

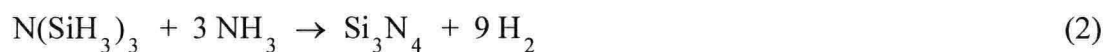
In general, the performance of any semi-empirical model is directly related to how well the parameterisation of the model reproduces the wavefunctions, but on a practical basis even the smallest basis set ab initio model will reproduce molecular structure better than the semi-empirical models. What the semi-empirical models do provide is information, such as heat of formation values for molecules that would be very difficult to obtain by other means. Use can be made use of this information when performing thermodynamic calculations on molecules where experimental information is not available or unstable species where experimental measurements cannot be performed.

4 THERMODYNAMIC CALCULATIONS

To be able to postulate a reaction for the formation of silicon nitride from trisilylamine and ammonia precursors requires that the reaction is initially thermodynamically feasible. The criterion for this is the Gibbs free energy change (ΔG_m°) which is related to the standard molar enthalpy change (ΔH_m°), the standard molar entropy change (ΔS_m°) and the temperature (T) by:

$$\Delta G_m^\circ = \Delta H_m^\circ - T\Delta S_m^\circ \quad (1)$$

For the reaction to be thermodynamically feasible requires that ΔG_m° is both negative and large. The value of ΔG_m° for the analogous formation reaction of silicon nitride from silane and ammonia precursors will also be calculated. The two formation equations can be written as:



This will allow a direct comparison of the thermodynamics of the two reactions from which we can evaluate the potential of the trisilylamine and ammonia reaction for semiconductor applications.

One of the required values is the standard molar enthalpy change (ΔH_m°) which is determined from the relationship:

$$\Delta H_m^\circ = \Delta H_f^\circ(\text{products}) - \Delta H_f^\circ(\text{reactants}) \quad (4)$$

Experimentally determined heat of formation values are available in the literature for all the molecules except for trisilylamine. In this case only values of semi-empirical calculations are available. An average of the two values will be used because there are no available data on the errors associated with the values.

The standard molar entropy change (ΔS_m°) can be obtained from the relationship:

$$\Delta S_m^\circ = S^\circ(\text{products}) - S^\circ(\text{reactants}) \quad (5)$$

and entropy of formation data are available on all products and reactants except trisilylamine.

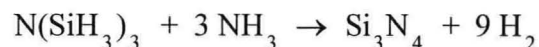
The absence of data requires that the entropy of trisilylamine must be calculated. The method of choice in this work involves calculating the entropy directly from spectroscopic data. As there is no experimental entropy value in the literature for comparison, the method requires verification by applying the calculation to a known substance and comparing the accuracy of the theoretical and measured values. Two methods have been considered to determine the accuracy of the entropy value:

- (a) Apply the calculation to a molecule of similar structure which has a known value of thermal entropy. In this case a suitable molecule is BCl_3 which possesses the identical shape and symmetry point group to the heavy-atom skeleton of trisilylamine and has a very similar molecular weight.
- (b) Use curve-fitted empirical equations to estimate the entropy from plots of M.W versus S° .

In all the above calculations it is implicit that the calculation of thermodynamic properties is for the standard temperature of 298 K.

4.1 STANDARD MOLAR ENTHALPY CHANGE (ΔH_m°) FOR THE FORMATION OF Si_3N_4

This section deals with the calculation of the value of ΔH_m° for the reactions of trisilylamine and ammonia to form silicon nitride (eqn. 2):



Substituting values from appendix 1 into equation (4):

$$\Delta H_m^\circ = \Delta H_f^\circ(\text{products}) - \Delta H_f^\circ(\text{reactants})$$

allows the value of ΔH_m° for the formation of silicon nitride from trisilylamine and ammonia to be obtained. The standard molar enthalpy of formation taken for trisilylamine was the mean of two MNDO calculations (Gmelin, 1989) converted from kcal/mol to kJ mol^{-1} using the factor 4.186

We have therefore:

$$\Delta H_m^\circ = \Delta H_f^\circ(\text{Si}_3\text{N}_4) + 9 \Delta H_f^\circ(\text{H}_2) - 3 \Delta H_f^\circ(\text{NH}_3) - \Delta H_f^\circ[\text{N}(\text{SiH}_3)_3] \quad (6)$$

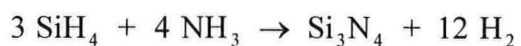
Substituting in the values gives:

$$\begin{aligned} \Delta H_m^\circ &= (-743.5 + 0) - (-137.7 + -131.0) \\ &= -474.8 \text{ kJ mol}^{-1} \end{aligned} \quad (7)$$

In chapter 5 a range of semi-empirical models were used to obtain a value of the standard molar enthalpy of formation (ΔH_f°) for trisilylamine. The value obtained from the mean of all the calculations was $-132.94 \text{ kJ mol}^{-1}$. Inserting this value in equation (6) permits a re-evaluation of the standard molar enthalpy change (ΔH_m°) for the formation of Si_3N_4 . Therefore:

$$\Delta H_m^\circ = (-743.5 + 0) - (-137.7 + -132.94) = -472.86 \text{ kJ mol}^{-1} \quad (8)$$

Repeating the calculation for the silane and ammonia reaction (eqn. 3):



we obtain the result:

$$\Delta H_m^\circ = -662.8 \text{ kJ mol}^{-1} \quad (9)$$

The values of ΔH_m° obtained for the reaction of trisilylamine with ammonia and silane with ammonia are both large and negative and as such indicate that both reactions are strongly exothermic and from the thermodynamic viewpoint would proceed to completion at standard room temperature and pressure.

4.2 STANDARD MOLAR ENTROPY OF FORMATION (S°) FOR TRISILYLAMINE

As no facilities exist at Middlesex University to measure the entropy of trisilylamine, nor is there a value available in the literature, the option considered was to evaluate the entropy from the relationship:

$$S^\circ (\text{spectroscopic}) = S^\circ (\text{translational}) + S^\circ (\text{rotational}) + S^\circ (\text{vibrational}) \quad (10)$$

When attempting to calculate entropy it is clear that the largest contribution, and fortunately the easiest value to determine, is the translational entropy.

4.2.1 Translational Entropy

This is given by the Sackur-Tetrode equation (James, 1976):

$$S^\circ (\text{translational}) = 28.72 \log M + 195.48 \text{ J K}^{-1} \text{ mol}^{-1} \quad (11)$$

where M = molecular weight (kg)

The molecular weight of trisilylamine is $0.10735 \text{ kg mol}^{-1}$ and substitution into equation (8) gives:

$$\begin{aligned} S^\circ (\text{translational}) &= 28.72 \log 0.107352 + 195.48 \\ &= (28.72 \times -0.96919) + 195.48 \\ &= -27.84 + 195.48 \\ &= +167.64 \text{ J K}^{-1} \text{ mol}^{-1} \end{aligned} \quad (12)$$

4.2.2 Rotational Entropy

The rotational entropy of a molecule is dependent on a knowledge of the symmetry of the molecule and the moments of inertia about the major symmetry axes. The most important consideration when determining the rotational contribution is to ensure that the structure and symmetry of the molecule are assigned correctly prior to analysing the moments of inertia and the principal axes. The rotational symmetry number can be

assigned from a knowledge of the point group and a useful table is given in the literature (Herzberg, 1960). In this work we have assigned trisilylamine to the D_{3h} point group (Aylett, 1994) and therefore have used a rotational symmetry number $\sigma = 6$ (obtained from Herzberg) in the evaluation of the rotational entropy. This is the number of indistinguishable positions that a rigid body assumes when subject to rotation about its axes of symmetry. In the case of trisilylamine this is made up of 1 rotation around the C_3 axis and 3 rotations around the C_2 axes. No contribution for excited states is assumed as no odd numbers of electrons are present in the structure. If A, B and C describe the moments of inertia for rotations around the principal axes taken as Cartesian axes, then we can obtain a relationship for a planar polyatomic molecule. In this case there are symmetry operations in only two of the three principal axes given by (Knox, 1971):

$$ABC = I_{xx}I_{yy}(I_{xx} + I_{yy}) \quad (13)$$

where $I_{xx} = 3mr^2$, $I_{yy} = 2m(r\sin 60^\circ)^2$, $r =$ bond length (metres) and $m = M.W$
(kg)

To evaluate the rotational entropy the relationship used is from Knox (Knox, 1971):

$$S^\circ(\text{rotational}) = R \ln \left[\left(\frac{\sqrt{\pi}}{\sigma} \right) * \left(\frac{8\pi^2 kT}{h^2} \right)^{3/2} \sqrt{ABC} \right] \quad (14)$$

where R is the universal gas constant, σ is the rotational symmetry number, h is Planck's constant, k is Boltzmann's constant and T is temperature (K)

Substitution into equation (14) gives :

$$S^\circ(\text{rotational}) = R \ln \left[(0.2954) \times \left(\frac{3.2501 \times 10^{-19}}{4.3907 \times 10^{-67}} \right)^{3/2} \sqrt{ABC} \right]$$

$$= R \ln \left(1.8813 \times 10^{71} \sqrt{ABC} \right)$$

To evaluate the value of \sqrt{ABC} we substitute the following values for trisilylamine:

$$\sigma = 6, m = 31.114 \text{ g mol}^{-1} \text{ and } R_{\text{N-Si}} = 1.738 \times 10^{-10} \text{ m}$$

Therefore:

$$3mr^2 = 3 \times \frac{31.114}{1000} \times \frac{(1.738 \times 10^{-10})^2}{6.022 \times 10^{23}} = 4.6819 \times 10^{-45}$$

$$2m(r \cdot \sin 60)^2 = 2 \times \frac{31.114}{1000} \times \frac{(1.738 \times 10^{-10} \times 0.866)^2}{6.022 \times 10^{23}} = 2.341 \times 10^{-45}$$

$$\begin{aligned} ABC &= 3mr^2 \times 2m(r \sin 60)^2 \times \{3mr^2 + 2m(r \sin 60)^2\} \\ &= 1.096 \times 10^{-89} \{7.0229 \times 10^{-45}\} \\ &= 7.6971 \times 10^{-134} \end{aligned}$$

$$\sqrt{ABC} = \sqrt{7.6971 \times 10^{-134}} = 2.7744 \times 10^{-67}$$

Substitution gives:

$$\begin{aligned} S^\circ (\text{rotational}) &= R \ln(1.8813 \times 10^{71} \times 2.7744 \times 10^{-67}) \\ &= R \ln(5.2195 \times 10^4) \\ &= (8.3143 \times 10.8627) = 90.3161 \\ &= +90.32 \text{ J K}^{-1} \text{ mol}^{-1} \end{aligned} \tag{15}$$

4.2.3 Vibrational Entropy

The vibrational contribution to the entropy can be obtained using the relationship given by Knox:

$$S^\circ (\text{vibrational}) = R \sum [x \cdot e^x \cdot (e^x - 1)^{-1}] - [\ln(e^x - 1)] \tag{16}$$

where $x = \frac{h \cdot \omega \cdot c}{k \cdot t}$ and ω is the vibrational frequency (cm^{-1}), h is Planck's

constant, c is the velocity of light, k is Boltzmann's constant and t is temperature (K)

All observable vibrational frequencies for trisilylamine (Gmelin, 1989) were included in the calculation and the contribution of the bonds to the entropy was evaluated. The results are shown in table 4.1.

Table 4.1

Calculation of the Vibrational Entropy Component of Trisilylamine

Band	ω (cm^{-1})	x	e^x	(e^x-1)	$(e^x-1)^{-1}$	$\ln(e^x-1)$	Sum (Σ)
v_1	2170	10.4724	35,327	35,326	2.8×10^{-5}	10.4724	0.0003
v_7	2166	10.4531	34,652	34,651	2.9×10^{-5}	10.4531	0.0003
v_{12}	2163	10.4386	34,153	34,152	2.9×10^{-5}	10.4386	0.0003
v_{19}	2152	10.3856	32,390	32,389	3.1×10^{-5}	10.3856	0.0003
v_{13}	2146	10.3566	31,464	31,463	3.2×10^{-5}	10.3566	0.0003
v_2	2138	10.3180	31,273	31,272	3.2×10^{-5}	10.3180	0.0003
v_3	1011	4.8791	131.5123	130.5123	0.0077	4.8715	0.0450
v_{14}	997	4.8115	122.9159	121.9159	0.0082	4.8033	0.0477
v_{15}	946	4.5654	96.1010	95.1010	0.0106	4.5549	0.0585
v_8	945	4.5606	95.6409	94.6409	0.0106	4.5501	0.0587
v_{20}	921	4.4448	85.1828	84.1828	0.0119	4.4330	0.0646
v_4	919	4.4351	84.3606	83.3606	0.01200	4.4232	0.0651
v_{16}	898	4.3338	76.2334	75.2334	0.0133	4.3206	0.0708
v_9	748	3.6099	36.9624	36.9624	0.0271	3.5825	0.1278
v_5	697	3.3637	28.8959	27.8959	0.0359	3.3285	0.1558
v_{21}	697	3.3637	28.8959	27.8959	0.0359	3.3285	0.1558
v_{17}	661	3.1900	24.2884	23.2884	0.0429	3.1480	0.1790
v_6	493	2.3792	10.7963	9.7963	0.1021	2.2820	0.3401
v_{10}	312	1.5057	4.5073	3.5073	0.2851	1.2549	0.6801
v_{18}	195	0.9411	2.5628	1.5628	0.6399	0.4465	1.0968

The full list of band assignments are given in table II, page 5050 of Wendel (Wendel et al., 1992) and page 101 of Gmelin (Gmelin, 1989). Evaluating equation (16) gives a value of the vibrational entropy. In this case:

$$S^{\circ} \text{ (vibrational) for trisilylamine} = + 26.17 \text{ J K}^{-1} \text{ mol}^{-1} \quad (17)$$

The substitution of entropy contributions from equations (10), (13) and (15) into equation (8) gives a value for the standard molar entropy of trisilylamine at 298 K:

$$S^{\circ} = 167.64 + 90.32 + 26.17 = 284.13 \text{ J K}^{-1} \text{ mol}^{-1} \quad (18)$$

Substituting the values listed in appendix 1 we can obtain a value for the standard molar entropy change (ΔS°_m) for the formation of Si_3N_4 from the relationship (eqn. 5):

$$\Delta S^{\circ}_m = S^{\circ} \text{ (products)} - S^{\circ} \text{ (reactants)}$$

$$\begin{aligned} \Delta S^{\circ}_m &= 101.3 + 1176.3 - 578.4 - 284.1 \\ &= + 415.1 \text{ J K}^{-1} \text{ mol}^{-1} \end{aligned} \quad (19)$$

For the formation of silicon nitride from the silane and ammonia reaction, evaluation of equation (5) gives a value of:

$$\Delta S^{\circ}_m = + 284.7 \text{ J K}^{-1} \text{ mol}^{-1} \quad (20)$$

It should be noted that the material discussed in this present work applies only to trisilylamine and other species in the gas phase. The positive entropy sign is an indication of a disordered state and upon attachment to a surface a molecule loses one degree of freedom and becomes less disordered. This implies that the entropy value will become less positive and in the limiting case where the molecule is attached to a surface and has lost all its three degrees of freedom the entropy will be at its minimum value.

As this is a theoretical study no account has been taken of the processes that occur in non-equilibrium systems such as in plasma CVD reactors. Where species are condensing onto surfaces there will be a number of factors that need to be taken into account. There are a number of different ways in which absorption onto a surface can

occur and the mechanisms are different in each case. This work does not assume any particular mechanism because the emphasis is on the gas phase reaction and the precursor species. Temperature and pressure will also have an effect on the thermodynamics and kinetics of reaction in CVD systems and for a fully comprehensive study on the deposition using trisilylamine as a precursor at elevated temperature the thermodynamic values would have to be determined as no values are available in the literature for this work. The pressure in this study is assumed to be atmospheric pressure but in a CVD system the partial pressures of the reactants would need to be considered as would the nature of the dilutant and its potential effect on the film growth in a non-equilibrium situation.

4.3 GIBBS FREE ENERGY CHANGE (ΔG_m°) FOR THE FORMATION OF Si_3N_4

The Gibbs free energy change is given by the relationship (eqn. 1):

$$\Delta G_m^\circ = \Delta H_m^\circ - T\Delta S_m^\circ$$

Using the values of $\Delta H_m^\circ = -472.86 \text{ kJ mol}^{-1}$ from equation (8) and $\Delta S_m^\circ = +415.1 \text{ J K}^{-1} \text{ mol}^{-1}$ from equation (19) we can substitute into equation (1) with temperature T equal to 298.15 K. The value of ΔG_m° obtained for the formation of Si_3N_4 from the reaction of trisilylamine and ammonia is:

$$\begin{aligned}\Delta G_m^\circ &= -472.86 - (298.15 \times 0.4151) \\ &= -472.86 - 123.76 \\ &= -596.62 \text{ kJ mol}^{-1}\end{aligned}\tag{21}$$

Repeating the calculation for the silane and ammonia reaction gives the result:

$$\Delta G_m^\circ = -747.7 \text{ kJ mol}^{-1}\tag{22}$$

4.4 THE ACCURACY OF THE STANDARD MOLAR ENTROPY OF FORMATION (S°) CALCULATION FOR TRISILYLAMINE

The boron trichloride molecule was chosen as a reference on which to perform a specimen calculation to determine whether the method used to calculate the standard molar entropy of formation for trisilylamine produced an acceptable value. The following values were assumed when repeating the calculation for BCl_3 :

$$\text{M.W} = 0.11716 \text{ kg mol}^{-1}, \sigma = 6, m = 35.45 \text{ g mol}^{-1}, R_{\text{B-Cl}} = 1.715 \times 10^{-10} \text{ m}$$

For the vibrational entropy the vibrational frequencies $\nu_1 - \nu_4$ (Gmelin, 1978) were used for both the $^{10}\text{B}^{35}\text{Cl}_3$ and $^{11}\text{B}^{35}\text{Cl}_3$ isotopic species. The values obtained for BCl_3 are as follows :

$$S^\circ (\text{translational}) = 168.7 \text{ J K}^{-1} \text{ mol}^{-1} \quad (23)$$

$$S^\circ (\text{rotational}) = 95.63 \text{ J K}^{-1} \text{ mol}^{-1} \quad (24)$$

$$S^\circ (\text{vibrational}) = 26.34 \text{ J K}^{-1} \text{ mol}^{-1} \quad (25)$$

Substituting these values into equation (11) gives an entropy for BCl_3 of:

$$S^\circ = 168.7 + 94.31 + 27.34 = 290.7 \text{ J K}^{-1} \text{ mol}^{-1} \quad (26)$$

which is in excellent agreement with the published value for BCl_3 of $290.1 \text{ J K}^{-1} \text{ mol}^{-1}$ in the Chemical Rubber Handbook (Lide, 1993).

A plot of molecular weight against S° for known polyatomic gaseous molecules provides a curve-fitted equation of sufficient accuracy that a good estimate of the value of S° for an unknown compound can be obtained. For polyatomic molecules with a molecular weight less than 250 a value of S° can be expressed by an empirical curve-fitted equation (Dasent, 1970):

$$S^\circ = 163 + 1.4M - (2.6 \times 10^{-3})M^2 \quad (27)$$

More recently two further curve-fitted equations have been developed dependent on the number of atoms in the molecule (Kubaschewski, 1993). The equation for 4 atoms is:

$$S^{\circ} = -7.53 + 146.44 \log M \quad (28)$$

and for 5 or more atoms:

$$S^{\circ} = -131.8 + 207.11 \log M \quad (29)$$

Equation (28) can be applied to trisilylamine if we assume that the SiH_3 groups are one entity with a mass of 31. This is the approach taken when determining values of mr^2 for the rotational entropy of a gas and allows a direct comparison of the equation with BCl_3 which has 4 atoms in the molecule. Table 4.2 gives a comparison of S° values for trisilylamine and BCl_3 from direct entropy calculation and equations generated from the graphical method.

Table 4.2

Comparison of Entropy Values of TSA and BCl_3

Entropy Equation	TSA	BCl_3
Equation (27) $\text{J K}^{-1} \text{mol}^{-1}$	283.4	291.4
Equation (28) $\text{J K}^{-1} \text{mol}^{-1}$	289.9	295.4
Equation (29) $\text{J K}^{-1} \text{mol}^{-1}$	288.8	293.4
Mean (26) - (28) $\text{J K}^{-1} \text{mol}^{-1}$	287.4	293.4
Equation (10) $\text{J K}^{-1} \text{mol}^{-1}$	284.1	290.7
Literature Value (Lide, 1993)	-	290.1

The results from the mean of the graphical method are within 1% of the literature value for boron trichloride and this agreement gives confidence that, within the limitations of the method, a value of entropy can be obtained for neutral molecules where no value exists in the published literature.

4.5 STANDARD EQUILIBRIUM CONSTANT

The generally held relationship between the standard enthalpy and entropy changes and the equilibrium constant K° is:

$$\log K^\circ(T) = \frac{\Delta S_m^\circ}{2.303R} - \frac{\Delta H_m^\circ}{2.303RT} \quad (30)$$

where R is the gas constant equal to $8.314 \text{ J K}^{-1} \text{ mol}^{-1}$ and $T = 298.15 \text{ K}$

Substituting our calculated values for ΔS_m° and ΔH_m° into the equation we obtain for the reaction of trisilylamine and ammonia to form silicon nitride:

$$\log K^\circ(T) = \frac{412.4}{19.15} - \frac{-474.8 \times 10^3}{5.71 \times 10^3} = 21.54 - (-83.15) = 104.69$$

$$K^\circ(T) = 4.9 \times 10^{104} \quad (31)$$

Repeating the calculation for the reaction of silane and ammonia to form silicon nitride:

$$K^\circ(T) = 8.91 \times 10^{130} \quad (32)$$

5 SEMI-EMPIRICAL CALCULATIONS

The main models available for semi-empirical calculation are MNDO, MNDO/d, AM1 and PM3. Due to the difference in parameterisation of the models it is not possible to say with any degree of certainty that one particular model will be most suitable for this work. To obtain some information on the models and their applicability some test runs will be performed to see what molecules they can handle and how the results compare for each of the models and the degree of reproducibility of each model.

Information available from the semi-empirical programmes includes data on bond length and angle, dipole moment, charge density on atoms, lowest unoccupied molecular orbital (LUMO), highest occupied molecular orbital (HOMO) and electron probability. Some or all of these will be useful in determining the potential for reaction of trisilylamine.

Three different commercially available molecular orbital programmes have been used to determine the standard molar enthalpy of formation for trisilylamine. Due to the limited number of semi-empirical models available there is insufficient data to perform a meaningful statistical analysis (F or t test) of the data. Therefore the standard deviation has been calculated to provide information on the standard deviation from the mean (Z factor) for each data point.

5.1 SOFTWARE

The main software package used in this programme of work was Chem3D Pro from CambridgeSoft Corporation. Chem3D incorporates the MOPAC semi-empirical calculation routines developed by Fujitsu and runs on a PC using the Windows operating system. The majority of the standard molar enthalpy of formation information was obtained using this package.

Additionally two other software packages containing molecular orbital routines were obtained on a time-limited demonstration basis. One was a personal computer (PC) version of Hyperchem 5.1 from Hypercube which was fully functional and obtained on a two week time-limited trial. The other was a fully functional copy of the Spartan molecular orbital software package obtained on a 30 day trial. The Spartan programme was run on an HP 700 UNIX workstation. These additional programmes were useful as they allowed comparisons to be made between the methods implemented in the software.

In all three software packages a graphical user interface (GUI) was provided so that a graphical representation of the molecule could be created rather than having to write a textual input file to represent the molecule. Each package provided a molecular mechanics routine to minimise the energy of the molecule. For Chem3D and Hyperchem 5.1 this was MM2 and for Spartan was SYBIL. The MNDO, AM1 and PM3 semi-empirical models were implemented in all the software packages and additionally Chem3D and Spartan had an implementation of MNDO/d. Two modes of operation were allowed:

- (a) single energy mode where one iteration of the algorithm is used or
- (b) an optimisation of the geometry which requires multiple iterations to converge the calculation below a preset level

For single energy calculations the result is highly dependent on the ability of the model to obtain a good result in one iteration and is therefore a function of the quality of the parameters in the model. For this programme of work it was decided that single energy calculations would not provide sufficient accuracy and would be ignored.

One of the problems with the implementation of semi-empirical models is that the parameterisation is different for different models and may vary for different implementations of the same model. There is no easy way of determining which of the models will perform best in predicting the structure, energy and thermodynamic properties of the molecules. From information in the Chem3D manual the programmes compute the standard molar enthalpy of formation from the relationship:

$$\Delta H_f^\circ = E_{\text{elec}} + E_{\text{nucl}} + E_{\text{isol}} + E_{\text{atom}} \quad (1)$$

where E_{elec} is obtained from the SCF calculation, E_{nucl} is the core-core repulsion and E_{isol} and E_{atom} are parameters supplied by the potential function

defined for the gas phase at 298 K for one mole of a compound from its elements in their standard state. The semi-empirical software used in this investigation originates in the USA and therefore all the energy values are given in units of kcal/mol. In this, and future chapters, all values of energy in kcal/mol have been converted to kJ mol^{-1} using the factor 4.186.

Prior to using the semi-empirical methods on trisilylamine, some calculations were performed on silane and ammonia to investigate the functioning of the models. Each model in the two PC programmes were used to determine the standard molar enthalpy of formation of silane and ammonia and the results are given in table 5.1.

Table 5.1

Values of ΔH_f° for Silane and Ammonia from Energy Minimisation Calculations using Chem3D

	ΔH_f° (kJ mol^{-1})			
	Silane		Ammonia	
	Chem3D	Hyperchem	Chem3D	Hyperchem
MINDO3	+ 33.97	+ 33.95	- 38.18	- 38.22
MNDO	+ 4.96	+ 4.73	- 26.72	- 26.83
MNDO/d	+ 43.53	N/A	- 26.67	N/A
AM1	+ 17.25	+ 17.04	- 30.53	- 30.68
PM3	+ 52.22	+ 51.99	- 12.87	- 12.98
Reference - Lide, 1993	+ 34.37		- 45.96	

It appears that for small, inorganic molecules the ability of the semi-empirical models to obtain a correct minimum convergence point is variable. However, all the models correctly predicted the formation of silane to be endothermic and the formation of ammonia to be exothermic. It is also interesting to note that the oldest of the semi-empirical models MINDO3, which is based on the INDO (Intermediate Neglect of Differential Overlap) integrals of Pople, performed better than the newer models. In this model every atom is represented by eight parameters and every pair of atoms by one parameter. This programme has also been used successfully for calculations of the electronic structure of silicon nitride (Gritsenko et al., 1997).

From the CambridgeSoft analysis of the semi-empirical models one can conclude that, in the absence of empirical data, the MNDO/d, AM1 and PM3 calculations currently represent the best means of obtaining a value for the standard molar enthalpy of formation of trisilylamine. All these models are based on the NDDO (Neglect of Differential Diatomic Overlap) principle with MNDO having seven atomic parameters and one for computing multipole interactions. In contrast AM1 and PM3 are very similar with about fourteen parameters per atom and varying only on their respective choice of parameter.

The analysis in table 5.1 demonstrates that newer models are not necessarily more accurate than older models and that improvements in the formulation of the model may have a detrimental effect in the calculation of wavefunctions for certain molecules. It appears then to be important to run baseline tests on molecules with each of the semi-empirical models prior to extracting thermodynamic, bonding and structural data. This is especially important where the representations of the orbitals (HOMO and LUMO) are to be used to infer information on reactivity and bonding. Parameterisation and atomic data can be seen in Appendix 2.

5.2 STANDARD MOLAR ENTHALPY OF FORMATION (ΔH_f°) FOR TRISILYLAMINE

The trisilylamine molecule was created in each of the GUI screens and saved as a default file after energy minimisation using the MM2 molecular mechanics programme. In each case the minimised molecular structure possessed C_{3v} symmetry with the van der Waals energy dominating the steric energy values. The steric energies obtained were:

Chem3D	- 0.985 kJ mol ⁻¹
Hyperchem 5.1	- 2.127 kJ mol ⁻¹
Spartan	- 3.684 kJ mol ⁻¹

The information about the progress of the calculation is stored as a file. In the case of Hyperchem 5.1 and Chem3D the output files are stored as MS Word readable files. An example is given for Hyperchem 5.1 in Appendix 3.

5.2.1 Standard Molar Enthalpy of Formation

Table 5.2 gives the values for the molar enthalpy of formation for trisilylamine from calculations that involve optimisation of the molecular geometry. The MINDO3 programme was unable to achieve self-consistency and the calculation terminated early. The MINDO3 method was no longer considered for use after this point.

Table 5.2

Values of ΔH_f° for Trisilylamine from Geometric Optimisation Calculations

Semi-empirical model	ΔH_f° for trisilylamine (kJ mol ⁻¹)		
	Hyperchem	Chem3D	Spartan
MNDO	- 245.01	- 250.35	- 244.04
MNDO/d	N/A	- 137.41	- 130.73
AM1	- 127.76	- 127.60	- 127.05
PM3	- 138.01	- 137.54	- 137.38
Reference Values	Livant et al., 1983 -130.31 kJ mol ⁻¹ Cuthbertson et al., 1983 -131.57 kJ mol ⁻¹		

In table 5.2 there are eight results from three different semi-empirical methods implemented in three different software programmes. The standard molar enthalpy of formation of trisilylamine is best calculated from the mean of the eight readings. This was achieved by calculating the standard deviation of the readings, S , from the equation:

$$S = \sqrt{\frac{\sum_{i=1}^N (x_i - \bar{x})^2}{N-1}} \quad (2)$$

where N is the number of readings, x_i are the individual readings and \bar{x} is the mean of the readings

Substituting the results from Table 5.3 into equation (2) gives:

$$\text{Standard deviation } S = \sqrt{\frac{181.48}{7}} = \sqrt{25.93} = 5.092 \quad (3)$$

Table 5.3

Calculation of Standard Deviation of ΔH_f° for Trisilylamine

Number	Mean	Number - Mean	(Number - Mean) ²	Z Score
137.41	132.94	4.47	19.98	0.87
130.73	132.94	2.21	4.88	0.43
127.05	132.94	- 5.89	34.69	- 1.16
127.60	132.94	- 5.34	28.52	- 1.05
127.76	132.94	- 5.18	26.83	- 1.02
138.01	132.94	5.07	25.71	0.99
137.54	132.94	4.60	21.16	0.90
137.38	132.94	4.44	19.71	0.87
Sum = 1063.48			Sum = 181.48	
Mean = 132.94				

We can convert the readings into a distribution by determining the relative standing of each reading in terms of standard deviations from the mean using the Z score equation:

$$Z = \frac{(x_i - \bar{x})}{S} \quad (4)$$

where S is the standard deviation

The Z scores obtained in table 5.3 indicate that the values of ΔH_f° for trisilylamine from geometric optimisation calculations using three different semi-empirical models and three implementations of the models are all around one standard deviation from the mean. However, all three implementations of the AM1 model are above one standard deviation and therefore this model is less applicable to trisilylamine than the others for the determination of ΔH_f° .

As these were results from one run and it was considered important to determine the variation in each semi-empirical programme as well as between them. Five energy minimisation runs were performed using the MNDO/d, AM1 and PM3 programmes with Chem3D starting each time with a new molecule of trisilylamine. By creating the molecules via text input of the chemical formula and moving a different hydrogen atom each time, the starting point of the calculation could be varied to obtain the maximum variation in the standard molar enthalpy of formation. The results of this experiment are given in table 5.4. Analysis of the results showed that there were minimal variations for the MNDO/d model whereas the AM1 model gave a small variation which may be explained by the Z factor calculated in table 5.3.

Table 5.4

Repeatability of ΔH_f° Value for MNDO/d, AM1 and PM3 Semi-empirical Methods from Energy Minimisation Calculations using Chem3D

Semi-empirical model	ΔH_f° for trisilylamine (kJ mol ⁻¹)		
	AM1	MNDO/d	PM3
Run 1	127.60234	137.41244	137.50604
Run 2	128.28713	137.41248	137.53580
Run 3	127.57529	137.41240	137.53044
Run 4	128.28709	137.41248	137.48691
Run 5	127.60255	137.41299	137.53137
Mean	127.87088	137.41256	137.51811

5.2.2 Molecular Geometry and Atomic Charges

Each of the semi-empirical methods provides an output file with the geometric data. The bond angle (degrees) and bond length (nm) data are given in table 5.5.

Table 5.5

Comparison of Bonding Data for Trisilylamine from Energy Minimisation Calculations using Chem3D

	Si - - Si (nm)	Si-N (nm)	Si-H (nm)	∠SiNSi (°)	∠HSiN (°)	∠HSiH (°)	Reference
MNDO/d	0.3121	0.1802	0.1416	120.0	109.8	109.1	this work
AM1	0.2976	0.1718	0.1470	120.0	112.5	106.3	this work
PM3	0.2997	0.1756	0.1501	117.1	111.1	107.3	this work
ED	0.2997	0.1734	0.1485	119.7	108.1	110.8	1
ED	0.2998	0.1736	0.1506	119.4	106.6	112.2	1
ED	0.3005	0.1738	0.154	119.6	N/A	N/A	2
MNDO+d	0.3043	0.1757	0.1443	120.0	109.3	N/A	3
MNDO+d	N/A	0.1758	0.1443	N/A	109.4	N/A	4
References	1 Beagley et al., 1970			3 Cuthbertson et al., 1983			
	2 Hedberg, 1955			4 Livant et al., 1983			

Where more than one bond length or bond angle is involved the mean value has been given in the table. There are two sets of values obtained from electron diffraction experiments by Beagley given in table 5.5. The results highlighted in **bold** text were obtained using a fixed value of 0.1485 nm for the Si-H bond length and are considered by chemists to represent the most accurate experimental results available with which to compare the results obtained from the semi-empirical models.

The MNDO/d model appears to be good at predicting bond angles but poor with bond lengths whereas almost the reverse is true of the AM1 and PM3 models. The performance of the MNDO/d model is not unreasonable as the geometry of the model was close to expectations. What is disappointing is the performance in predicting the bond lengths which were noticeably worse than the AM1 and PM3 models.

The charge on the atoms is an indication of the polarisation and delocalisation effects within the molecule. Table 5.6 gives a comparison of the atomic charges. In all cases the charges on the nitrogen, silicon and hydrogen atoms follow the same sequence:

$$\text{MNDO/d} > \text{AM1} > \text{PM3}$$

Table 5.6

Comparison of Atomic Charge Data for Trisilylamine from Energy Minimisation Calculations using Chem3D

Atom	MNDO/d	AM1	PM3
N(1)	-1.47876	-1.20803	-0.56813
Si(2)	1.79325	1.15038	0.66838
Si(3)	1.79328	1.15204	0.66852
Si(4)	1.79328	1.15448	0.66842
H(5)	-0.43381	-0.23496	-0.14658
H(6)	-0.43322	-0.25258	-0.18125
H(7)	-0.43333	-0.26154	-0.15120
H(8)	-0.43331	-0.23078	-0.15150
H(9)	-0.43383	-0.26263	-0.14656
H(10)	-0.43320	-0.25929	-0.18106
H(11)	-0.43382	-0.23047	-0.14671
H(12)	-0.43320	-0.26409	-0.18118
H(13)	-0.43333	-0.25666	-0.15114

5.2.3 Molecular Structure

The structure of trisilylamine is generated by semi-empirical methods via quantum mechanical techniques and varies with the parameterisation of the model. From the work of Varma (Varma et al., 1963) we know that the dipole moment of trisilylamine is zero as would be expected for a perfectly symmetrical, planar molecule. The magnitude is the dipole moment of the molecule determined by the vector sum of the constituent moments obtained by summation over all nuclei and electrons in the molecule. This can be represented by an equation of the form:

$$\mu = \sum_{i=1}^N e_i (X_i i + Y_i j + Z_i k) \quad (5)$$

where μ is the dipole moment, N is the number of atoms, e_i is the charge of the i^{th} particle and i, j and k are unit vectors

The dipole moments for trisilylamine from semi-empirical models are given in table 5.7.

Table 5.7

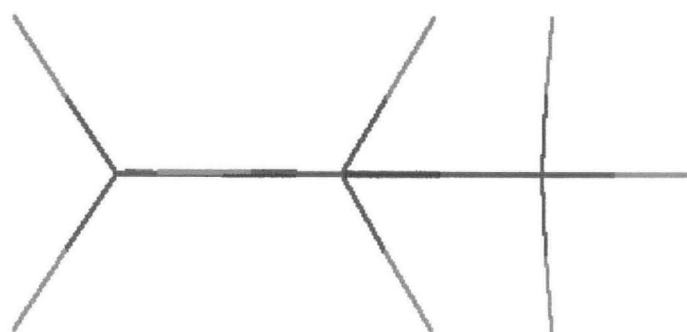
Values of Dipole Moment for Trisilylamine from Energy Minimisation Calculations using Chem3D

Semi-empirical model	Dipole Moment (Debye)			
	X	Y	Z	Magnitude
MNDO/d	0.000	0.003	0.000	0.003
AM1	- 0.179	0.062	- 0.060	0.198
PM3	- 0.062	0.147	0.087	0.181

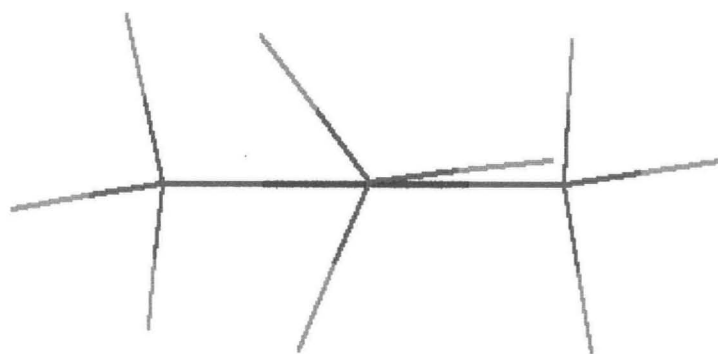
From the results obtained it is evident that the MNDO/d model has managed to optimise the structure of trisilylamine sufficiently well that it has almost, but not quite, produced a planar and symmetrical molecule. From the output file the symmetry point group for the energy minimisation of trisilylamine by MNDO/d and AM1 models is C_s and C_{3v} for geometric optimisation by the PM3 model. In the following figures we can see information available from the semi-empirical programmes. In figure 5.1 by utilising the wire bond models it is possible to take a Newman projection along a bond to see how close the semi-empirical models get to the planar structure of trisilylamine after energy minimisation. Figure 5.2 shows the total charge density surfaces which represent the probability of finding electrons in space and provides the best "shape" for the molecule.

In figures 5.3, 5.4 and 5.5 the highest occupied molecular orbital (HOMO) and lowest unoccupied molecular orbital (LUMO) have been mapped onto the electron density surfaces. This provides a colour-coded visualisation of the distribution of the molecular orbitals over the atoms in the molecule. Areas of highest occupancy are coloured red and lowest occupancy are coloured violet and the mid colour is green. The AM1 and PM3 models show a distinct similarity in the delocalisation of the molecular orbitals mapped onto the total electron distribution surface. Variation in colour is apparent

indicating differences in occupation. In comparison the MNDO/d model shows complete localisation of orbitals and very even occupancy of molecular orbitals. These differences are due to the different algorithm used in the MNDO/d model but which is the most appropriate cannot be decided on calculation alone.



(a) MNDO/d



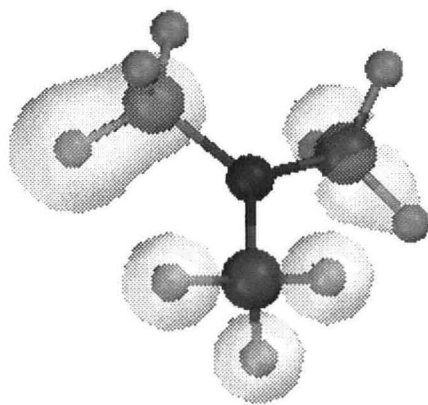
(b) AM1



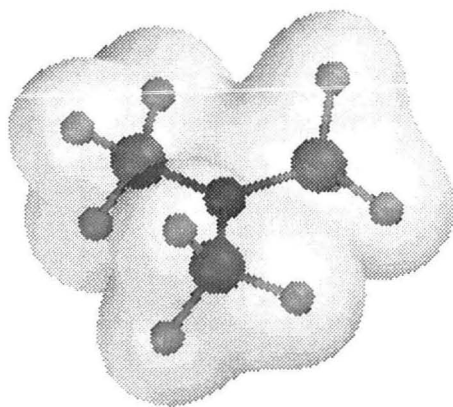
(c) PM3

Figure 5.1

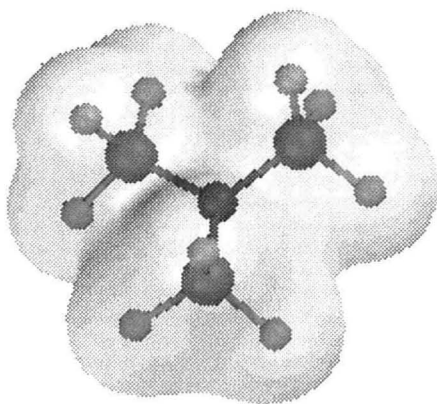
Newman Projection of Trisilylamine from Semi-empirical Models



(a) MNDO/d



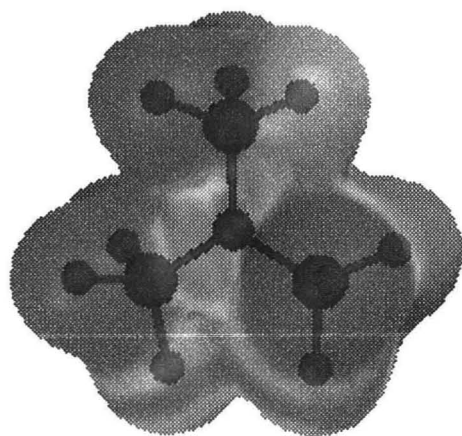
(b) AM1



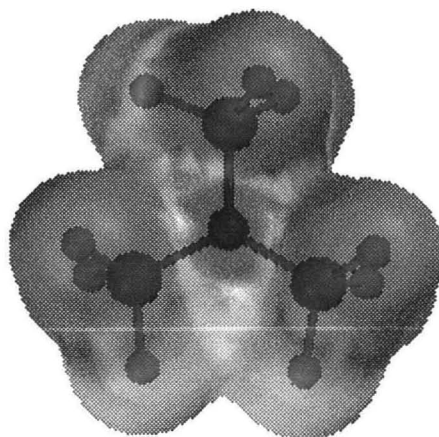
(c) PM3

Figure 5.2

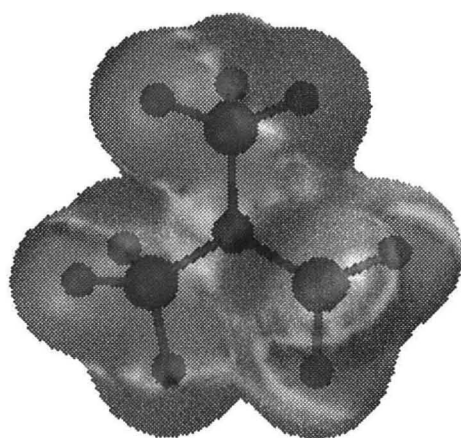
Total Charge Density of Trisilylamine from Various Semi-empirical Models



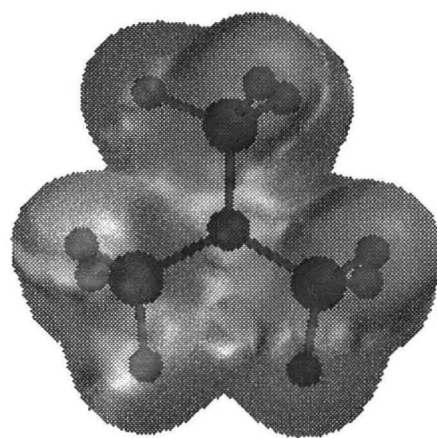
(a) HOMO - top view



(b) HOMO bottom view



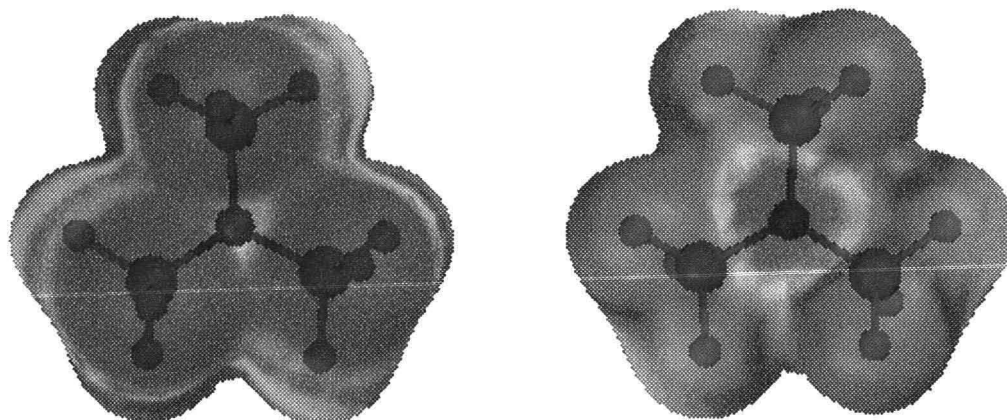
(c) LUMO - top view



(d) LUMO bottom view

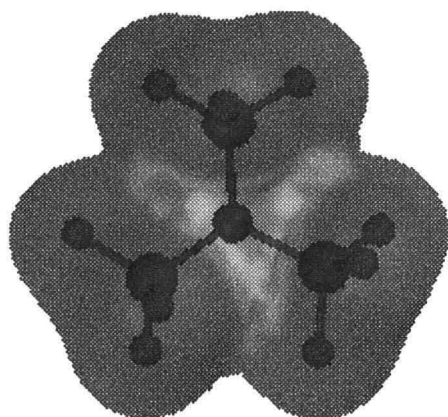
Figure 5.3

HOMO and LUMO of Trisilylamine from AM1 Semi-empirical Model

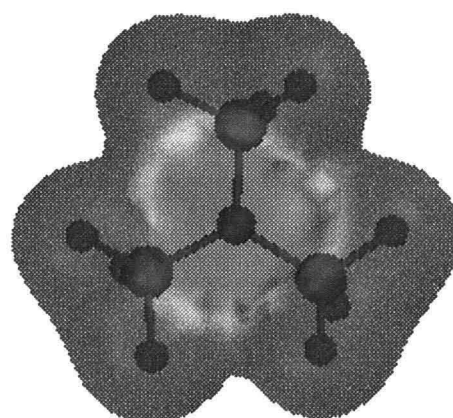


(a) HOMO - top view

(b) HOMO bottom view



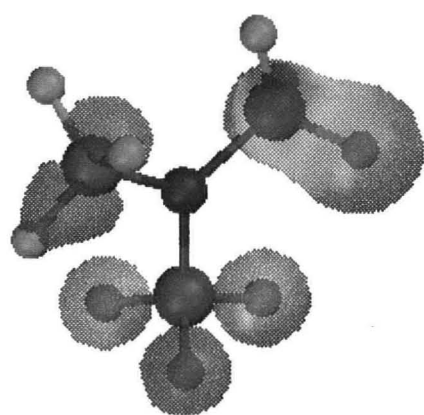
(c) LUMO - top view



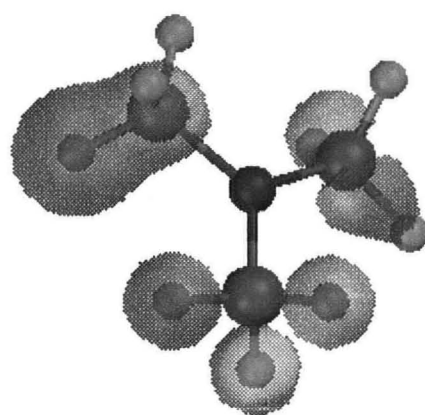
(d) LUMO bottom view

Figure 5.4

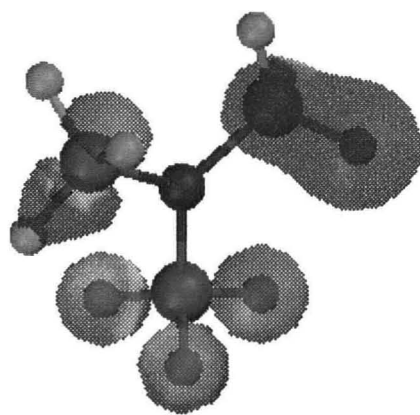
HOMO and LUMO of Trisilylamine from PM3 Semi-empirical Model



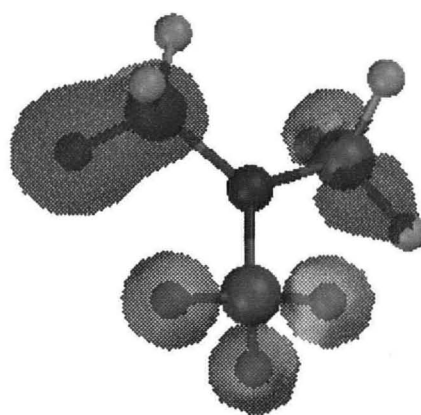
(a) HOMO - top view



(b) HOMO bottom view



(c) LUMO - top view



(d) LUMO bottom view

Figure 5.5

HOMO and LUMO of Trisilylamine from MNDO/d Semi-empirical Model

5.3 THE EFFECT OF HYDROGEN REMOVAL

Molecular orbital programmes allow the investigation of the potential for triaminosilyl radicals to be involved in reaction mechanisms in an analogous way to silyl radicals in silane radical reactions. One possibility is that trisilylamine loses hydrogen atoms and that -NH_2 groups attach onto the silicon atoms from the position where the hydrogen atom was lost. The values of the molar enthalpy of formation for partial dehydrogenation of trisilylamine has been determined and the results are given in table 5.8.

Table 5.8

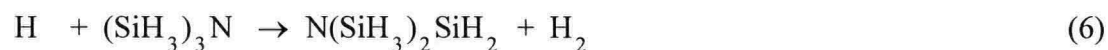
Values of ΔH_f° of Dehydrogenated Trisilylamine from Energy Minimisation

Calculations using Chem3D

	ΔH_f° (kJ mol ⁻¹)		
	MNDO/d	AM1	PM3
$\text{N}(\text{SiH}_3)_3$	- 135.96	- 127.59	- 137.47
$\text{N}(\text{SiH}_3)_2\text{SiH}_2$	- 0.77	- 60.83	- 51.42
$\text{N}(\text{SiH}_3)_2\text{SiH}$	+ 6.28	+ 5.60	- 4.17
$\text{NSiH}_3(\text{SiH}_2)_2$	+ 10.57	+ 7.24	+ 3.24
$\text{N}(\text{SiH}_2)_3$	+ 74.65	+ 25.75	+ 23.75

Of the results obtained there are considerable variations in the values. This is not altogether unexpected because, in general, the algorithms in semi-empirical methods are parameterised with molecules rather than radicals. The $\text{N}(\text{SiH}_3)_2\text{SiH}$ radical species produced a difference in sign for the PM3 model which was unexpected. In order to analyse these differences reference needs to be made to ab initio calculations or empirically determined results which are currently unavailable.

Information can be obtained on the standard molar enthalpy change from the reaction for the formation of $\text{N}(\text{SiH}_3)_2\text{SiH}_2$ via hydrogen extraction with H:



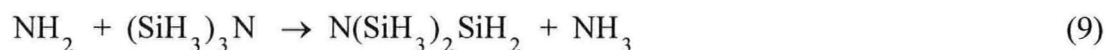
by substituting values from appendix 1 into equation (7):

$$\Delta H_m^\circ = \Delta H_f^\circ(\text{products}) - \Delta H_f^\circ(\text{reactants}) \quad (7)$$

Therefore:

$$\begin{aligned} \Delta H_m^\circ &= \Delta H_f^\circ(\text{N}(\text{SiH}_3)_2\text{SiH}_2) + \Delta H_f^\circ(\text{H}_2) - \Delta H_f^\circ(\text{N}(\text{SiH}_3)_3) + \Delta H_f^\circ(\text{H}) \\ &= (-37.67 + 0) - (+218.0 + -132.94) \\ &= -122.73 \text{ kJ mol}^{-1} \end{aligned} \quad (8)$$

For the formation of $\text{N}(\text{SiH}_3)_2\text{SiH}_2$ via the reaction of NH_2 we can substitute values from appendix 1 into equation (7):



to obtain the standard molar enthalpy change:

$$\begin{aligned} \Delta H_m^\circ &= \Delta H_f^\circ(\text{N}(\text{SiH}_3)_2\text{SiH}_2) + \Delta H_f^\circ(\text{NH}_3) - \Delta H_f^\circ(\text{N}(\text{SiH}_3)_3) + \Delta H_f^\circ(\text{NH}_2) \\ &= (-37.67 + -45.9) - (+109.37 + -132.94) \\ &= -59.97 \text{ kJ mol}^{-1} \end{aligned} \quad (10)$$

What is of interest is that both hydrogen extraction reactions are exothermic.

5.4 AN ESTIMATION OF THE Si-N AND Si-H BOND STRENGTH

With information on the value of ΔH_m° for $(\text{SiH}_3)_3\text{N}$ and $(\text{SiH}_3)_2\text{NSiH}_2$ it is possible to obtain an estimate of the mean bond energy for the Si-N and Si-H bonds (see OU, 1975). The complete dissociation of trisilylamine is given by the equation:



For which the value of ΔH_m° is given by:

$$\Delta H_m^\circ = \Delta H_f^\circ (\text{N}, \text{g}) + 3\Delta H_f^\circ (\text{Si}, \text{g}) + 9\Delta H_f^\circ (\text{H}, \text{g}) - \Delta H_f^\circ ((\text{SiH}_3)_3\text{N}, \text{g})$$

Substituting values from appendix 1 gives a value of ΔH_m° as follows:

$$\begin{aligned} \Delta H_m^\circ &= (472.7 + 1350 + 1962) - (-132.94) \\ &= +3917.64 \text{ kJ mol}^{-1} \end{aligned} \quad (12)$$

If we now repeat the calculation for $\text{N}(\text{SiH}_3)_2\text{SiH}_2$ which is trisilylamine minus one hydrogen atom we can obtain an approximation for the Si-H bond strength. Therefore:



For which the value of ΔH_m° is given by:

$$\Delta H_m^\circ = \Delta H_f^\circ (\text{N}, \text{g}) + 3\Delta H_f^\circ (\text{Si}, \text{g}) + 8\Delta H_f^\circ (\text{H}, \text{g}) - \Delta H_f^\circ (\text{N}(\text{SiH}_3)_2\text{SiH}_2, \text{g})$$

Substituting values from appendix 1 allows us to calculate the value of ΔH_m° for the total dissociation as follows:

$$\begin{aligned} \Delta H_m^\circ &= (472.7 + 1350 + 1744) - (-37.67) \\ &= +3604.37 \text{ kJ mol}^{-1} \end{aligned} \quad (14)$$

We can write ΔH_m° in terms of the mean bond energy $E_m(\text{Si-H})$ as the value of ΔH_m° is directly related to the sum of all the bond energies in the molecule. We have:

$$\Delta H_m^\circ (\text{N}(\text{SiH}_3)_3) = 3 E_m (\text{Si-N}) + 9 E_m (\text{Si-H})$$

$$\Delta H_m^\circ ((\text{SiH}_3)_2\text{NSiH}_2) = 3 E_m (\text{Si-N}) + 8 E_m (\text{Si-H})$$

which gives respectively:

$$3917.64 = 3 E_m (\text{Si-N}) + 9 E_m (\text{Si-H})$$

$$3604.37 = 3 E_m (\text{Si-N}) + 8 E_m (\text{Si-H})$$

On subtracting simultaneous equations the value of $E_m(\text{Si-H})$ is given by:

$$\text{Si-H} = 3917.64 - 3604.37 = 313.27 \text{ kJ mol}^{-1} \quad (15)$$

the mean bond energy $E_m(\text{Si-N})$ can be obtained by calculating the total Si-H bond energy and subtracting this from ΔH_m° and dividing the resultant energy by three. Therefore:

$$3917.64 - 9 E_m (\text{Si-H}) = 3917.64 - 9 (313.27) = 3917.64 - 2819.43 = 1098.21/3$$

$$3604.37 - 8 E_m (\text{Si-H}) = 3604.37 - 8 (313.27) = 3604.37 - 2506.16 = 1098.21/3$$

$$E_m (\text{Si-N}) = \frac{1098.21}{3} = 366.07 \text{ kJ mol}^{-1}$$

If the calculation is repeated for the Si-H bond in silane we have:

$$\Delta H_m^\circ = \Delta H_f^\circ (\text{Si}, \text{g}) + 4\Delta H_f^\circ (\text{H}, \text{g}) - \Delta H_f^\circ ((\text{SiH}_4, \text{g}))$$

Substituting values from Appendix 1 provides a value of ΔH_m° for the total dissociation as follows:

$$\begin{aligned} \Delta H_m^\circ &= (+ 450 + 872) - (+ 34.3) \\ &= + 1287.7 \text{ kJ mol}^{-1} \end{aligned}$$

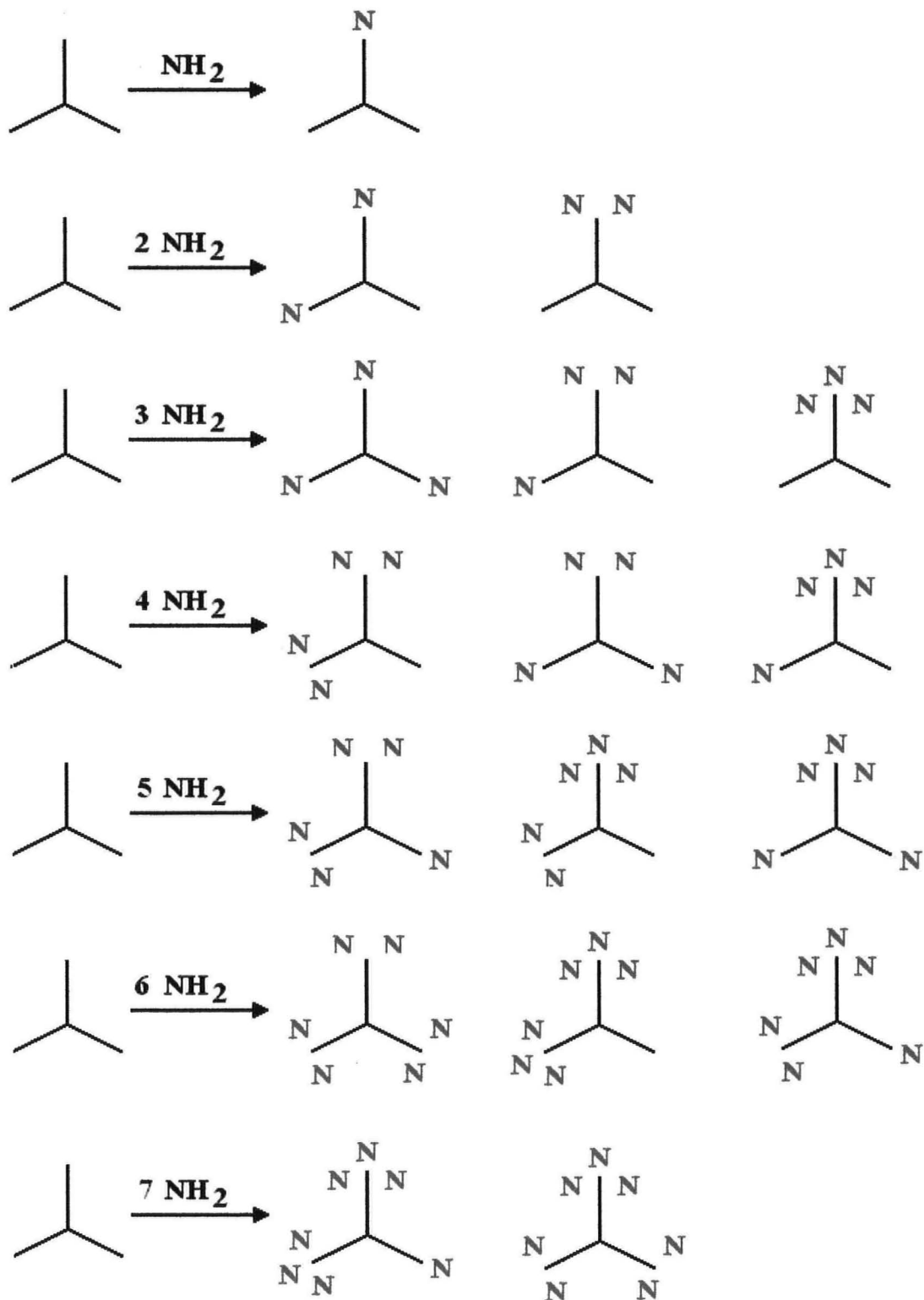
Therefore:

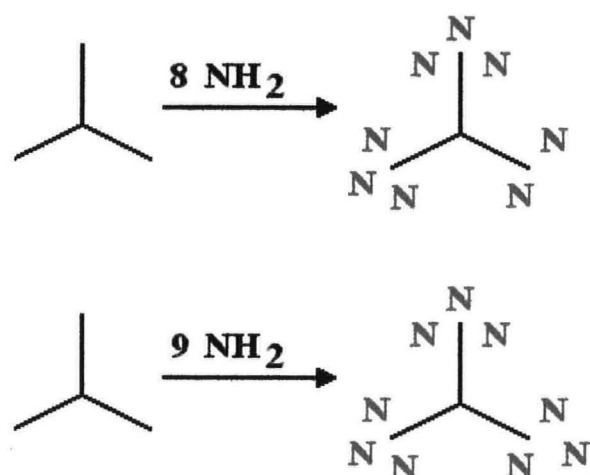
$$E_m(\text{Si-H}) = \frac{1287.7}{4} = 321.9 \text{ kJ mol}^{-1}$$

Similar values are given for the Si-H bond strength in silane of 325.5 kJ mol⁻¹ by Trotman-Dickenson (Trotman-Dickenson, 1973) and 339.1 kJ mol⁻¹ from pyrolysis in Gmelin (Gmelin, 1982).

5.5 THE FORMATION OF AMINOTRISILYLAMINES

The formation of aminotrisilylamines requires that -NH_2 groups will substitute for hydrogen atoms in the trisilylamine structure. There exists the possibility that in a plasma reaction any level of substitution may occur from mono- to nona-substitution. This being the case all molecules that could be formed are shown in figure 5.6.





Key :

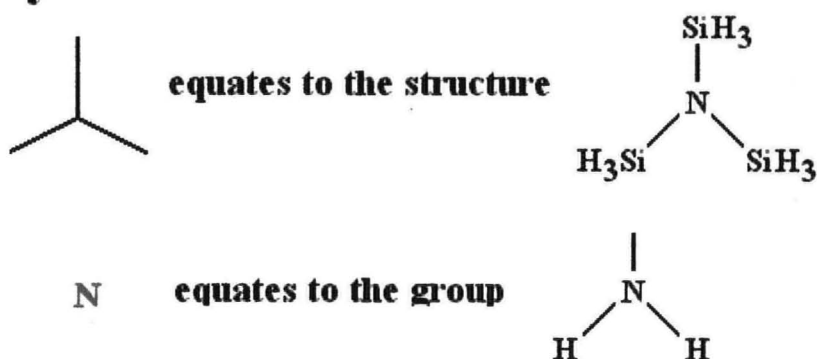


Figure 5.6

Formation of Molecules by Amination of Trisilylamine

The standard molar enthalpy of formation for all the species shown in figure 5.6 has been determined. In view of the anomalous standard molar enthalpy of formation for trisilylamine obtained from the MNDO model, a decision was taken only to use the MNDO/D, AM1 and PM3 molecular orbital models. The results are given in table 5.9. The values given in table 5.9 do not clearly show any trends that might be present in the way that the energy associated with the addition of amino groups is affected by the position of the hydrogen that is being substituted and any amino groups that are already present. The main observation from table 5.9 is that all the standard molar enthalpy of formation values are negative and increase with increasing numbers of Si-N bonds. To show this the data in table 5.9 is presented graphically in figure 5.7.

Table 5.9

Values of ΔH_f° of Substituted Trisilylamines from Energy Minimisation Calculations using Chem3D

ΔH_f° (kJ mol ⁻¹)				
Molecule	Semi-empirical model			Number of Atoms
	MNDO/d	AM1	PM3	
N(SiH₃)₃	- 137.41	- 127.60	- 137.54	13
N(SiH ₃) ₂ SiH ₂ NH ₂	- 205.02	- 238.67	- 231.01	15
N(SiH ₃) ₂ SiH(NH ₂) ₂	- 264.80	- 360.49	- 329.30	17
NSiH ₃ (SiH ₂ NH ₂) ₂	- 270.87	- 348.65	- 324.84	17
N(SiH ₃) ₂ Si(NH ₂) ₃	- 316.41	- 480.99	- 427.09	19
NSiH ₃ SiH ₂ NH ₂ SiH(NH ₂) ₂	- 330.15	- 467.68	- 421.44	19
N(SiH ₂ NH ₂) ₃	- 334.79	- 456.85	- 412.19	19
NSiH ₃ SiH ₂ NH ₂ Si(NH ₂) ₃	- 379.59	- 589.02	- 520.38	21
NSiH ₃ (SiH(NH ₂) ₂) ₂	- 383.35	- 588.62	- 512.48	21
N(SiH ₂ NH ₂) ₂ SiH(NH ₂) ₂	- 389.90	- 576.82	- 507.65	21
NSiH ₂ NH ₂ (SiH(NH ₂) ₂) ₂	- 449.36	- 693.60	- 601.92	23
NSiH ₃ SiH(NH ₂) ₂ Si(NH ₂) ₃	- 434.50	- 710.77	- 615.38	23
N(SiH ₂ NH ₂) ₂ Si(NH ₂) ₃	- 439.51	- 696.78	- 606.92	23
NSiH ₃ (Si(NH ₂) ₃) ₂	- 479.26	- 825.55	- 711.18	25
NSiH ₂ NH ₂ (SiH(NH ₂) ₂ Si(NH ₂) ₃)	- 494.38	- 818.06	- 699.56	25
N(SiH(NH ₂) ₂) ₃	- 500.76	- 814.38	- 703.77	25
NSiH ₂ NH ₂ (Si(NH ₂) ₃) ₂	- 538.21	- 933.96	- 823.17	27
N(SiH(NH ₂) ₂) ₂ Si(NH ₂) ₃	- 546.98	- 933.41	- 798.18	27
NSiH(NH ₂) ₂ (Si(NH ₂) ₃) ₂	- 585.83	- 1052.78	- 898.88	29
N(Si(NH ₂) ₃) ₃	- 624.26	- 1168.70	- 991.34	31

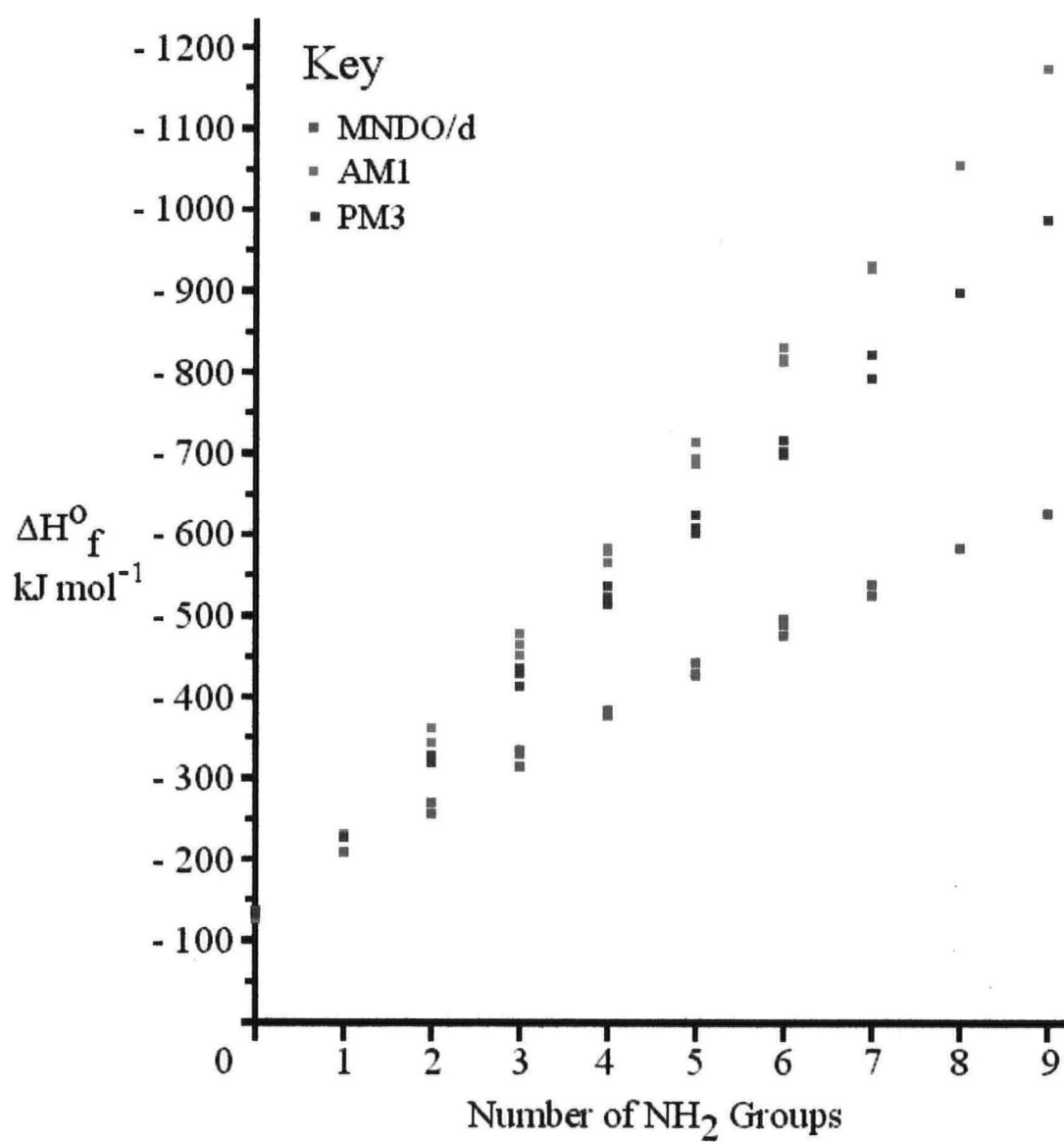


Figure 5.7

Graph of Standard Molar Enthalpy of Formation vs. Number of NH_2 Groups for MNDO/d, AM1 and PM3 Semi-empirical Models

A limited amount of information was obtained from the AM1 and PM3 models in Hyperchem 5.1 and these results are given in table 5.10. A comparison of results obtained from Chem3D and Hyperchem 5.1 are given in table 5.11.

Table 5.10

Values of ΔH_f° for Substituted Trisilylamines from Geometric Optimisation Calculations using Hyperchem 5.1

ΔH_f° for trisilylamine (kJ mol^{-1})			
Molecule	Semi-empirical model		Number of Atoms
	AM1	PM3	
$\text{N}(\text{SiH}_3)_2\text{SiH}_2\text{NH}_2$	- 238.60	- 224.70	15
$\text{N}(\text{SiH}_3)_2\text{SiH}(\text{NH}_2)_2$	- 348.74	- 307.76	17
$\text{NSiH}_3(\text{SiH}_2\text{NH}_2)_2$	- 348.95	- 308.84	17
$\text{N}(\text{SiH}_2\text{NH}_2)_3$	- 457.36	- 403.78	19
$\text{N}(\text{SiH}_3)_2\text{Si}(\text{NH}_2)_3$	- 481.52	- 426.60	19

Table 5.11

Comparison of ΔH_f° Values for Substituted Trisilylamines from Chem3D and Hyperchem 5.1 Semi-empirical Models

Molecule	ΔH_f° (kJ mol^{-1})			
	Chem3D		Hyperchem 5.1	
	AM1	PM3	AM1	PM3
$\text{N}(\text{SiH}_3)_2\text{SiH}_2\text{NH}_2$	- 238.67	- 231.01	- 238.60	- 224.70
$\text{N}(\text{SiH}_3)_2\text{SiH}(\text{NH}_2)_2$	- 360.49	- 329.30	- 348.74	- 307.76
$\text{NSiH}_3(\text{SiH}_2\text{NH}_2)_2$	- 348.65	- 324.84	- 348.95	- 308.84
$\text{N}(\text{SiH}_2\text{NH}_2)_3$	- 456.85	- 412.19	- 457.36	- 403.78
$\text{N}(\text{SiH}_3)_2\text{Si}(\text{NH}_2)_3$	- 480.99	- 427.09	- 481.52	- 426.60

In table 5.12 the values from table 5.9 have been reformulated to show the molecular weight of the molecules and a factor of standard molar enthalpy of formation divided by the molecular weight to normalise the energy. Figure 5.8 illustrates the normalisation

factor for each of the possible aminated trisilylamine molecules shown in figure 5.6 plotted against the number of NH_2 groups.

Table 5.12

Normalisation Factor Derived from Mean Values of ΔH_f° and Molecular Weight for Trisilylamine and Derivatives

Molecule	ΔH_f°	MW	Factor
$\text{N}(\text{SiH}_3)_3$	- 134.18	107.35	1.25
$\text{N}(\text{SiH}_3)_2\text{SiH}_2\text{NH}_2$	- 224.90	122.37	1.84
$\text{N}(\text{SiH}_3)_2\text{SiH}(\text{NH}_2)_2$	- 318.20	137.39	2.32
$\text{NSiH}_3(\text{SiH}_2\text{NH}_2)_2$	- 314.79	137.39	2.29
$\text{N}(\text{SiH}_3)_2\text{Si}(\text{NH}_2)_3$	- 408.16	152.40	2.68
$\text{NSiH}_3\text{SiH}_2\text{NH}_2\text{SiH}(\text{NH}_2)_2$	- 406.42	152.40	2.67
$\text{N}(\text{SiH}_2\text{NH}_2)_3$	- 401.28	152.40	2.63
$\text{NSiH}_3\text{SiH}_2\text{NH}_2\text{Si}(\text{NH}_2)_3$	- 496.33	167.42	2.97
$\text{NSiH}_3(\text{SiH}(\text{NH}_2)_2)_2$	- 494.82	167.42	2.96
$\text{N}(\text{SiH}_2\text{NH}_2)_2\text{SiH}(\text{NH}_2)_2$	- 491.46	167.42	2.94
$\text{NSiH}_3\text{SiH}(\text{NH}_2)_2\text{Si}(\text{NH}_2)_3$	- 586.88	182.44	3.22
$\text{N}(\text{SiH}_2\text{NH}_2)_2\text{Si}(\text{NH}_2)_3$	- 581.07	182.44	3.19
$\text{NSiH}_2\text{NH}_2(\text{SiH}(\text{NH}_2)_2)_2$	- 581.63	182.44	3.19
$\text{NSiH}_2\text{NH}_2(\text{SiH}(\text{NH}_2)_2\text{Si}(\text{NH}_2)_3)$	- 670.67	197.46	3.40
$\text{NSiH}_3(\text{Si}(\text{NH}_2)_3)_2$	- 672.00	197.46	3.40
$\text{N}(\text{SiH}(\text{NH}_2)_2)_3$	- 672.97	197.46	3.41
$\text{NSiH}_2\text{NH}_2(\text{Si}(\text{NH}_2)_3)_2$	- 765.11	212.48	3.60
$\text{N}(\text{SiH}(\text{NH}_2)_2)_2\text{Si}(\text{NH}_2)_3$	- 759.52	212.48	3.58
$\text{NSiH}(\text{NH}_2)_2(\text{Si}(\text{NH}_2)_3)_2$	- 845.83	227.49	3.72
$\text{N}(\text{Si}(\text{NH}_2)_3)_3$	- 928.10	242.51	3.83

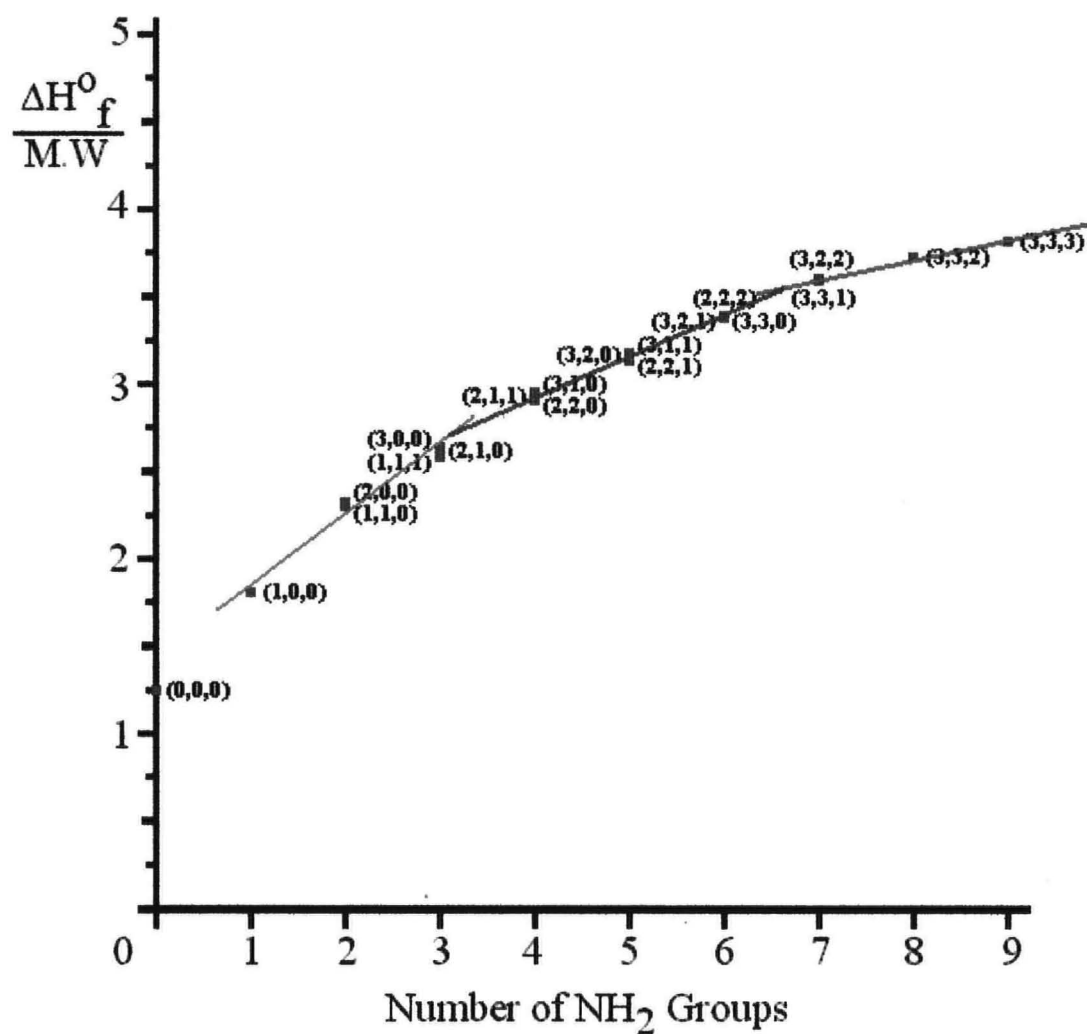


Figure 5.8

Graph of Normalisation Factor vs. Number of NH₂ Groups

6 PLASMA ENHANCED DEPOSITION OF SILICON NITRIDE

In this chapter an attempt will be made to postulate a mechanism for the reaction of trisilylamine and ammonia in a plasma. Available for comparison are the known reactions of silane and ammonia and the conditions of temperature and pressure under which they occur.

There are two initiation reactions that will be considered. One is the initial step in the reaction of silane and ammonia proposed by Tachibane et al:



in which their reaction involves the lone pair of electrons centered on the nitrogen atom of ammonia attacking a silicon atom which is positively polarised.

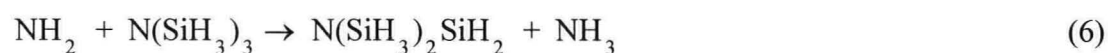
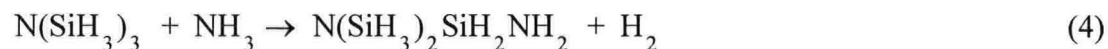
The other initiation process involves the formation and reaction of radical species as suggested by Tachibane (Tachibane et al., 1992):



and Jasinski (Jasinski et al., 1989):



If trisilylamine reacts in the same mechanistic way then we can propose the formation of the respective analogous products:



In the case of energy supplied by a plasma for CVD reactions the most likely occurrence is the formation of neutral, ion and radical species.

From the review of the literature it is evident that most authors consider that under conditions of excess ammonia the reaction of silane and ammonia proceeds via triaminosilane and/or tetraaminosilane species. The deposition of silicon nitride is very dependent on the plasma conditions and especially on the gas phase ratio of silane to ammonia precursors. Unlike silane, trisilylamine is a convenient precursor and therefore it cannot be assumed that the reaction will proceed in an analogous way to that with silane and ammonia. The most appropriate approach therefore is to consider all the possible species that could be formed by the interaction of trisilylamine and ammonia having due consideration to the potential reactions of silane and ammonia.

By using semi-empirical MO methods the standard molar enthalpy of formation of all the reactant species can be determined and from these values can be calculated the value of ΔH_m° . This will provide information on the stability of the species and the exothermic or endothermic nature of the reactions.

From the work of Lucovsky and others it is known that silicon nitride does not contain measurable quantities of Si-Si and N-N bonds, which limits the reactions that can occur. In terms of the structure of trisilylamine and silicon nitride there is evidence in the literature of the structural similarity between planar trisilylamine and crystalline silicon nitride (Lucovsky et al., 1983) and that the planar NSi_3 skeleton in trisilylamine is nearly identical to that of NSi_3 in the framework of α and β -silicon nitride (Julian et al., 1988). It is not unreasonable to suggest therefore that reaction with ammonia to form silicon nitride requires little structural modification from the trisilylamine precursor to the product.

6.1 THE CHARACTERISTICS OF A PLASMA

For PECVD applications, a glow discharge plasma is produced at reduced pressure (i.e. a vacuum) and consists of a highly complex mixture of ions, electrons, radicals and neutrals maintained in a continuous state of generation and recombination. The characteristics of the plasma state are defined by the electron density and electron energy, and various plasmas are shown in figure 6.1.

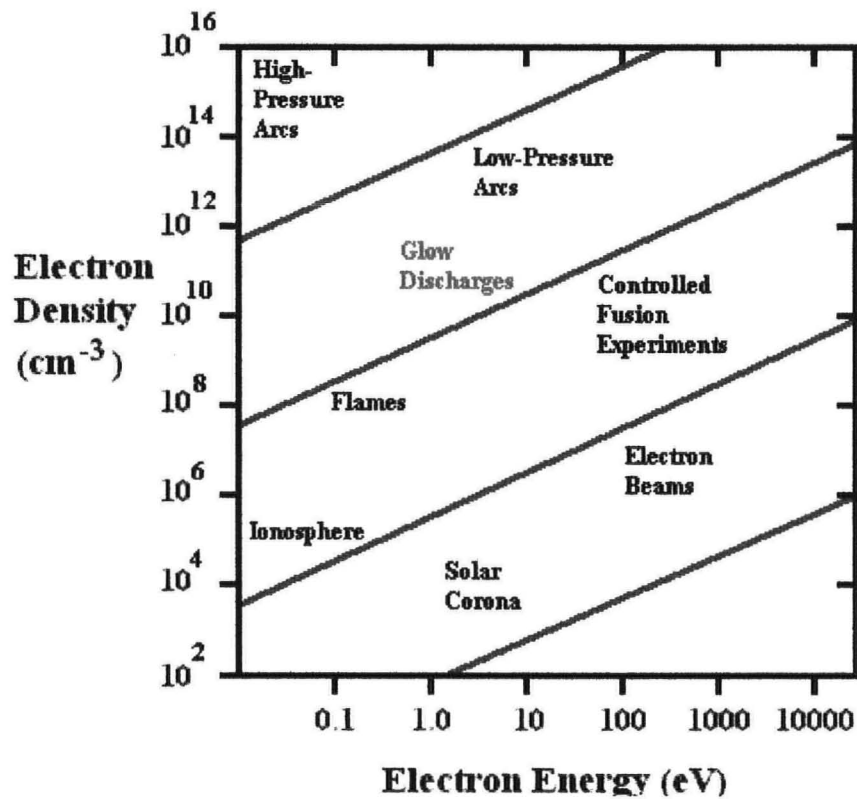


Figure 6.1

Characterisation of a Plasma by Electron Density and Energy
(after Rosler et al, 1976)

In the case of plasma deposition of insulators the plasma is a glow discharge generated by an applied voltage. The application of glow discharges in semiconductor fabrication technology is a technologically mature process.

In PECVD reactors the system chamber is evacuated to a base pressure, then a precursor gas (or mixture of gases) is introduced to increase the pressure to within the operating pressure range for a glow discharge plasma to be initiated and sustained. The plasma is initiated by applying a voltage across horizontal, parallel electrode plates. A typical set-up is shown in figure 6.2.

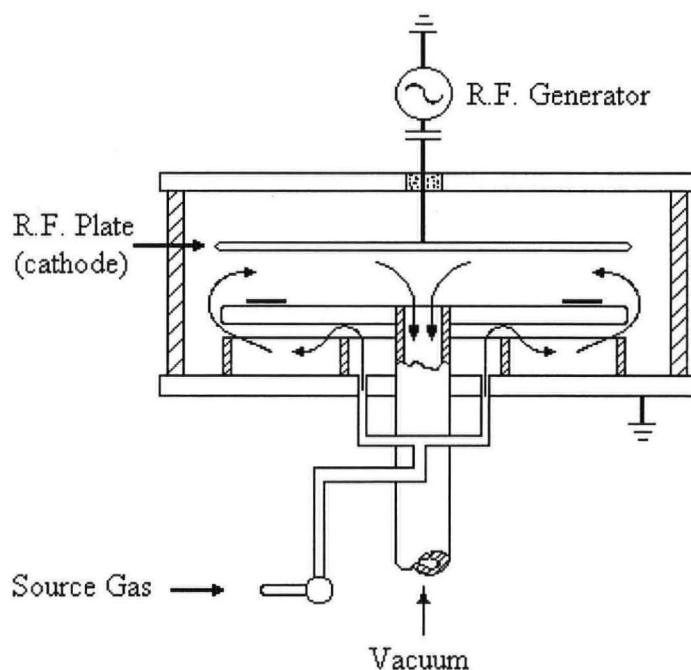


Figure 6.2

Radial Flow Parallel Plate Reactor

(after Bunshah et al, 1982)

The production of reactive species in a plasma occurs via two main processes. These are impact ionisation and impact excitation. In the case of argon:



The external energy source acts on both ions and electrons, but due to the mass difference the much lighter electrons can be accelerated by the field while the heavier ions will have only slightly higher kinetic energy than the neutrals. The acceleration

and inelastic collisions of electrons and neutral atoms produces ions and propagates and multiplies electrons. The avalanche collisions of electrons and neutral atoms continues until a plasma density is achieved concomitant with the applied external field. For this type of plasma the electron density is between $10^9 - 10^{12}/\text{cm}^3$ with electron energies of between 1 - 10 eV. Assuming $1 \text{ eV} \sim 100 \text{ kJ mol}^{-1}$ it is clear that within this energy range almost any chemical bond can be broken by electron impact.

Consider as an example the case of carbon tetrafluoride which dissociates under electron impact to give a pair of radicals:



To maintain the essential neutrality of the plasma the creation processes must be balanced by recombination and relaxation processes forming neutral atoms. In the case of argon:



a quanta of energy is released, the wavelength of which is dependent on the pathway from excited state to ground state. Energy with a wavelength between 4000 and 7000 Å will be in the visible region and responsible for the phenomena known as the "plasma glow" observed in the plasma. A large number of other processes occur in the plasma region with varying degrees of importance.

With a DC voltage the large disparity in mass between electrons and ions will cause problems with an insulator in the system. The consequence of this thousand fold difference in speed is that the electron flux will charge an insulator up to a floating potential, V_f , which is always less than the overall plasma potential, V_p . When fully charged the insulator will begin to repel further incoming electrons and a positively charged sheath will develop around the insulator. This charging effect is not compatible with good film deposition of insulators.

In practice DC power supplies are seldom used to power PECVD systems because the capacitive coupling means the voltage characteristics show a time dependence and the

discharge will extinguish itself every time the voltage at the insulator surface drops below the discharge sustaining voltage. With an AC discharge it has been determined empirically that frequencies above 100 kHz are sufficient to maintain a continuous discharge and the alternating positive and negative charge ensures that no build-up of charge occurs. Most systems use the 13.56 MHz radio frequency (RF) band assigned to commercial users, but lower frequencies and dual frequencies have been utilised to tailor thin film dielectric characteristics. For more information see, for example, the account given by Hess and Graves of plasma-assisted chemical vapour deposition (Hitchman et al., 1993).

6.2 MEAN FREE PATH FOR TRISILYLAMINE

We can estimate a value for the mean free path, λ , of trisilylamine at temperature, T and pressure, p , from the equation:

$$\lambda = \frac{k.T}{\sqrt{2}.p.\pi.d^2} \quad (12)$$

where k is Boltzmann's constant, T is temperature, p is pressure and d is molecular diameter

The molecular diameter of trisilylamine, d , is obtained as the mean of the largest distance across the energy minimised structure measured from each of the four semi-empirical programmes. The actual values provided by MNDO, MNDO/d, AM1 and PM3 were 5.079, 5.266, 5.212 and 5.328 Å respectively and the mean value obtained was 5.2×10^{-8} cm. From equation 12 and using a pressure of 0.5 Torr:

$$\lambda = \frac{1.38 \times 10^{-23} \times 298}{1.414 \times 3.142 \times 0.5 \times (5.2 \times 10^{-8})^2}$$

$$\lambda = \frac{4.11 \times 10^{-21}}{6.01 \times 10^{-15}} = 6.84 \times 10^{-7} \text{ J Torr}^{-1} \text{ cm}^{-2} \quad (13)$$

We require the mean free path to be in centimetres and so we have to multiply by the appropriate factors to remove the energy and pressure terms:

$$\lambda = 6.84 \times 10^{-7} \times \frac{8.206 \times 10^{-2}}{8.31} \times 1000 \times 760 = 5.14 \times 10^{-3} \text{ cm} \quad (14)$$

This method was obtained from a specimen calculation available on the internet at URL <http://mulliken.chem.hope.edu/~polik/Chem345-1997/vacuumtechniques/vacuumtechniques1.htm>

At reduced pressure the mean free path (distance between collisions) and the collision diameter (\sim molecular diameter) are so disparate that bimolecular reactions are not feasible. In a gas phase plasma there are also many reactive ions and radicals in the process of formation and recombination and these are sufficiently energetic that kinetics would favour reaction with these species.

6.3 THERMODYNAMICS OF REACTIONS

Tachibane et al. suggest that the formation of silylamine SiH_3NH_2 is the initiation step in the reaction involving silane and ammonia. Values of ΔH_f° for the three compounds silylamine, triaminosilane and tetraaminosilane have been obtained using Chem3D and the results are given in table 6.1. A value of $-41.67 \text{ kJ mol}^{-1}$ was obtained for the standard molar enthalpy of formation for silylamine as a mean value. This compares favourably with the estimated value from the literature of $-50.23 \text{ kJ mol}^{-1}$ (Gmelin, 1989).

Table 6.1

Values of ΔH_f° for Silylamine, Triaminosilane and Tetraaminosilane from Chem3D

	$\Delta H_f^\circ (\text{kJ mol}^{-1})$		
	MNDO/d	AM1	PM3
SiH_3NH_2	- 28.09	- 22.52	- 74.43
$\text{Si}(\text{NH}_2)_3$	- 43.21	- 254.24	- 140.66
$\text{Si}(\text{NH}_2)_4$	- 224.58	- 441.70	- 316.05

The values of standard molar enthalpy of formation in appendix 1 can be used to determine the standard molar enthalpy change for the overall reaction for the formation of silylamine from silane and ammonia. Taking equation (1):



and inserting values from table 6.1 for the 3 semi-empirical models gives equation 15 (MNDO/d), equation 16 (AM1) and equation 17 (PM3):

$$\begin{aligned} \Delta H_m^\circ &= \Delta H_f^\circ (\text{SiH}_3\text{NH}_2) + \Delta H_f^\circ (\text{H}_2) - \Delta H_f^\circ (\text{SiH}_4) + \Delta H_f^\circ (\text{NH}_3) \\ &= (- 28.09 + 0) - (+ 34.3 + - 45.9) \\ &= - 16.49 \text{ kJ mol}^{-1} \end{aligned} \quad (15)$$

$$\Delta H_m^\circ = \Delta H_f^\circ (\text{SiH}_3\text{NH}_2) + \Delta H_f^\circ (\text{H}_2) - \Delta H_f^\circ (\text{SiH}_4) + \Delta H_f^\circ (\text{NH}_3)$$

$$\begin{aligned}
 &= (-22.52 + 0) - (+34.3 + -45.9) \\
 &= -10.92 \text{ kJ mol}^{-1}
 \end{aligned}
 \tag{16}$$

$$\begin{aligned}
 \Delta H_m^\circ &= \Delta H_f^\circ (\text{SiH}_3\text{NH}_2) + \Delta H_f^\circ (\text{H}_2) - \Delta H_f^\circ (\text{SiH}_4) + \Delta H_f^\circ (\text{NH}_3) \\
 &= (-74.43 + 0) - (+34.3 + -45.9) \\
 &= -62.82 \text{ kJ mol}^{-1}
 \end{aligned}
 \tag{17}$$

Considerable variation exists between the models and therefore care needs to be exercised when using the results from individual models. While the MNDO/d and AM1 results are in reasonable accord the PM3 value is very high in comparison. This result is unexpected because the AM1 and PM3 models have similar algorithms whereas the MNDO/d model is different. Further work would need to be performed to determine the accuracy of the models. Meanwhile taking the mean value which is in reasonable accord with the published value may offer an alternate approach:

$$\begin{aligned}
 \Delta H_m^\circ &= \Delta H_f^\circ (\text{SiH}_3\text{NH}_2) + \Delta H_f^\circ (\text{H}_2) - \Delta H_f^\circ (\text{SiH}_4) + \Delta H_f^\circ (\text{NH}_3) \\
 &= (-41.67 + 0) - (+34.3 + -45.9) \\
 &= -30.07 \text{ kJ mol}^{-1}
 \end{aligned}
 \tag{18}$$

The equivalent reaction for trisilylamine and ammonia shown in equation (4):



results in the formation of $(\text{SiH}_3)_2\text{SiH}_2\text{NH}_2$ and the standard molar enthalpy change for this reaction is:

$$\begin{aligned}
 \Delta H_m^\circ &= \Delta H_f^\circ [(\text{SiH}_3)_2\text{SiH}_2\text{NH}_2] + \Delta H_f^\circ (\text{H}_2) - \Delta H_f^\circ [\text{N}(\text{SiH}_3)_3] + \Delta H_f^\circ (\text{NH}_3) \\
 &= (-224.90 + 0) - (-132.94 + -45.9) \\
 &= -46.06 \text{ kJ mol}^{-1}
 \end{aligned}
 \tag{19}$$

For this reaction the values for the standard molar enthalpy change for both silane and trisilylamine are negative and of the same order of magnitude.

In most of the literature on the low temperature plasma deposition of silicon nitride from silane and ammonia the triaminosilyl radical and the tetraaminosilane species are

considered to be the key intermediates in film formation (see for example Smith et al., 1990a). The standard enthalpy of formation of these two intermediates has been determined using the MNDO/d, AM1 and PM3 routines in Chem3D and the results are given in table 6.1. Both sets of results suggest that formation is an exothermic process. Jasinski et al. suggested from their studies that the reaction of silane and ammonia may be initiated via the formation of a silyl radical in one of two ways:



Calculating the value of ΔH_m° for these reactions gives, for equation (2) and equation (3) gives $-41.33 \text{ kJ mol}^{-1}$ and $+21.4 \text{ kJ mol}^{-1}$ respectively:

$$\begin{aligned} \Delta H_m^\circ &= \Delta H_f^\circ(\text{SiH}_3) + \Delta H_f^\circ(\text{H}_2) - \Delta H_f^\circ(\text{SiH}_4) + \Delta H_f^\circ(\text{H}) \\ &= (+210.97 + 0) - (+34.3 + 218.0) \\ &= -41.33 \text{ kJ mol}^{-1} \end{aligned} \quad (20)$$

$$\begin{aligned} \Delta H_m^\circ &= \Delta H_f^\circ(\text{SiH}_3) + \Delta H_f^\circ(\text{NH}_3) - \Delta H_f^\circ(\text{SiH}_4) + \Delta H_f^\circ(\text{NH}_2) \\ &= (+210.97 + -45.9) - (+34.3 + 109.37) \\ &= +21.4 \text{ kJ mol}^{-1} \end{aligned} \quad (21)$$

Comparing the reactions shows that the standard molar enthalpy change for hydrogen abstraction via ammonia (equation 2) is endothermic whereas the standard molar enthalpy change for hydrogen abstraction by hydrogen (equation 3) is exothermic.

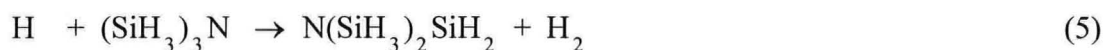
Tachibane (Tachibane et al., 1992) have also suggested that for chemical vapour deposition of silicon nitride the formation of silylamine can be achieved via a radical process involving a two step reaction:



The standard molar enthalpy change for the formation of silylamine is given by:

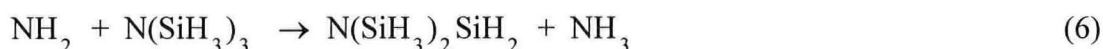
$$\begin{aligned}
 \Delta H_m^\circ &= \Delta H_f^\circ(\text{SiH}_3\text{NH}_2) + \Delta H_f^\circ(\text{H}) - \Delta H_f^\circ(\text{SiH}_3) + \Delta H_f^\circ(\text{NH}_3) \\
 &= (-41.67 + 218.0) - (+210.97 + -45.9) \\
 &= +11.26 \text{ kJ mol}^{-1}
 \end{aligned}
 \tag{23}$$

If we apply the same calculation to trisilylamine we have from Chapter 5, section 5.3 that the standard molar enthalpy change from the formation of $\text{N}(\text{SiH}_3)_2\text{SiH}_2$ via hydrogen extraction with H:



has a value of $\Delta H_m^\circ = -122.73 \text{ kJ mol}^{-1}$. This value is three times larger than the equivalent reaction for silane ($-41.33 \text{ kJ mol}^{-1}$).

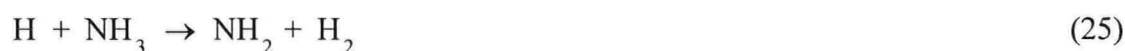
By substituting values from appendix 1 into equation (6):



we can obtain a value for the standard molar enthalpy change for the abstraction of hydrogen from trisilylamine with NH_2 :

$$\begin{aligned}
 \Delta H_m^\circ &= \Delta H_f^\circ[(\text{SiH}_3)_2\text{SiH}_2] + \Delta H_f^\circ(\text{NH}_3) - \Delta H_f^\circ[\text{N}(\text{SiH}_3)_3] + \Delta H_f^\circ(\text{NH}_2) \\
 &= (-37.67 + -45.9) - (-132.94 + 109.37) \\
 &= -60.0 \text{ kJ mol}^{-1}
 \end{aligned}
 \tag{24}$$

In this case the value obtained is negative indicating an exothermic reaction. In the equivalent reaction for silane the value is positive and therefore energy may be required from the plasma for the silane reaction to occur. Hydrogen abstraction from ammonia to form NH_2 is given by the equation:



Evaluation of ΔH_m° for this reaction gives:

$$\begin{aligned}\Delta H_f^\circ &= \Delta H_f^\circ(\text{NH}_2) + \Delta H_f^\circ(\text{H}_2) - \Delta H_f^\circ(\text{H}) + \Delta H_f^\circ(\text{NH}_3) \\ &= (+109.37 + 0) - (+218.0 + -45.9) \\ &= -62.73 \text{ kJ mol}^{-1}\end{aligned}\tag{26}$$

6.4 INITIATION OF THE PLASMA REACTION

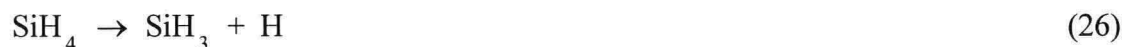
When power is applied to the parallel electrodes of the plasma deposition rig, the gas between the electrodes will be subjected to a sufficiently large input of energy that the molecules form a gas plasma. There are various reactions that occur but in general the rate at which dissociation occurs is related to the input energy and the energy of the bonds that are ruptured. In the case of silane and ammonia it is well documented that silane dissociates before ammonia because the silane Si-H bond is weaker than the ammonia N-H bond. In this case an assumption can be made that the plasma energy is sufficient to rupture the weakest bonds in the trisilylamine and ammonia system and produce radical species. From the work presented in section 5.4 we know that the Si-H bond is around 45 kJ mol^{-1} weaker than the Si-N bond and therefore the most likely reaction is:



The standard molar enthalpy change for trisilylamine is given by:

$$\begin{aligned} \Delta H_m^\circ &= \Delta H_f^\circ(\text{N}(\text{SiH}_3)_2\text{SiH}_2) + \Delta H_f^\circ(\text{H}) - \Delta H_f^\circ(\text{N}(\text{SiH}_3)_3) \\ &= (-37.67 + 218.0) - (-132.94) \\ &= +313.27 \text{ kJ mol}^{-1} \end{aligned} \quad (25)$$

and for silane:



$$\begin{aligned} \Delta H_m^\circ &= \Delta H_f^\circ(\text{SiH}_3) + \Delta H_f^\circ(\text{H}) - \Delta H_f^\circ(\text{SiH}_4) \\ &= (+210.97 + 218.0) - (+34.3) \\ &= +394.67 \text{ kJ mol}^{-1} \end{aligned} \quad (27)$$

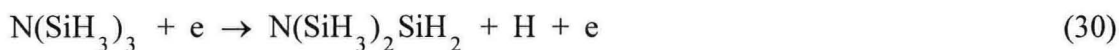
If we perform the same calculation for the ammonia reaction:



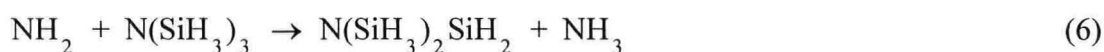
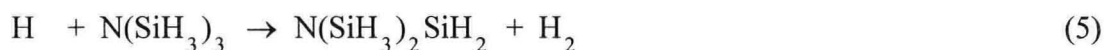
$$\begin{aligned} \Delta H_m^\circ &= \Delta H_f^\circ(\text{NH}_2) + \Delta H_f^\circ(\text{H}) - \Delta H_f^\circ(\text{NH}_3) \\ &= (+109.37 + 218.0) - (-45.9) \\ &= +373.27 \text{ kJ mol}^{-1} \end{aligned} \quad (29)$$

These dissociation reactions are very endothermic and can be induced thermally at elevated temperatures, however due to the applied RF voltage there is sufficient energy in a glow discharge for these reactions to occur at low temperatures. From figure 6.1 the typical energy values in a glow discharge plasma range from 1 - 10 eV, which is equivalent to 96.5 - 965 kJ mol⁻¹.

In this case the most abundant neutral molecules in the plasma are trisilylamine and ammonia molecules and therefore we can postulate that initiation of the reaction involves electron impact:



Only a very small fraction of a plasma consists of reactive species and therefore the most likely event for a radical is that it will collide with a neutral molecule. There are a number of possible reactions involving hydrogen abstraction and regeneration of radical species, e.g.:



For the deposition of silicon nitride films the important reactions are:



For the deposition of silicon nitride films from trisilylamine and ammonia the work of Jasinski suggests that, in an analogous way to silane and ammonia, most of the lower aminotrisilylamine compounds would be formed initially in the plasma. It is evident from the mass spectral work of Brooks (Brooks et al., 1988) that only a limited number of these compounds would have the required stability that their concentration and residence time in the plasma would be sufficient for reaction to occur.

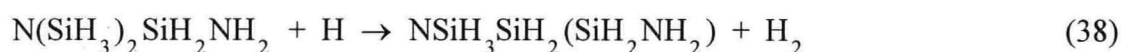
In the case of silane and ammonia Brooks suggests that these compounds are triaminosilane and tetraaminosilane, both of which have negative values of standard molar enthalpy of formation. One cannot rely entirely on the thermodynamic properties of the compounds, as the kinetic effects are not be accounted for. However, comparison of the ΔH_f° values from, for example, the PM3 semi-empirical model for triaminotrisilylamine (- 412.19 kJ mol⁻¹) with triaminosilane (- 140.66 kJ mol⁻¹) and tetraaminotrisilylamine (- 512.48 kJ mol⁻¹) with tetraaminosilane (- 316.05 kJ mol⁻¹) shows comparable values for the standard molar enthalpy of formation and therefore the potential exists for using the ΔH_f° value to assess the potential stability of species in plasma reactions.

6.5 PROPAGATION REACTIONS

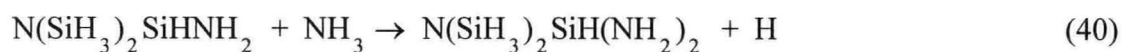
By a continual process of radical formation the reaction can be propagated leading to the formation of higher molecular weight species. If we consider the molecule $N(\text{SiH}_3)_2\text{SiH}_2\text{NH}_2$ there are a number of options for reaction. The molecule can lose hydrogen from an aminosilyl group, from one of the two remaining silyl groups or from the NH_2 group, either by dissociation in the plasma by electron impact:



or by hydrogen abstraction reactions via interaction with either H or NH_2 :



In equation (40) we can see how a radical species can be created by the loss of hydrogen from a Si-H bond followed by reaction with a neutral ammonia molecule to add another NH_2 group:



A representation of the molecule $N(\text{SiH}_3)_2\text{SiH}(\text{NH}_2)_2$ can be seen in figure 6.3.

Where the radical species has been created by the loss of hydrogen from a N-H bond a reaction can occur with neutral trisilylamine:



This process adds considerably to the molecular weight and size of the product and a representation of the molecule $N(\text{SiH}_3)_2\text{SiH}_2\text{NHSiH}_2(\text{SiH}_3)_2\text{N}$ can be seen in figure 6.4.

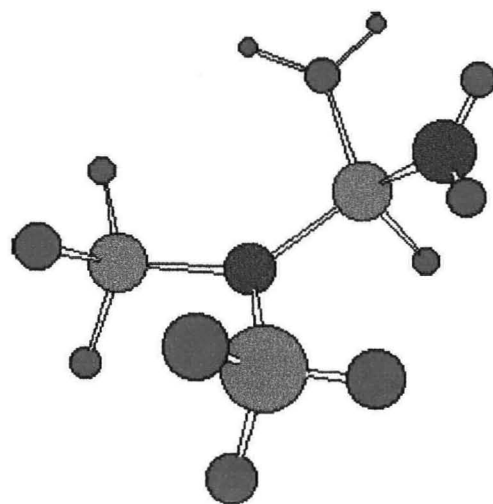


Figure 6.3

Structure of $N(SiH_3)_2SiH(NH_2)_2$ from PM3 Semi-empirical Model

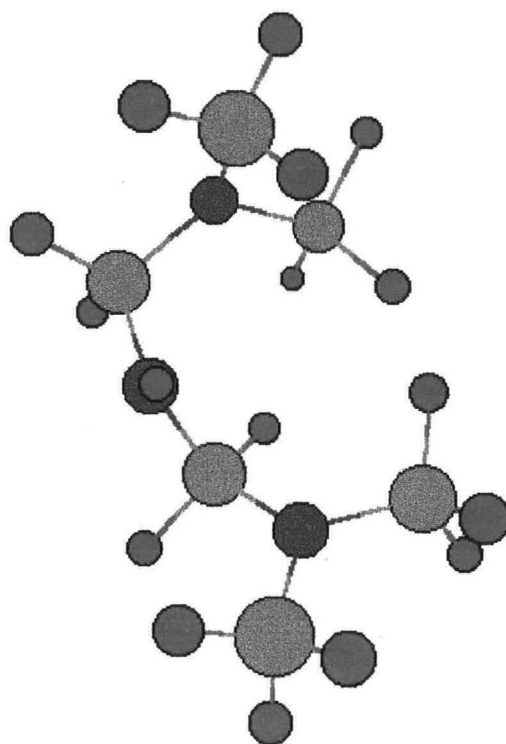


Figure 6.4

Structure of $N(SiH_3)_2SiH_2NHSiH_2(SiH_3)_2N$ from PM3 Semi-empirical Model

By a continual process of radical formation by the loss of hydrogen from Si-H and N-H groups and the reaction of the subsequently formed radicals with neutral ammonia or trisilylamine a series of higher molecular weight species can be generated which will incorporate into a growing solid film with the general stoichiometry of $\text{Si}_x\text{N}_y\text{H}_z$.

6.6 TERMINATION REACTIONS

Termination of radical reactions can be by annihilation of two radical species either directly as in equation (42) or by reaction with a third body which in this case includes all the internal surfaces of the PECVD reaction chamber (denoted as M) as shown in equation (43).



The annihilation reaction of two extremely unstable and reactive species is a highly exothermic event. For example, if we look at the following reactions from section 6.4:



the reverse of these equations is the formation of trisilylamine, silane and ammonia from the respective radical species and the standard molar enthalpy of formation is also the reverse being $\Delta H_m^\circ = - 313.27, - 394.67$ and $- 373.27 \text{ kJ mol}^{-1}$ respectively.

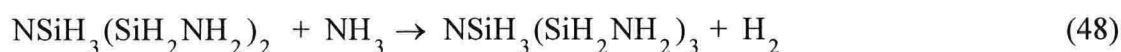
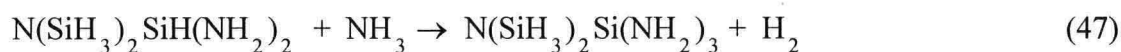
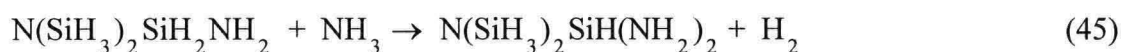
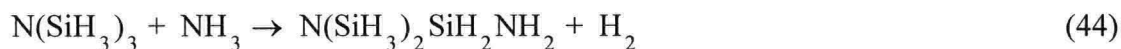
However, the proportion of radical species in the chamber is minute in comparison to the quantity of neutral species the probability of termination process by a radical-radical reaction is remote. The most likely termination reaction therefore is the interaction with the inside of the deposition chamber.

The rate of reaction is dependent on applied temperature as well as applied RF energy and the platen on which the substrates are situated can be heated and thermostatically controlled. The rate of film growth on the substrates and platen will be considerably higher than elsewhere inside the chamber. The ideal situation is that the film growth should occur only on the substrates and platen as the de-lamination of films built up on the vertical walls of the deposition chamber can lead to particulate contamination of the growing films. In many deposition systems the facility to cool the vertical chamber walls can lead to a reduction in unwanted film deposition and particulation.

6.7 THE USE OF ΔH_m° IN PLACE OF ΔG_m° IN REACTION ANALYSIS

In the reaction analysis carried out so far the values for the standard molar enthalpy change have been calculated to compare and investigate the potential reactions. This has been necessary due to the lack of availability in the literature of standard molar enthalpy values, structural information or other thermodynamic data on aminated trisilylamine compounds that would have facilitated the determination of the Gibbs free energy change. It is generally the case that the sign and magnitude of ΔH_m° is reflected in the value of ΔG_m° . Some experimental results were used to check the validity of this assertion as applied to the case of trisilylamine.

A search was conducted on the NIST WebBook internet page to determine whether an analogous compound could be found to provide entropy change information. Unfortunately the information available was sufficiently limited to be unusable in these cases. Therefore the entropy was calculated using the equations of entropy versus molecular weight developed by Kubaschewski and introduced in chapter 5. Using this data applied to some standard reaction equations allows the correlation between the standard molar enthalpy change and the Gibbs free energy change to be tested. Using the following reaction equations:



and taking values of ΔH_f° from appendix 1 we can obtain values for ΔH_m° . The results of these calculations are given in table 6.2.

From the experience with the entropy of trisilylamine and BCl_3 there is no one entropy versus molecular weight equation that is best for all molecules therefore an average of the three equations was used (see table 4.2 in chapter 4).

Table 6.2

Values of ΔH_m° for Substituted Trisilylamines Using AM1 and PM3 Models

	ΔH_m° (kJ mol ⁻¹)	
	AM1	PM3
Equation (44)	- 64.9	- 40.7
Equation (45)	- 63.2	- 37.1
Equation (46)	- 64.3	- 38.2
Equation (47)	- 87.7	- 72.8
Equation (48)	- 63.9	- 48.9

The equations are given below:

$$S^\circ = 163 + 1.4M - (2.6 \times 10^{-3})M^2 \quad (49)$$

$$S^\circ = - 7.53 + 146.44 \log M \quad (50)$$

$$S^\circ = - 131.8 + 207.11 \log M \quad (51)$$

and the results of the calculation are given in table 6.3.

Table 6.3

Values of S° for Substituted Trisilylamines from Entropy vs. Molecular Weight Equations

Reaction Species	S° (J K ⁻¹ mol ⁻¹)			
	Equation 49	Equation 50	Equation 51	Average
$N(SiH_3)_2SiH_2NH_2$	295.39	298.19	300.58	298.05
$N(SiH_3)_2SiH(NH_2)_2$	306.27	305.55	310.99	307.6
$NSiH_3(SiH_2NH_2)_2$	306.27	305.55	310.99	307.6
$N(SiH_3)_2Si(NH_2)_3$	315.97	312.15	320.32	316.15
$N(SiH_2NH_2)_3$	315.97	312.15	320.32	316.15

Substituting the values into the equation:

$$\Delta S_m^\circ = S^\circ(\text{products}) - S^\circ(\text{reactants}) \quad (50)$$

we can obtain the standard molar entropy change (ΔS_m°) for the reaction species and the results of the calculations are given in table 6.4.

To ensure equivalence, the entropy value used for trisilylamine is that obtained in chapter 4 for the average of the three entropy vs. MW equations ($287.4 \text{ J K}^{-1} \text{ mol}^{-1}$) and not the value calculated from the spectroscopic entropy ($286.8 \text{ J K}^{-1} \text{ mol}^{-1}$).

Table 6.4

Values of ΔS_m° for Substituted Trisilylamines

Reaction Products	$\Delta S_m^\circ (\text{J K}^{-1} \text{ mol}^{-1})$
Equation (44)	- 51.45
Equation (45)	- 52.55
Equation (46)	- 52.55
Equation (47)	- 53.55
Equation (48)	- 53.55

As we have seen from chapter 4 the standard molar enthalpy change (ΔH_m°) for the formation of products from reactants is given by:

$$\Delta G_m^\circ = \Delta H_m^\circ - T\Delta S_m^\circ \quad (47)$$

Substituting into this equation and setting T equal to 298.15 K, values of ΔG_m° obtained for the formation of substituted trisilylamines are given in table 6.5.

From table 6.5 we can see that all the reactions are thermodynamically feasible. The trends in the standard molar enthalpy results given in table 6.2 are reflected in the Gibbs free energy change values in table 6.5 because there is little apparent difference in the values of the standard molar entropy change given in table 6.4.

Table 6.5

Values of ΔG_m° for Substituted Trisilylamines Using AM1 and PM3 Models

	ΔG_m° (kJ mol ⁻¹)	
	AM1	PM3
Equation (44)	- 49.57	- 25.37
Equation (45)	- 47.54	- 21.44
Equation (46)	- 48.64	- 22.54
Equation (47)	- 71.74	- 56.84
Equation (48)	- 47.94	- 32.94

7 DISCUSSION

An extensive review of the literature has been undertaken to determine what information is currently available related to the physical properties and reactions of trisilylamine. Extensive use was made of the BIDS and Compendex on-line database searches and the facilities of the reading room at the Science Reference Library in London. The most useful source of accumulated information on trisilylamine is the Gmelin Handbook of Inorganic Chemistry.

What emerged was rather limited in breadth and depth and it can only be concluded that this was due to the absence of significant amounts of information from commercial applications of trisilylamine. Clearly, from the semiconductor industry viewpoint, the succession of patents taken out relating to the deposition of silicon nitride by glow discharge methods with trisilylamine as a precursor, demonstrates that the potential of the material has been identified but this has not, as yet, been translated into practice. This is not really surprising given the maturity of silane based chemistries and the reluctance of manufacturers to alter processes that have run successfully over long time periods with high product yield.

The literature review reveals a considerable amount of activity in finding a replacement for silane in silicon nitride deposition. In three decades the complexity of the precursors under investigation has increased from simple inorganic silanes like SiBr_4 (proposed in 1969 by Androshuk et al. and Aboaf) to organosilane compounds such as $\text{Si}[\text{N}(\text{CH}_3)_2]_4$ (proposed by Hoffman et al. in 1995). There is still much to be said for the principle of simplicity and in this respect trisilylamine has many virtues. In common with the current trends for semiconductor precursors, trisilylamine is liquid at room temperature and stable under inert conditions. The analysis of the elemental composition of precursors given in Chapter 2, table 2.6 indicates that only trisilylamine and disilazane have similar silicon and hydrogen composition to silane and, with additional nitrogen, the potential exists for the reaction with ammonia to form silicon nitride in an analogous fashion to silane and ammonia without incorporating extraneous atoms into the film.

Comparisons have been drawn in the literature review to other precursors used for silicon nitride deposition. From Chapter 2, table 2.4 we can see that the heat of formation of trisilylamine is negative in comparison to silane or its higher homologues which all have positive values. In the case of the silane series, increasing molecular weight does not lead to an increase in stability. Trisilane and trisilylamine have

comparable boiling point, melting point and molecular weight, yet in terms of the heat of formation trisilylamine is some $238.6 \text{ kJ mol}^{-1}$ (57 kcal/mol) more stable than trisilane.

In the vapour phase silane, in common with most gaseous or volatile silanes, reacts spontaneously with oxygen and/or water vapour to form silicon dioxide. What sets silane apart is the fact that it is a pyrophoric gas and has been known to be detonatable. This clearly leads to severe handling and operational difficulties both in manufacturing and research and there have been innumerable cases of silane fires and explosions recorded in semiconductor and related laboratories. In the case of trisilylamine the risk is considerably reduced as we are dealing with vapour from a liquid rather than a pressurised gas from a cylinder.

The liquid precursor trichlorosilane has been used over many years for the LPCVD deposition of silicon nitride and from the information given in Chapter 2, table 2.5 the precursor is categorised as flammable and corrosive. Trisilylamine has a boiling point of 52°C , higher than that of trichlorosilane and almost identical to trisilane (52.9°C) whereas, in comparison, silane has a very low boiling point at -110°C . The enthalpy of formation of both trisilylamine and trichlorosilane is negative while that of silane is positive. This positive value indicates that silane is very reactive and less stable than its decomposition products whereas the reverse is true for the other two precursors. Finally, the critical temperature of both trichlorosilane and trisilylamine exceeds 200°C whereas that of silane is below 0°C . Having used trichlorosilane in semiconductor production for many years it is unlikely that handling a liquid precursor such as trisilylamine would cause significant additional problems.

To change the precursor in a fabrication process often requires a very substantial change to the equipment and the deposition conditions and such a change will be driven by forces encompassing changes in technology, market or external regulation. In the case of most gaseous precursors (e.g. arsine, diborane, phosphine, etc.) the change to organometallic liquid precursors, for deposition and ion implantation applications, has been on the grounds of safety and this situation also applies to the need to find a replacement precursor for silane. This has been effectively achieved for silicon dioxide deposition with TEOS but the commercial acceptance of TEOS has taken over a decade. At this moment in time none of the precursors that have been proposed for glow discharge deposition of silicon nitride has achieved any form of acceptability.

7.1 SEMI-EMPIRICAL MODELLING

Over the course of the research access was obtained to three different molecular orbital programmes - Spartan, Hyperchem 5.1 and Chem3D all of which had semi-empirical routines available for structural and thermodynamic calculations on molecules. Spartan was the earliest programme obtained on a 30 day trial and due to the long time spent learning to use the programme running under UNIX not a large amount of information was obtained. Hyperchem 5.1 and Chem3D both ran under a Windows environment and therefore were more intuitive for PC users.

7.1.1 Limitations of the Models

It is evident from Chapter 3, table 3.4 that all the models are able to predict the equilibrium geometry with some degree of accuracy. In general the ab initio models are far better at predicting across the range of properties than the other models. There are some exceptions to this rule; this is the case with the molecular mechanics models which can predict some properties with the same level of accuracy as the larger basis set ab initio models.

In general the ab initio methods are necessary to obtain the correct geometry of a molecule. Semi-empirical models can be used to obtain molecular information but are far less reliable than even simple ab initio basis sets. However the advantage is the speed of calculation for a compound. For less well studied compounds this provides valuable information which may not be available from published literature sources.

The use of semi-empirical routines can be a problem area due to the approximations used in the models to circumvent the direct computation of the two-electron integrals, as would be performed in an ab initio calculation. These approximations are generally:

- the minimum basis set has only s and p STO's for valence electrons
- core electrons are added to the nucleus which reduces the nuclear charge for an atom
- many of the direct computations of the Coulomb and Exchange integrals are replaced with element dependent parameters

The main difficulty is that there is no way of ensuring that the molecules from which the element dependent parameters have been obtained will have any similarity to the test

molecules on which semi-empirical calculations are being performed. It is therefore to be expected that the most reliable results will be obtained where there is a close relationship between the parameterisation molecules and the test molecules and less reliable results where they are more diverse. Where there is experimental information available some account may be made for this, but this is not the case for molecules such as trisilylamine where little semi-empirical MO information is available in the literature. In an effort to quantify the problem a test run was performed, using silane and ammonia, to calculate the standard molar enthalpy of formation. Two programmes were used, Hyperchem 5.1 and Chem3D, in which four semi-empirical methods were common and one, MINDO3, was available only in one programme. The results are given in Chapter 5, table 5.1 and demonstrate that all the models could correctly predict the sign but only the oldest model, MINDO3, was able to accurately predict the standard molar enthalpy of formation for both silane and ammonia when compared to the literature value. This is a special case because the model has a different implementation of the Hamiltonian, being parameterised in terms of diatomic pairs. These include N-H and Si-H diatomic pairs which are found in silane and ammonia. The other models varied as to how well they mirrored the literature value and this demonstrates that problems can arise if only one model is used. For both silane and ammonia the precision of the semi-empirical models was exceptionally good but only the MINDO3 model computed an accurate value. The worst matches were the MNDO model for silane and the PM3 model for ammonia. In the Chem3D users guide there is a brief discussion of the applicability and limitations of the various semi-empirical models in the programme and the following extracts are taken from the users guide:

- “AM1 is a distinct improvement over MNDO, in that the overall accuracy is considerably improved. Specific improvements are : In general, errors in ΔH_f° obtained using AM1 are about 40 % less than those given by MNDO.”
- “PM3 is a distinct improvement over AM1.”
- “Overall errors in ΔH_f° are reduced by about 40 % relative to AM1.”
- “Results obtained from MNDO-d are generally superior to those obtained from MNDO. The latter method should mainly be used in cases where it is necessary to compare or repeat calculations previously performed using MNDO.”

7.1.2 Molecular Structure of Trisilylamine

The limitations of the semi-empirical routines, discussed in section 7.1.1, are evident from the molecular structures produced after a geometric optimisation run has been performed. From the electron diffraction work of initially Hedberg and then Beagley the gas phase structure of trisilylamine is trigonal planar. Ab initio calculations with large basis sets are able to correctly predict the structure of trisilylamine but this is not so with the semi-empirical routines. From the work of Varma the dipole moment of trisilylamine has been determined to be zero which is a reflection of the symmetry of the molecule. None of the semi-empirical models were able to produce a zero dipole although the overall value of 0.003 Debye returned by the MNDO/d model included zero dipole contribution from both the X and Z vectors with 0.003 Debye in the Y vector showing that the energy minimisation of the molecule was almost, but not quite 100% symmetrical.

By on-screen manipulation of the orientation of the molecular images it was possible to provide a Newman projection down one bond to facilitate ease of comparison between the energy minimised structure outputs for trisilylamine from each model. These images are clearly seen in Chapter 5, figure 5.1. Information from the output files indicate that the MNDO/d and AM1 models generated a C_s point group and PM3 minimised to C_{3v} . In reality D_{3h} (or C_{3h}) would have been expected. This being the case some care needs to be exercised when trying to draw meaningful conclusions from the visual representations of the total charge density and molecular orbitals generated by the models. It is reasonable to expect that if the LCAO procedure had correctly created the necessary molecular orbitals then the correct structure and symmetry would be displayed on the screen. The fact that this is not the case indicates that the approximations made in the programmes are insufficient to predict the orbital structures. Plots of the highest occupied molecular orbitals (HOMO) and lowest occupied molecular orbitals (LUMO) have been produced to see the quality of the graphical output provided by the package. Due to the uncertainties in the determination of the structure and therefore the orbital representations it was decided that meaningful comparative bonding data using these molecular orbital representations was not appropriate for trisilylamine.

In Chapter 5, table 5.5 a table has been constructed giving all the structural bonding information from the semi-empirical models and the known values from the literature.

The quality of the agreement between the models and the electron diffraction results of Beagley have been summarised in table 7.1. An analysis of the data in this format allows us to directly compare the relative performance of the models.

Table 7.1

Quality of Agreement between Electron Diffraction and Semi-empirical Bonding Data for Trisilylamine

	Si - - Si	Si-N	Si-H	$\angle\text{SiNSi}$	$\angle\text{HSiN}$	$\angle\text{HSiH}$
MNDO/d	1	1	1	3	2	2
AM1	2	2	2	3	1	1
PM3	3	2	2	2	1	1

where 3 = excellent 2 = good 1 = poor

Clearly the restrictions and limitations associated with semi-empirical models in general completely outweighs any specific advantage of having d orbital representation in the MNDO/d code.

Although the AM1 and PM3 models predict a different symmetry point group the general performance of the two models was similar. Specifically, the AM1 model always underestimated the bond length compared to PM3 and, other than for $\angle\text{HSiH}$ overestimated the bond angle. Comparison of the models is difficult as none appear to be successful in modeling actual bonding in trisilylamine. Considering that there is little consensus in the literature (see Chapter 2, section 2.4.1) as to the real reason for the lack of reactivity and shorter than expected Si-N bond length in trisilylamine, it is not surprising that the models cannot correctly predict the geometry. In his analysis of semi-empirical models Hehre (Hehre et al., 1995) associates many of the known problems with molecules to the lack of representation of these compounds in the parameterisation of the models.

The main conclusion that comes from this section of the work is that great care needs to be exercised when deciding on one of the semi-empirical models rather than any of the others. Attempting to predict which model will provide the best results cannot evidently be done on the basis of atomic coverage or molecular size capabilities. Informed researchers may decide that the most appropriate action is to refer to the literature from Dewar concerning the MINDO3, MNDO and AM1 models, Stewart for the PM3 model

and Thiel for MNDO/d and decide the most suitable model from the papers. The alternative method is to run the molecule on all the models and make a decision based on the empirical results obtained.

7.1.3 Atomic and Electron Charge Distribution

Chapter 5, table 5.5 provides a comparison of the atomic charges on the atoms from energy minimisation of trisilylamine by each of the semi-empirical models. The highest charges are produced by the oldest programme and runs in the order:

MNDO/d > AM1 > PM3

The total charge density represents the electron density in the space surrounding the nuclei of the molecule and defines the shape of the molecule. It is interesting to note that the plot from the MNDO/d model [compare Chapter 5, figure 5.2 (a) with (b) and (c)] produces a considerably different output than the other two models. In this case the central nitrogen atom has no associated electron density whereas for the AM1 and PM3 models all the atoms are enclosed within the electron density surface. In the light of the problems highlighted with orbital and structure prediction it is unclear how much credence can be given to these electron density surface plots. This also applies to the molecular orbitals plots as shown in Chapter 2, figures 5.3 - 5.5.

This problem is beyond the scope of this programme of research but may be resolved by comparison with other molecules of similar structure and bonding (see Conclusion and Future Work).

7.2 HYDROGEN REMOVAL AND THE ESTIMATION OF Si-N AND Si-H BOND STRENGTH

Thermodynamic calculations were performed to determine the stability of compounds formed by the removal of 1, 2 and 3 hydrogen atoms from the basic trisilylamine structure. The MNDO/d, AM1 and PM3 models managed to energy minimise all the structures from $\text{N}(\text{SiH}_3)_3$ to $\text{N}(\text{SiH}_2)_3$ and provide a value for the standard molar enthalpy of formation. The values for $\text{N}(\text{SiH}_3)_2\text{SiH}_2$ were all exothermic, although in the case of MNDO/d only just so ($-0.77 \text{ kJ mol}^{-1}$). Standard molar enthalpies of formation of all other species were endothermic.

The availability of a value of ΔH_f° for $\text{N}(\text{SiH}_3)_2\text{SiH}_2$ meant that by solving simultaneous equations a value could be obtained for the mean bond energy of the Si-N and Si-H bonds (see Chapter 5, section 5.4). Using the same method a value of $E_m(\text{Si-H})$ for silane was obtained for comparative purposes by substituting values for SiH_4 and SiH_3 from Appendix 1. As ΔH_m° is equal to the mean bond energy in the molecule (E_m) we can therefore solve simultaneous equations to obtain the result:

$$E_m(\text{Si-N}) = 366.1 \text{ kJ mol}^{-1} \text{ (for trisilylamine)}$$

$$E_m(\text{Si-H}) = 313.3 \text{ kJ mol}^{-1} \text{ (for trisilylamine)}$$

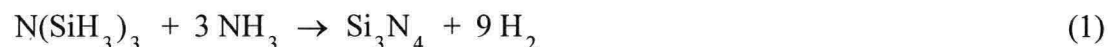
$$E_m(\text{Si-H}) = 321.9 \text{ kJ mol}^{-1} \text{ (for silane)}$$

The silane value agrees extremely well with the Si-H bond energy in silane of $325.5 \text{ kJ mol}^{-1}$ given by Trotman-Dickenson (Trotman-Dickenson, 1973) and is within $\sim 5\%$ of the $339.1 \text{ kJ mol}^{-1}$ given in Gmelin (Gmelin, 1982). This gives good confidence for the $E_m(\text{Si-H})$ value of $313.3 \text{ kJ mol}^{-1}$ obtained for trisilylamine.

The value of $E_m(\text{Si-N})$ for trisilylamine at $366.1 \text{ kJ mol}^{-1}$ is $\sim 6.7\%$ higher than the bond dissociation value of $343.25 \text{ kJ mol}^{-1}$ derived from stretching force constants and equilibrium bond lengths by Kreigsmann (Kreigsmann et al., 1959).

7.3 THERMODYNAMIC VALUES

In the early stages of the project one of the key issues was the feasibility of the reaction of trisilylamine and ammonia to form silicon nitride as defined by the Gibbs free energy change (ΔG_m°). How this value compared with the reaction of silane and ammonia was also an important issue. The overall reaction equation for silane and ammonia is well documented and by analogy, a similar overall reaction equation can be written for the reaction of trisilylamine and ammonia:



The Gibbs free energy change (ΔG_m°):

$$\Delta G_m^\circ = \Delta H_m^\circ - T\Delta S_m^\circ \quad (2)$$

assumes that values are known for the standard molar enthalpy change (ΔH_m°) and the standard molar entropy change (ΔS_m°) for the formation of Si_3N_4 .

7.3.1 Standard Molar Enthalpy of Formation (ΔH_f°) for Trisilylamine

Searches of the literature failed to find any thermodynamic values for trisilylamine other than the standard molar enthalpy of formation (ΔH_f°). The reference on page 98 in Gmelin (Gmelin, 1989) was found to be somewhat confusing because the first reference [22] is incorrectly quoted and is actually reference [23] (Livant et al, 1983) and both values are quoted as being determined by the MNDO method. Although not explicitly stated in the text of the papers the results of the work given in Chapter 5, table 5.2 suggests that in both cases the results are consistent with the use of the MNDO/d method and not strictly MNDO. As the values quoted in Gmelin for the standard molar entropy of formation of trisilylamine were within 1% of each other the mean of the two values was used in the calculation of the standard molar enthalpy change (ΔH_m°) for the formation of Si_3N_4 . This was justified on the grounds that the accuracy of the semi-empirical method was probably much worse than the 1% difference between the two

values. The ΔH_m° values obtained for silane and trisilylamine are both large and negative and therefore both reactions are strongly exothermic.

The availability of various molecular orbital modeling programmes provided an opportunity to evaluate and compare the standard molar enthalpy of formation values for trisilylamine. Since Livant and Cuthbertson published their respective works in 1983 the AM1 and PM3 semi-empirical models have both become available. Chapter 5, table 5.2 gives the results obtained from three different software packages and four different semi-empirical methods. What is evident is the disparity between the results for the MNDO model compared to MNDO/d, AM1 and PM3 models. The parameterisation of the MNDO model is clearly at odds with the others. This is not to say that this model is necessarily wrong. Without an experimentally determined value as a reference it is impossible to say with 100% confidence and it is conceivable that the MNDO/d, AM1 and PM3 models are parameterised in a similar way that incorrectly calculates the standard molar enthalpy of formation. However, with regard to the comments on the accuracy of the models detailed in section 7.1.1 there is little scientific evidence to support the standard molar enthalpy of formation generated by this model.

The number of results available is insufficient to perform a statistical distribution analysis (student t test) so the standard deviation has been calculated and the value of the "Z factor" determined. This is the standard deviation around the mean value. This shows that the MNDO/d and PM3 models are both within one standard deviation of the mean value and positive in value (see table 5.3). The AM1 values are within one to two standard deviations of the mean and negative in value. We can say therefore that the results generated by the PM3 and MNDO/d models are statistically different to the AM1 model. The reasons for the statistical difference are unclear and further investigations are required.

7.3.2 Standard Molar Entropy of Formation for Trisilylamine

To determine the standard molar entropy change (ΔS_m°) requires a value for trisilylamine of the standard molar entropy of formation (S°). As no such value could be found from the literature, to proceed further required that a value be calculated. With no heat capacity or other usable entropy parameter the option taken was to calculate a value using the relationship for the spectroscopic entropy:

$$S^{\circ} (\text{spectroscopic}) = S^{\circ} (\text{translational}) + S^{\circ} (\text{rotational}) + S^{\circ} (\text{vibrational}) \quad (3)$$

This approach can be justified on the grounds that the total entropy of a gas can be partitioned into translational, rotational and vibrational components (James, 1976). For the translational entropy the Sackur-Tetrode equation was used which requires only that the molecular weight of the compound be substituted into the equation.

In determining the rotational entropy of the molecule the symmetry becomes an important factor as it has a direct bearing on the value of the rotational symmetry number (σ). Some authors assign the point group of trisilylamine as C_{3h} point which assumes that there is hindered rotation around the Si-H bond. There appears to be little evidence to support this view and therefore the D_{3h} point group is a more appropriate assignment. This means that a value of $\sigma = 6$ was used in the calculation of the rotational entropy.

The vibrational entropy of a polyatomic molecule cannot be obtained from simple gas phase spectra due to rotational-vibrational coupling. It is therefore necessary to consider the contribution from every bond in the infrared and Raman spectra. Due to the planarity and high level of symmetry of trisilylamine it is an easy molecule on which to perform these calculations relative to other multi-atom molecules. This is because, as noted by Robinson (Robinson, 1958), even with 13 atoms in the molecule the infrared spectrum contains a relatively small number of peaks. The calculation of the vibrational entropy contribution relies on the availability of the spectral peak information which in this case was readily available in Gmelin. An analysis of the data shows that the major contribution is the 3 bending bands between 493 - 195 cm^{-1} which account for 67.24% of the total vibrational entropy. The 11 bands between 1011 - 661 cm^{-1} contribute 32.68% of the total with the contribution from the stretching bands between 2138 - 2170 cm^{-1} less than 0.1%.

The value of the standard molar entropy of formation (S°) calculated for trisilylamine was 286.8 $\text{J K}^{-1} \text{mol}^{-1}$. The individual contributions to the entropy were determined to be:

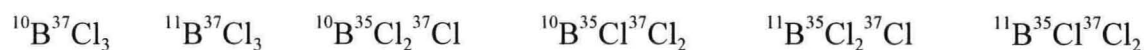
translational	167.64 $\text{J K}^{-1} \text{mol}^{-1}$	59.0%
rotational	90.32 $\text{J K}^{-1} \text{mol}^{-1}$	31.8%
vibrational	26.17 $\text{J K}^{-1} \text{mol}^{-1}$	9.2%

As there is no experimentally determined literature value for comparison it is not possible to say how accurate this calculated value really is. To overcome this problem boron trichloride (BCl_3) was chosen for a specimen calculation. The main criteria had to be that the molecule was as comparable as possible to trisilylamine in its structure and constitution to minimise sources of error. Boron trichloride proved suitable for the following reasons:

- both molecules have trigonal planar structure
- the central boron atom is very close in the periodic table to nitrogen
- the atomic weight of chlorine atoms of 35.45 is very close to SiH_3 groups at 31.11
- the bond lengths for Si-N and B-Cl were comparable (0.1738 nm and 0.1715 nm respectively)
- no fluorine atoms are present which may cause anomalous results

Repeating the calculation in an identical manner using the appropriate values for boron trichloride gave a value of $290.7 \text{ J K}^{-1} \text{ mol}^{-1}$. This compares very favourably to the literature value of $290.1 \text{ J K}^{-1} \text{ mol}^{-1}$.

An uncertainty in the vibrational entropy calculation of BCl_3 is the effect of the presence of isotopic species in the molecule. In this work only the $^{10}\text{B}^{35}\text{Cl}_3$ and $^{11}\text{B}^{35}\text{Cl}_3$ bonds have been taken to represent all bonds. However a number of other isotopic bonding arrangements may be present:



For a rigorous treatment of the vibrational entropy their contributions would have to be taken into account by averaging over a range of isotopic distributions.

Additional information was obtained by using plots of entropy against molecular weight. The values obtained are given in table 4.2 and the mean value of the three methods used were 287.4 and $293.4 \text{ J K}^{-1} \text{ mol}^{-1}$ respectively for trisilylamine and boron trichloride. Comparing the calculated value for trisilylamine of $284.1 \text{ J K}^{-1} \text{ mol}^{-1}$ the difference is less than 1.2% and for boron trichloride around 1%. Some disparity between empirically and experimentally determined values of S° is to be expected because:

- (a) the contribution of molecular weight to entropy is via S° (translational) whose major contribution to the overall entropy of a gas occurs at lower molecular weights
- (b) no account is taken of other molecular parameters that may have an influence on the entropy of the gas.

7.3.3 Gibbs Free Energy Change (ΔG_m°) for the Formation of Si_3N_4

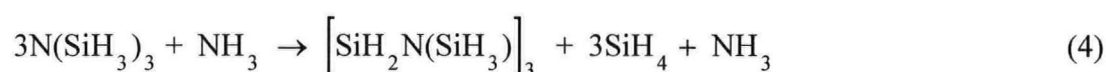
The result obtained for the reaction of trisilylamine and ammonia to form silicon nitride $\Delta G_m^\circ = -596.6 \text{ kJ mol}^{-1}$ and for the reaction of silane and ammonia to form silicon nitride $\Delta G_m^\circ = -747.7 \text{ kJ mol}^{-1}$ indicate that both values are large and negative and therefore that the reactions are highly feasible in thermodynamic terms at room temperature. This is also confirmed by the calculation of the standard equilibrium constant in Chapter 4, section 4.5 that shows $K^\circ(T) > 10^{100}$ for both reactions.

These values for the Gibbs free energy change have been calculated at 298 K but in reality neither the silane and ammonia reaction nor the trisilylamine and ammonia reaction occur in the gas phase at room temperature. This is generally an indication that there are kinetic factors to consider and this is certainly the case with silane and ammonia which react via a radical mechanism whose energy of activation cannot be overcome by normal collision energies at room temperature.

7.4 REACTION OF TRISILYLAMINE AND AMMONIA

The Gibbs free energy change (ΔG_m°) applies only to the reaction equation as written and says nothing about the mechanisms or pathways of reaction. For many reactions which apparently have a large and negative value of ΔG_m° at room temperature the reaction does not occur due to other factors such as kinetic and/or mechanistic considerations.

Wells found that in the liquid phase the reaction of trisilylamine and ammonia proceeded via the elimination of silane to form a ring compound:



This is possible because the inter-molecular distances are very close and the solvation energy of the solvent can easily promote elimination reactions. It is very difficult to conceive how, in the gas phase, three trisilylamine molecules can orientate themselves such that the base catalysed elimination of silane can take place with the formation of the six membered ring compound. This does not mean that this, or any other ring compound cannot be formed, only that the mechanism is likely to be different.

If we consider the experimental evidence for the silane and ammonia reaction we see that the thermal reaction to form silicon nitride by APCVD takes place at temperatures between 700 - 900°C with LPCVD deposition occurring between 650 - 750°C (however for production purposes dichlorosilane is preferred to silane as a precursor, see for example Sze, 1983). At reduced pressure the plasma assisted CVD process occurs typically between 200 - 350°C. The difference in reaction temperature between APCVD and PECVD deposition from silane and ammonia is very significant (~ 500°C) and can be ascribed to the difference in reaction mechanism.

At normal pressures and at elevated temperatures a bimolecular reaction occurs whereby silane and ammonia atoms become coincident for sufficient time and with sufficient energy for a 4 centered reaction to take place. The 4 centered transition state is illustrated in figure 7.1.

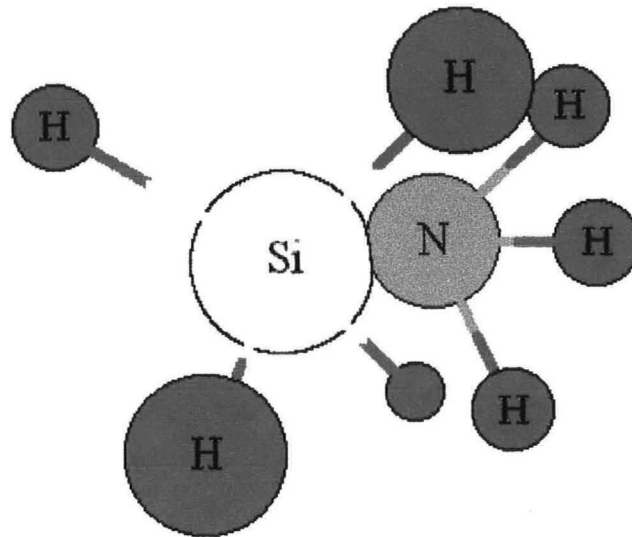


Figure 7.1

Bimolecular Reaction of Silane and Ammonia

In this case one Si atom, one N atom and two H atoms form a transient structure leading to breakage of one Si-H bond in silane and one N-H bond in ammonia and the formation of one Si-N bond and one H-H bond to form products according to the reaction:



In the case of plasma CVD reactions these occur at reduced pressures in the so called "glow region" where a gas phase plasma can be sustained. There is a considerable body of evidence to support the theory that silane pyrolyses and reacts via a radical reaction. The difference in temperature between the atmospheric pressure ($\sim 900^\circ\text{C}$) and reduced pressure plasma assisted ($\sim 300^\circ\text{C}$) reactions of silane and ammonia is due to the difference in activation energy associated with reactive radical species compared to neutral molecules.

7.4.1 Feasibility of Reaction

The only experimental information available concerning the gas phase mixing of trisilylamine and ammonia is the work of Wells who determined that in the gas phase no elimination of silane was detected either after 16 hours at room temperature or 1 hour at

100°C within the limits of experimental error. As the thermodynamic calculations performed in this work indicate that the reaction of trisilylamine and ammonia is, like that of silane and ammonia, feasible at room temperature then the thermodynamics is clearly at odds with experimental observation.

At reduced pressures of ~ 500 mTorr used for PECVD, the mean free path (distance between collisions) calculated for trisilylamine of 5.14×10^{-3} cm is five orders of magnitude larger than the molecular diameter (\sim collision diameter) at 5.2×10^{-8} cm obtained from the mean of the semi-empirical calculations. In this case, coincidence of atoms with sufficient residence time for reaction to occur is physically impossible.

The Gibbs free energy change is the most appropriate measure of the feasibility of the reaction but the lack of direct entropy data means that this cannot easily be determined. Zarowin (Zarowin, 1985) has suggested that in many cases the Gibbs free energy change is correlated with, and often (but not always) dominated by, the enthalpy term. Comparing the results given in Chapter 6, tables 6.2 and 6.5 it is evident that the trends in the thermodynamic data follow an identical pattern and therefore using the standard molar enthalpy change rather than the Gibbs free energy change is acceptable for comparative results in this work. This is shown clearly in table 7.2.

Table 7.2

Trends in Values of ΔH_m° and ΔG_m° for AM1 and PM3 Semi-empirical Models

Reaction	AM1		PM3	
	ΔH_m°	ΔG_m°	ΔH_m°	ΔG_m°
	kJ mol ⁻¹		kJ mol ⁻¹	
$(\text{SiH}_3)_2\text{NSiH}_2\text{NH}_2 + \text{H}_2$	- 64.9	- 49.57	- 40.7	- 25.37
$(\text{SiH}_3)_2\text{NSiH}(\text{NH}_2)_2 + \text{H}_2$	- 63.2	- 47.54	- 37.1	- 21.44
$\text{SiH}_3\text{N}(\text{SiH}_2\text{NH}_2)_2 + \text{H}_2$	- 64.3	- 48.64	- 38.2	- 22.54
$(\text{SiH}_3)_2\text{NSi}(\text{NH}_2)_3 + \text{H}_2$	- 87.7	- 71.74	- 72.8	- 56.84
$(\text{SiH}_2\text{NH}_2)_3\text{N} + \text{H}_2$	- 63.9	- 47.94	- 48.9	- 32.94

The only occasions when the correlation of ΔG_m° and ΔH_m° becomes a problem is where the value of ΔH_m° is positive or where the value of ΔS_m° is negative. In these cases it would be necessary to evaluate the equation directly to obtain the size and sign of ΔG_m° .

7.4.2 Formation of Products

Clearly the addition of amino groups to trisilylamine can lead to a large number of different reaction products. There are 19 different possibilities for the addition of amino groups to the basic trisilylamine structure via substitution of the hydrogen atoms and these are shown in Chapter 5, figure 5.6. Values for the standard molar enthalpy of formation were obtained for all the possible species using Chem3D while a few values were obtained with Hyperchem 5.1. Table 7.3 contains a comparison of results from the two semi-empirical programmes and in general one can see that there is very good agreement between the models.

For the AM1 routine implemented in Hyperchem and Chem3D the difference between the results varied between 1.8% - 5.0% and for the implementation of the PM3 routines 0.4% - 6.7%. This is considered to be a creditable result given the different origins of the programmes and the semi-empirical codes.

Table 7.3

Values of ΔH_f° for Addition of Amino Groups to Trisilylamine using AM1 and PM3 Semi-empirical Models

	ΔH_f° (kJ mol ⁻¹)			
	AM1		PM3	
	Chem3D	Hyperchem	Chem3D	Hyperchem
N(SiH ₃) ₂ SiH ₂ NH ₂	- 234.29	- 238.60	- 216.96	- 224.70
N(SiH ₃) ₂ SiH(NH ₂) ₂	- 332.03	- 348.74	- 315.70	- 307.76
N(SiH ₃) ₂ Si(NH ₂) ₃	- 470.51	- 481.52	- 428.14	- 426.60
NSiH ₃ (SiH ₂ NH ₂) ₂	- 333.37	- 348.95	- 289.46	- 308.84
N(SiH ₂ NH ₂) ₃	- 448.78	- 457.36	- 391.27	- 403.78

In Chapter 5, figure 5.7 the ΔH_m° values for all aminotrisilylamine species have been plotted against the number of amino groups to elucidate trends in the semi-empirical programmes. All three plots are linear but vary by the inclination of the line. One feature of the plot is the general lack of scatter of data points.

An attempt was made to see whether trends in the energy related to the addition of amino groups could be better visualised by normalising the plot to remove the effect of

increasing molecular weight with enthalpy of formation. This was done by recalculating and re-plotting with the appropriate factor to remove the effects of molecular weight with enthalpy. The values and resultant plot are shown in Chapter 5, table 5.11 and figure 5.8 respectively. Neither a straight line or curve fitted the data points in a satisfactory manner and the best fit was obtained by fitting three lines to the data points. This suggests that there are three distinct regions associated with 1 - 3, 4 - 6 and 7 - 9 NH_2 groups with differing rates of steepness of the slope. As the standard molar enthalpy of formation is a measure of the relative stability of a molecule, it can be postulated that these small, but relatively stable, species are ideal candidates as building blocks for larger molecules and ultimately solid films. This suggestion is corroborated by the work of Jasinski (Jasinski et al., 1989) who found lower molecular weight aminosilanes in the laser dissociation of silane and ammonia.

7.4.3 Radical Reactions

It is convenient from a chemistry viewpoint to consider reactions in molecular terms; nucleophilic and electrophilic reactions are both important cases. It is also a convenient standpoint from which ab initio molecular orbital calculations can be performed on reaction species to see how structural changes may take place. For non-plasma reactions the idea of a nucleophilic attack on a positively polarised silicon atom in a silyl group by a nitrogen atom in ammonia with a lone pair of electrons is entirely reasonable. However, in a plasma environment this type of reaction is very unlikely to occur for many reasons including:

- the power applied to the electrodes to create the glow discharge promotes rapid dissociation of precursor molecules
- the mean free path at reduced pressure precludes close contact between reacting species
- in a plasma neutral nitrogen atoms with lone pair electrons are very un-reactive when compared to gas phase radicals

Two processes can be seriously considered for the formation of reactive radical species that would lead to the deposition of silicon nitride from trisilylamine and ammonia precursor. These are:

- (a) dissociation by electron bombardment where sufficient electron energy is available in the plasma to break bonds in the range 100 - 900 kJ mol⁻¹
- (b) formation by hydrogen abstraction where calculations performed in chapter 6 have given values for the standard molar enthalpy change for hydrogen abstraction by H radicals and NH₂ radicals of - 142.73 kJ mol⁻¹ and - 80.0 kJ mol⁻¹ respectively

Given the tiny fraction of radicals in a plasma and the mean free path at 500 mTorr pressure the most likely reactions are radical-molecule interactions to propagate the reaction and radical-third body reactions to terminate the reaction. Examples of these reactions have been given in Chapter 6, sections 6.5 and 6.6. Unfortunately, facilities are not available to provide experimental verification by quadrupole mass spectrometry (QMS) in the plasma nor are there software packages available that have algorithms capable of providing simulation of the plasma deposition process by which the initiation, propagation and termination reactions proposed in this work can be compared.

CONCLUSION

The formation of silicon nitride from trisilylamine and ammonia has been investigated by thermodynamic calculations and semi-empirical molecular orbital computations and as a consequence a mechanism for radical reaction has been postulated.

Most of the thermodynamic values required to assess the potential reactions of trisilylamine and ammonia were unavailable in the literature or had been determined by more indirect methods. It was therefore necessary to determine all the values required and these are presented along with any previously determined values. The overall reaction equation proposed for trisilylamine and ammonia is:



and the thermodynamic values determined in this work for this reaction equation are:

- (1) standard molar enthalpy change $\Delta H_m^\circ = -472.86 \text{ kJ mol}^{-1}$
- (2) standard molar entropy change $\Delta S_m^\circ = +415.1 \text{ J K}^{-1} \text{ mol}^{-1}$
- (3) Gibbs free energy change $\Delta G_m^\circ = -596.62 \text{ kJ mol}^{-1}$

The author has been unable to locate any of the above values in the literature.

Specific thermodynamic values related to trisilylamine were required to obtain the above reaction values. These thermodynamic values were determined to be:

- (5) standard molar enthalpy of formation $\Delta H_f^\circ = -132.94 \text{ kJ mol}^{-1}$.
- (6) standard molar entropy of trisilylamine $S^\circ = +284.13 \text{ J K}^{-1} \text{ mol}^{-1}$
- (7) translational entropy $S^\circ = +167.64 \text{ J K}^{-1} \text{ mol}^{-1}$
- (8) rotational entropy $S^\circ = +90.32 \text{ J K}^{-1} \text{ mol}^{-1}$
- (9) vibrational entropy $S^\circ = +26.17 \text{ J K}^{-1} \text{ mol}^{-1}$

From the literature, values of ΔH_f° for trisilylamine of $-130.31 \text{ kJ mol}^{-1}$ and $-131.57 \text{ kJ mol}^{-1}$ are available (Livant et al, 1983 and Cuthbertson et al, 1983 respectively).

Using the method of solving simultaneous equations, values for the standard molar enthalpy change ΔH_m^0 for trisilylamine $N(SiH_3)_3$ and the triaminosilyl radical $N(SiH_3)_2SiH_2$ were used to obtain values of the mean bond energy E_m for the Si-H and Si-N bonds in trisilylamine. The results obtained were comparable to values in the literature:

$$(10) \text{ mean bond energy } E_m(\text{Si-N}) = 366.07 \text{ kJ mol}^{-1}$$

$$(11) \text{ mean bond energy } E_m(\text{Si-H}) = 313.27 \text{ kJ mol}^{-1}$$

and provide a new and additional method of calculation to that currently available. From the literature a value of $E_m(\text{Si-N})$ for trisilylamine of $343.25 \text{ kJ mol}^{-1}$ is available (Kreigsmann et al., 1959). Comparative literature values of $E_m(\text{Si-H})$ for silane are $325.5 \text{ kJ mol}^{-1}$ and $339.1 \text{ kJ mol}^{-1}$ (Trotman-Dickenson, 1973 and Gmelin, 1982 respectively).

The standard molar enthalpy of formation values of all possible $-NH_2$ group substitutions of hydrogen in the trisilylamine molecule have been shown to be exothermic using the MNDO/d, AM1 and PM3 semi-empirical models. The relationship of standard molar enthalpy of formation with addition of $-NH_2$ groups is shown to increase linearly while the relationship of the factor $\Delta H_f^0/MW$ with addition of $-NH_2$ groups shows three distinct regions where the steepness of the slope of the graph is in the relation $1 - 3 > 4 - 6 > 7 - 9$ amino groups.

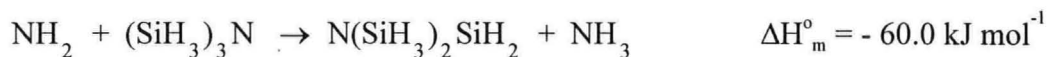
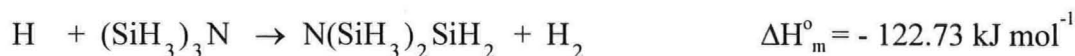
The molecular diameter of trisilylamine has been estimated as $5.2 \times 10^{-8} \text{ cm}$ and for gas phase reactions the mean free path of trisilylamine at 500 mTorr has been calculated to be $5.14 \times 10^{-3} \text{ cm}$.

The energy imparted by electron impact is sufficient to generate radical species from neutral molecules. The standard molar enthalpy of formation of important radicals in the trisilylamine/ammonia reaction has been determined:



These electron bombardment reactions are complemented in the plasma state by hydrogen abstraction reactions which dissociate neutral molecules into radicals. The

standard molar enthalpy change for the initiation of radical reactions in a gas phase plasma of trisilylamine and ammonia by hydrogen extraction has been shown to be exothermic with:



The triaminosilyl radical $\text{N}(\text{SiH}_3)_2\text{SiH}_2$ is proposed as the initial radical species in the gas phase plasma reaction of trisilylamine and ammonia to form silicon nitride films.

In Chapter 6, sections 6.4 - 6.6 the initiation, propagation and termination reactions by a combination of electron dissociation and hydrogen abstraction reactions are considered fully and lead to the conclusion that trisilylamine has potential as a convenient precursor for the deposition of silicon nitride.

One of the unexpected outcomes of this programme of research is the discovery that there exists significant variations in the results produced by the different semi-empirical models when performing calculations on the same molecule. These anomalies require further investigation but are a warning to chemists who are not familiar with molecular orbital calculations using semi-empirical methods that matching of the model to the problem is essential to ensure the best possible result.

RECOMMENDATIONS FOR FURTHER WORK

Three areas of work still need to be investigated to obtain additional information on the physical properties, bonding and reactions of trisilylamine.

(1) Structural Studies by Semi-empirical Methods

Information on the structure and bonding of trisilylamine could be obtained by semi-empirical computation and analysis on a range of $X(YH_3)_3$ molecules as given in Chapter 2, table 2.1. Both $N(SiH_3)_3$ and $N(GeH_3)_3$ have planar geometry whereas $N(CH_3)_3$ is pyramidal. All the $(YH_3)_3$ derivatives of phosphorus, namely $P(CH_3)_3$, $P(SiH_3)_3$ and $P(GeH_3)_3$ are known to be pyramidal.

(2) Structural Studies by Ab Initio Methods

It is possible, though not straight forward, to obtain the standard molar enthalpy of formation from ab initio methods. Using the 6-31G* or 6-31G** basis sets would provide an additional value for comparison with that obtained in this work.

Due to the inability of the semi-empirical methods to correctly predict the structure of trisilylamine there has been no structural analysis of any of the aminated derivatives of trisilylamine. This information may prove important in determining those species that are active intermediates for the deposition of silicon nitride.

(3) In-situ Reaction Studies by Mass Spectrometry

With a sample of trisilylamine and ammonia in a PECVD or RPECVD reactor with an in-situ QMS it would be possible to record the mass and energy spectra at different intensities and obtain direct information on the mass and energy of species that were in the plasma. The mass of the species can then be compared to those in Chapter 5, table 5.8 to identify the important reaction intermediates. With a silicon or other substrate on the heated platen in the PECVD chamber a film can be deposited for subsequent characterisation using physical measurement techniques such as FTIR, SIMS, AES, etc.

(4) Semi-empirical Modeling

The work performed in Chapter 5, section 5.1 suggests that although the MINDO3 semi-empirical programme is old, it is nevertheless very effective for smaller molecules when compared to the newer AM1 and PM3 programmes. The potential exists to modify the computer code (available in WinMOPAC 2.0 for Windows 95 from Fujitsu) to incorporate Si-N diatomic pair information to the existing N-H and Si-H diatomic pairs (currently only Si-H, Si-C and Si-Si diatomic pairs are available). This may provide the basis for a molecular orbital modeling programme that is specific to Si-N-H compounds.

GLOSSARY OF TERMS

III-V	compound semiconductor materials belonging to the periodic groups III and V
AES	Auger electron spectrometry
AFM	atomic force microscope
AMI	Austin Method 1 which is a semi-empirical programme
APCVD	atmospheric pressure chemical vapour deposition
AZS	azidotrimethylsilane $(\text{CH}_3)_3\text{SiN}_3$
BARL	bottom anti-reflection layer
BIPADS	1,2 - bis(di-i-propylamino)disilane $[(\text{C}_3\text{H}_7)_2\text{NSiH}_2]_2$
BPSG	borophosphosilicate glass
CFD	computational fluid dynamic
CGS	centimetre gram second units
CMOS	complimentary metal oxide semiconductor device
CVD	chemical vapour deposition
ED	electron diffraction
EDX	energy dispersive x-ray analysis
EELS	electron energy loss spectroscopy
ERDA	elastic recoil detection analysis
ESCA	electron spectroscopy for chemical analysis
ESR	electron spin resonance
FTIR	Fourier transform infra red spectroscopy
GaAs	gallium arsenide compound semiconductor
GTO	gaussian type orbital
GUI	graphical user interface
HMCTS	hexamethylcyclotrisilazane $[\text{Si}(\text{CH}_3)_2\text{NH}]_3$
HMCTSZN	hexamethylcyclotrisilazane $[\text{Si}(\text{CH}_3)_2\text{NH}]_3$
HMDS	hexamethyldisilazane $(\text{CH}_3)_6\text{Si}_2\text{NH}$
IBM	International Business Machines the computer manufacturer
LCAO	linear combination of atomic orbitals
LOCOS	LOCAl Oxidation of Silicon
LPCVD	low pressure chemical vapour deposition

LTEL	long term exposure limit
MINDO	modified intermediate neglect of differential overlap
MO	molecular orbital
MNDO	modified neglect of differential overlap
MNDO/d	as MNDO but with the addition of d orbital representations
MOS	metal oxide semiconductor
MNOS	metal nitride oxide semiconductors
MW	molecular weight
NDDO	neglect of diatomic differential overlap
NTP	normal temperature and pressure
OES	optical electron spectroscopy
PECVD	plasma enhanced chemical vapour deposition
PM3	Parametric Method 3 which is a semi-empirical programme
PMR	proton magnetic resonance
QCPE	quantum chemical programme exchange
QMS	quadrupole mass spectrometer
RAM	random access memory
RBS	Rutherford backscattering spectrometry
RF	radio frequency
RPECVD	remote plasma enhanced chemical vapour deposition
SCF	self consistent field
SI units	système internationale d'unités
SIMS	secondary ion mass spectrometry
STEL	short term exposure limit
STO	Slater type orbital
STP	standard temperature and pressure
TDSA	tris(dimethylamino)silylazide $[(\text{CH}_3)_2\text{N}]_3\text{SiN}$
TEB	triethylborate $(\text{C}_2\text{H}_5\text{O})_3\text{B}$
TEOS	tetraethoxysilane or tetraethylorthosilicate $(\text{C}_2\text{H}_5\text{O})_4\text{Si}$
TBA	tert-butylarsine $\text{C}_4\text{H}_9\text{AsH}_2$
TBP	tert-butylphosphine $\text{C}_4\text{H}_9\text{PH}_2$
TDMAS	trisdimethylaminosilane $[(\text{CH}_3)_2\text{N}]_3\text{SiH}$
TLV	threshold limit value

TMB	trimethylborate (C ₃ H ₉ O) ₃ B
TMPi	trimethylphosphite (CH ₃ O) ₃ P
TMPo	trimethylphosphate (CH ₃ O) ₃ PO
TSA	trisilylamine (SiH ₃) ₃ N
ULSI	ultra large scale integration
URL	universal resource locator
VLSI	very large scale integration
XPS	x-ray photoelectron spectroscopy (also known as ESCA)
ZDO	zero differential overlap

REFERENCES

- Aberle, A.G. and Hezel, R. "Progress in Low-Temperature Surface Passivation of Silicon Solar Cells using Remote-Plasma Silicon Nitride", *Progress in Photovoltaics*, 5, 1, (1997), pp.29-50.
- Aboaf, J.A. "Some Properties of Vapor Deposited Silicon Nitride Films Obtained by the Reaction of SiBr_4 and NH_3 ", *J. Electrochem. Soc.*, 116, 12, (1969), p.1736-1740.
- Adams, A.C. Schinke, D.P. and Capio, C.D. "An Evaluation of the Prism Coupler for Measuring the Thickness and Refractive Index of Dielectric Films on Silicon Substrates", *J. Electrochem. Soc.*, 126, 9, (1979), pp.1539-1543.
- Aleksandrov, L.N. Belousov, I.I. and Efimov, V.M. "Regularities of Growth and Electrical Properties in the Plasma-Enhanced Deposition of Silicon Nitride", *Thin Solid Films*, 157, (1988), pp.337-343.
- Aleksandrov, S.E. and Hitchman, M.L. "Remote Plasma-Enhanced CVD of Fluorinated Silicon Nitride Films", *Chemical Vapour Deposition*, 3, (1997), pp.111-117.
- Aleksandrov, S.E., Hitchman, M.L., Grekov, F.F. and Ivanov, V.S. "Remote Plasma Enhanced Chemical Vapour Deposition of Silicon Nitride Films in the System $\text{SiH}_4 - \text{N}_2 - \text{NF}_3$ ", *Russian Journal of Applied Chemistry*, 69, (1996), pp.1118-1125.
- Allaert, K. Van Calster, A. Loos, H. and Lequesne, A. "A Comparison Between Silicon Nitride Films Made by PCVD of $\text{N}_2\text{-SiH}_4/\text{Ar}$ and $\text{N}_2\text{-SiH}_4/\text{He}$ ", *J. Electrochem. Soc.*, 132, 7, (1985), pp.1763-1766.
- Alt, L.L., Ing Jr., S.W. and Laendle, K.W. "Low-Temperature Deposition of Silicon Oxide Films", *J. Electrochem. Soc.*, 110, (1963), p.465.
- Androshuk, A., Bergh, A.A. and Erdman, W.C. "Method of Conducting Chemical Reactions in a Glow Discharge", US Patent, 3,424,661, (1969).

Anonymous, "Photochemical Deposition of Silicon Nitride", Research Disclosure, 27343, (1987), January, p.32.

Arkles, B. "Silicon Nitride from Organosilazane Cyclic and Linear Prepolymers", J. Electrochem. Soc., 133, 1, (1986), pp.233-234.

Avasthi, D.K. Acharya, M.G. Tarey, R.D. Malhotra, L.K. and Mehta, G.K. "Hydrogen Profiling and the Stoichiometry of an a-SiN_x:H Film", Vacuum, 46, 3, (1995), pp.265-267.

Aylett, B. J. Private Communication, 1994.

Aylett, B.J. "Purposeful Chemical Design of MOCVD Precursors for Silicon Based Systems", Symposium Proceedings on Chemical Perspectives of Microelectronic Materials, MRS, Vol. 131, Pittsburgh, 1989, pp383-388.

Aylett, B.J. and Hakim, M.J. "Silicon-Nitrogen Compounds. Part VI. The Preparation and Properties of Disilazane", J. Chem. Soc. (A), (1969), pp.639-642.

Aylett, B.J. and Hakim, M.J. "The Preparation and Some Properties of Disilylamine", Inorg. Chem., 5, (1966), p.167.

Azuma, K. and Tanaka, M. "Plasma Chemical Vapour Deposition of Silicon Nitride", Japan Kokai Tokkyo Koho, 62,253,771, (1987).

Bárdos, L. Musil, J. and Taras, P. "Nitrogen Activation for Plasma Chemical Synthesis of Thin Si₃N₄ Films", Thin Solid Films, 102, (1983), pp.107-110.

Bárdos, L., Musil, J. and Taras, P. "Differences Between Microwave and RF Activation of Nitrogen for the PECVD Process", J. Phys. D: Appl. Phys., 15, (1982), pp.L79-82.

Barrow, M.J. and Ebsworth, E.A.V., "Crystal and Molecular Structure of Trisilylamine at 115 K", J. Chem. Soc. Dalton Trans., (1984), pp.563-565.

Bartle, D.C. Andrews, D.C. Grange, J.D. Harris, P.G. Trigg, A.D. and Wickenden, D.K. "Plasma Enhanced Deposition of 'Silicon Nitride' for use as an Encapsulant for Silicon Ion Implanted Gallium Arsenide", *Vacuum*, 34, 1-2, (1984), pp.315-320.

Baybutt, P., Guest, M.F. and Hillier, I.H. "The Rôle of d Functions in the Si-N Bond", *Proc. Roy. Soc. Lond. A*, 333, (1973), pp.225-236.

Beagley, B. and Conrad, A.R. "New Electron-Diffraction Study of the Molecular Dimensions and Planarity of Trisilylamine", *Trans. Faraday Soc*, 66, (1970), pp.2740-2744.

Bell, C.F. *Syntheses and Physical Studies of Inorganic Compounds*, (Pergamon Press, 1972), pp.49-55.

Belyi, V.I., Vasilyeva, L.L., Ginovker, A.S., Gritsenko, V.A., Repinsky, S.M., Sinita, S.P., Smirnova, T.P. and Edelman, F.L. *Materials Science Monographs 34, SILICON NITRIDE IN ELECTRONICS*, (Elsevier, 1988).

Belyi, V.I., Smirnova, T.P., Solov'ev, A.P., Yashkin, I.L., Khramova, L.V and Marakhovka, I.I. "Plasmachemical Methods for Obtaining Silicon and Boron Nitrides on Indium Antimonide", *Mikroelektronika*, 15, 2, (1986), pp.91-94.

Benninghoven, A. Sichtermann, W. and Storp, S. "Comparative Study of Si(111), Silicon Oxide, SiC and Si₃N₄ Surfaces by Secondary Ion Mass Spectroscopy (SIMS)", *Thin Solid Films*, 28, (1975), pp.59-64.

Blaauw, C. "Preparation and Characterisation of Plasma Deposited Silicon Nitride", *J. Electrochem. Soc.*, 131, 5, (1984), pp.1114-1118.

Bohn, P.W. and Manz, R.C. "A Multiresponse Factorial Study of Reactor Parameters in Plasma Enhanced CVD Growth of Amorphous Silicon Nitride", *J. Electrochem. Soc.*, 132, 8, (1985), pp.1981-1984.

Borreson, R.W., Yaws, C.L., Hsu, G. and Lutwack, R. "Physical and Thermodynamic Properties of Silane", *Solid State Tech.*, Jan, (1978), pp.43-46.

Brinkmann, R.P. "Modelling of RF-Discharges in the PCVD Regime", *Proceedings of the Tenth International Conference on Gas Discharges and their Applications*, Swansea, UK, 13-18 Sept, 1992, Vol. 2, pp.896-899.

Britton, L.G. and Taylor, P. "Improving your Handling of Silane", *Semicond. Int.*, April, (1991), pp.88-92.

Brooks, T.A. and Hess, D.W. "Deposition Chemistry and Structure of Plasma-Deposited Silicon Nitride Films from 1,1,3,3,5,5,-Hexamethylcyclotrisilazane", *J. Appl. Phys.*, 64, 2, (1988), pp.841-848.

Brooks, T.A. and Hess, D.W. "Characterisation of Silicon Nitride and Silicon Carbonitride Layers from 1,1,3,3,5,5,-Hexamethylcyclotrisilazane Plasmas", *J. Electrochem. Soc.*, 135, 12, (1988), pp.3086-3093.

Brouwer, F. "Quantum Chemistry in Molecular Modeling", *Lab. of Organic Chemistry, University of Amsterdam*, Chapter 5.

Brown, H.L. Bunyard, G.B. and Lin, K.C. "Applications of Mass Spectrometers to Plasma Process Monitoring & Control", *Solid State Tech.*, July, (1978), pp.35-38.

Bruce, R.H. "Ion Response to Plasma Excitation Frequency", *J. Appl. Phys.*, 52(12), (1981), pp.7064-7066.

Budhani, R.C. Bunshah, R.F. and Flinn, P.A. "Kinetics of Structural Relaxation and Hydrogen Evolution from Plasma Deposited Silicon Nitride", *Appl. Phys. Lett.*, 52(4), (1988), pp.284-286.

Bunshah R.F. (Series Editor), *Deposition Technologies for Films and Coatings*, (Noyes Publications, 1982), p.372.

Burggraaf, P.S. "Plasma Deposition Production Trends", *Semiconductor International*, 3, 3, (1980), pp.23-34.

Cai, L., Rohatgi, A., Han, S., May, G. and Zou, M. "Investigation of the Properties of Plasma-Enhanced Chemical Vapor Deposited Silicon Nitride and its Effect on Silicon Surface Passivation", *J. Appl. Phys.*, 83, 11, (1998), pp.5885-5889.

CambridgeSoft Corp., *CS Chem3D Users Guide*, (CambridgeSoft Corp., 1997), Chapter 9, pp. 130-131.

Caquineau, H. and Despax, B. "Influence of the Reactor Design in the Case of Silicon Nitride PECVD", *Chemical Engineering Science*, 52, 17, (1997), pp.2901-2914.

Centre for Molecular Modelling, "The NIH Guide to Molecular Modelling", http://cmm.info.nih.gov/modeling/guide_documents/tocs/computation_toc.html.

Chang, C-P., Flamm, D.L., Ibbotson, D.E. and Mucha, J.A. "Fluorinated Chemistry for High-Quality, Low Hydrogen Plasma-Deposited Silicon Nitride Films", *J. Appl. Phys.*, 62(4), (1987), pp.1406-1415.

Chang, M. Wong, J. and Wang, D.N.K. "Low Stress, Low Hydrogen Nitride Deposition", *Solid State Tech.*, May, (1988), pp.193-195.

Chiang, J.N. and Hess, D.W. "Mechanistic Considerations in the Plasma Deposition of Silicon Nitride Films" *J. Electrochem. Soc.*, 137, 7, (1990), pp.2222-2226.

Chowdhury, F.M. "Bulk Silane Release and Vapor Cloud Explosion", *Semiconductor International*, June, (1996), pp.155-160.

Cicala, G., Bruno, G., Capezzuto, P. and Losurdo, M. "Study of $\text{SiF}_4\text{-N}_2\text{-H}_2$ Plasmas for the Deposition of Fluorinated Silicon Nitride Films", *Mat. Res. Soc. Symp. Proc.*, Vol. 284, 1993, pp.27-32.

Claasen, W.A.P. "Ion Bombardment-Induced Mechanical Stress in Plasma Enhanced Deposited Silicon Nitride and Silicon Oxynitride Films", *Plasma Chem, Plasma Proc.*, 7, 1, (1987), pp.109-124.

Collins, D.J., Strojwas, A.J. and White Jr, D.D. "A CFD Model for the PECVD of Silicon Nitride", *IEEE Trans. Semicond. Manuf.*, 7, 2, (1994), pp. 176-183.

Cotter, D. "A Critical Study in Main-group Pi Bonding", *Molecular Modelling in the Undergraduate Curriculum* University of Massachusetts, January 18, 1996.

Cuthbertson, A.F. and Glidewell, C. "Ligands of Low Electronegativity in the VSEPR Model: Molecules and Ions Isoelectronic with Primary, Secondary and Tertiary Amines", *J. Mol. Structure*, 92, (1983), pp. 353-359.

Dahlhaus, J., Jutzi, P., Frenck, H-J. and Kulisch, W. " $(\text{Me}_5\text{C}_5)\text{SiH}_3$ and $(\text{Me}_5\text{C}_5)_2\text{SiH}_2$ as Precursors for Low-Temperature Remote Plasma-Enhanced CVD of Thin Si_3N_4 and SiO_2 Films", *Advanced Materials*, 5, 5, (1993), pp.377-380.

Dange, M.D., Lee, J.Y. and Sooriakumar, K. "New Applications of Low Temperature PECVD Silicon Nitride Films for Microelectronic Device Fabrication", *Microelect. Journal*, 22, 7-8, (1991), pp.19-26.

Dasent W. E., *Inorganic Energetics*, (Penguin, 1970), pp.126-129.

Dharmadhikari, V.S. "Summary Abstract: Comparative Study of Plasma-Enhanced Chemical Vapour Deposited Silicon Nitride Films", *J. Vac. Sci. Tech.*, A6 (3), (1988), pp.1922-1923.

Donzelli, G.P. and Gabbrielli, B. "Comparative Effects of Polyimide and PECVD Silicon Nitride as Passivating Layers on GaAs Power MESFET Characteristics", *Applied Surface Science*, 30, (1987), pp.95-99.

Drews, M.A., Schenck W.L., Smith, J.D., Walker, J. and Yaws, C.L. "Physical Properties of Semiconductor Industry Chlorosilanes", *Solid State Tech.*, Jan, (1973), pp.39-42.

Dun, H., Pan, P., White, F.R. and Douse, R.W. "Mechanism of Plasma-Enhanced Silicon Nitride Deposition Using SiH_4/N_2 Mixture", *J. Electrochem. Soc.*, 128, 7, (1981), pp.1555-1563.

Ebsworth, E.A.V., Hall, J.R., MacKillop, M.J., McKean, D.C., Sheppard, N. and Woodward, L.A. "Vibrational Spectra and Structure of Trisilylamine and Trisilylamine-*d*₉", *Spectrochimica Acta*, 13, (1958), pp.202-211.

Egitto, F.D. "Radial Wafer to Wafer Uniformity of Plasma-Deposited Si-N Films", *J. Electrochem. Soc.*, 127, 6, (1980), pp.1354-1359.

Engle, G.M. US Patent, 4,223,048, (1978).

Fainer, N.I., Rumyantsev, Y.M., Kosinova, M.L., Yurjev, G.S., Maximovskii, E.A. and Kuznetsov, F.A. "The Investigation of Properties of Silicon Nitride Films Obtained by RPECVD from Hexamethyldisilazane" *Applied Surface Science*, 113/114, (1997), pp.614-617.

Field, D Klemperer, D.F and Wade I.T "Spectroscopic Studies of Fluorescent Emission in Plasma Etching of Silicon Nitride", *J. Vac. Sci. Tech.*, B6 (2), (1988), pp.551-558.

Fitzgerald, M. "Liquid Replacements for Arsine/Phosphine", *Solid State Tech.*, May, (1991), pp.53-54.

Fthenakis, V.M. and Moskowitz, P.D. "An Assessment of Silane Hazards", *Solid State Tech.*, 33, 1, (1990), pp.81-85.

Fujita, S., Toyoshima, H., Ohishi, T. and Sasaki, A. "Plasma-Enhanced Chemical Vapor Deposition of Fluorinated Silicon Nitride", *Japanese Journal of Applied Physics*, 23, 3, (1984a), pp.L144-L146.

Fujita, S., Toyoshima, H., Ohishi, T. and Sasaki, A. "Plasma-Deposited Silicon Nitride Films from SiF_2 as Silicon Source", Japanese Journal of Applied Physics, 23, 5, (1984b), pp.L268-L270.

Gereth, R. and Scherber, W. "Properties of Ammonia-Free Nitrogen- Si_3N_4 Films Produced at Low Temperatures", J. Electrochem. Soc., 119, 9, (1972), pp.1248-1254.

Glidewell, C. "Some Chemical and Structural Consequences of Non-bonded Interactions", Inorg. Chim. Acta, 12, (1975), pp.219-227.

Glidewell, C. and Thomson, C. "The Structure and Acid-Base Properties of Methyl and Silyl Amines and Phosphines: An Ab-Initio SCF Study", J. Comp. Chem., 3, 4, (1982), pp.495-506.

Gmelin Handbook of Inorganic Chemistry, 8th edition, Si supplement B 5c, (Springer-Verlag, 1990).

Gmelin Handbook of Inorganic Chemistry, 8th edition, Si supplement B 4, (Springer-Verlag, 1989).

Gmelin Handbook of Inorganic Chemistry, 8th edition, Si supplement B 1, (Springer-Verlag, 1982).

Gmelin Handbook of Inorganic Chemistry, Borverbindungen Teil 19, (Springer-Verlag, 1978).

Gordon, R.G., Hoffman, D.M. and Riaz, U. "Silicon Dimethylamido Complexes and Ammonia as Precursors for the Atmospheric Pressure Chemical Vapor Deposition of Silicon Nitride Thin Films", Chem. Mater., 2, 5, (1990), pp. 480-482.

Gorowitz, B. Gorczyca, T.B. and Saia, R.J. "Applications of Plasma Enhanced Chemical Vapour Deposition in VLSI", Solid State Tech., 28, June, (1985), pp.197-203.

Gritsenko, V.A., Novikov, Y.N. and Morokov, Y.N. "MINDO/3 Calculation of the Electronic Structure of Silicon Nitride", *Physics of the Solid State*, 39, 8, (1997), pp.1191-1196.

H&SE, EH40/98 - Occupational Exposure Limits 1998, (HSE Books, 1998).

Hamaya, T., Yamazaki, S., Nagayama, S., Abe, M., Kanehana, M. and Fukada, T. "Silicon Nitride Film", *Japan Kokai Tokkyo Koho*, 61,234,533, (1986a).

Hamaya, T. and Yamazaki, S. "Silicon Nitride Film", *Japan Kokai Tokkyo Koho*, 61,234,534, (1986b).

Hammond, M.L. "Safety in Chemical Vapor Deposition", *Solid State Tech.*, 23, 12, (1980), pp.104-109.

Han, I.K. Lee, Y.J. Jo, J.H. Lee, J.I. and Kang, K.N. "Heating Effect in Plasma-Enhanced Chemical Vapour Deposition of Silicon Nitride", *J. Mater. Sci. Lett.*, 10, (1991), pp.526-528.

Hasegawa, S., Matsuda, M. and Kurata, Y. "Bonding Configuration and Defects in Amorphous $\text{SiN}_x\text{:H}$ Films", *Appl. Phys. Lett.*, 58 (7), 18 February, (1991), pp.741-743.

Hasegawa, S., Matsuda, M. and Kurata, Y. "Si-H and N-H Vibrational Properties in Glow-Discharge Amorphous $\text{SiN}_x\text{:H}$ Films ($0 < x < 1.55$)", *Appl. Phys. Lett.*, 57 (21), 19 November, (1990), pp.2211-2213.

Hedberg, K. "The Molecular Structure of Trisilylamine (SiH_3)₃N", *J. Am. Chem. Soc.*, 77, (1955), pp.6491-6492.

Hehre, W.J. and Huang, W.W., *Chemistry with Computation*, (Wavefunction, Inc, 1995), pp.54-60.

Helix, M.J. Vaidyanathan, K.V. Streetman, B.G. Dietrich, H.B. and Chatterjee, P.K. "RF Plasma Deposition of Nitride Layers", *Thin Solid Films*, 55, (1978), pp.143-148.

Herzberg, G., *Molecular Spectra and Molecular Structure. II. Infrared and Raman Spectra of Polyatomic Molecules*, (Van Nostrand, 1960), Chapter V.

Heslop, R.B. and Jones, K., *Inorganic Chemistry - A Guide to Advanced Study*, (Elsevier Scientific, 1976), p.276.

Hess, D.W. "Plasma Enhanced CVD: Oxides, Nitrides, Transition Metals, and Transition Metal Silicides", *J. Vac. Sci. Tech.*, A2 (2), (1984), pp.244-252.

Hezel, R. and Lieske, N. "Characterisation of Plasma-Deposited Silicon Nitride Films by Auger Electron Spectroscopy and Electron Energy Loss Spectroscopy", *J. Appl. Phys.*, 53 (3), (1982), pp.1671-1674.

Hicks, S.E. and Gibson, R.A.G. "A Spectroscopic Investigation of Growth Regimes in Silane-Ammonia Discharges Used for Plasma Nitride Deposition", *Plasma Chem. And Plasma Proc.*, 11, 4, (1991), pp.455-472.

Hitchman, M.L. and Jensen, K.F. (eds.), *Chemical Vapor Deposition - Principles and Applications*, (Academic Press, 1993), Chapter 7.

Hoffman, D.M., Rangarajan, S.P., Athavale, S.D. and Economou, D.J. "Plasma-Enhanced Chemical Vapour Deposition of Silicon, Germanium and Tin Thin Films from Metalorganic Precursors", *J. Vac. Sci. Tech.*, A13 (3), (1995), pp.820-825.

Hoffman, D.M., Rangarajan, S.P., Athavale, S.D., Deshmukh, S.C., Economou, D.J., Lui, J.-R., Zheng, Z. and Chu, W.-K. "Plasma-Enhanced Chemical Vapour Deposition of Silicon Nitride Films from a Metal-organic Precursor", *J. Mater. Res.*, 9, 12, (1994), pp.3019-3021.

Hrsak, D., Zuljevic, J.S. and Cosic, M. "Structure, Properties and Application of Silicon Nitride", *Metalurgija*, 37, 1, (1998), pp.39-43.

Hsieh, S.W. Chang, C.Y. Lee, Y.S. Lin, C.W. & Hsu, S.C. "Properties of Plasma-Enhanced-Chemical-Vapor-Deposited $a\text{-SiN}_x\text{:H}$ by Various Dilution Gases", *J. Appl. Phys.*, 76 (6), (1994), pp.3645-3655.

IBM Corp., IBM Technical Disclosure Bulletin, 28, 9, Feb, (1986), p.4170.

Ing, S.W. and Davern, W. "Useful Low Temperature Deposited Silicon Dioxide Films as Diffusion Masks in GaAs", *J. Electrochem. Soc.*, 111, (1964), pp.120-122.

Integrated Circuit Engineering Corp., Practical VLSI Fabrication for the 90's, (I.C.E Corp, 1990), Section 12.

Ishihara, R., Kanoh, H., Uchida, Y., Sugiura, O. and Matsumara, M. "Low-Temperature Chemical-Vapor Deposition of Silicon-Nitride from Tetra-Silane and Hydrogen Azide", *Mat. Res. Soc. Symp. Proc.*, Vol. 284, 1993, pp3-8.

Ishii, Y. Aoki, T. and Miyazawa, S. "Silicon Nitride Film Deposition by Hot Wall Plasma-Enhanced CVD for GaAs LSI", *J. Vac. Sci. Tech.*, B2 (1), (1984), pp.49-53.

Ishikawa, H. "Chemical Vapor Growth Method", Japan Kokai Tokyo Koho, 06,338,497, (1994).

Ishitani, A. and Koseki, S. "Non-Empirical Modelling on SiN_x CVD", *NEC Res. Dev.*, 33, 1, (1992), pp.1-6.

Ishitani, A. and Koseki, S. "A Model for SiN_x CVD Film Growth Mechanism by Using SiH_4 and NH_3 Source Gases", *Extended Abstracts of the 22nd (1990 International) Conference on Solid State Devices and Materials, Sendai*, (1990), pp.187-190.

James A. M., *A Dictionary of Thermodynamics*, (Macmillan Press, 1976).

Janca, J., Necasova, M. and Sikola, T. "Plasma-Deposited Silicon-Nitride Films in HMDS (Hexamethyldisilazane) Vapours", *Acta Physica Slov.*, 33, 3, (1983), pp. 187-193.

Jasinski, J.M., Beach, D.B. and Estes, R.D. "Excimer Laser Induced Photochemistry of Silane-Ammonia Mixtures", *Mat. Res. Soc. Symp. Proc.* Vol. 131, (1989), pp.501-506.

Jousse, D. Kanicki, J. Krick, D.T. and Lenahan, P.M. "Electron-Spin-Resonance Study of Defects in Plasma-Enhanced Chemical Vapour Deposited Silicon Nitride", *Appl. Phys. Lett.*, 52(6), (1988), pp.445-447.

Julian, M.M. and Gibbs, G.V. "Modeling the Configuration about the Nitrogen Atom in Methyl- and Silyl-Substituted Amines", *J. Phys. Chem.*, 92, (1988), pp.1444-1451.

Jun, B.H., Han, S.S., Lee, J.S., Kim, Y.B., Kang, H.Y., Koh, Y.B., Jiang, Z.T., Bae, B.S. and No, K. "Fluorinated Silicon Nitride Film for the Bottom Antireflective Layer in Quarter Micron Optical Lithography", *Semicond. Science and Tech.*, 12, 7, (1997), pp.921-926.

Kaganowicz, G and Robinson, J.W. "Relation Between Flow, Power, and Presence of Carrier Gas During Plasma Deposition of Thin Films", *J. Vac. Sci. Tech.*, A4 (4), (1986), pp.1901-1904.

Kanoh, H., Sugiura, O., Fujioka, S., Aramaki, Y., Hattori, T. and Matsumura, M. "Low Temperature Formation Chemical Vapour Deposition of Silicon Nitride", *Journal de Physique II*, 1, 7, (1991), pp.831-837.

Katoh, K. Yasui, M. and Watanabe, H. "Plasma-Enhanced Deposition of Silicon Nitride from $\text{SiH}_4\text{-N}_2$ Mixture" *Jap. J. Appl. Phys.*, 22, 5, (1983), pp.L321-L323.

Keqiang, C., Erli, Z., Jinfu, W., Hansheng, Z., Zuoyao, G. and Bangwei, Z. "Microwave Electron Cyclotron Resonance Plasma for Chemical Vapour Deposition and Etching", *J. Vac. Sci, Tech.*, A4 (3), (1986), pp.828-831.

Kim, M.J. "MOS-FET Fabrication Problems", *Solid State Electronics*, 12, (1969), pp.557-571.

Kitoh, H. and Muroyama, M. "Formation of SiN Films by Plasma-Enhanced Chemical Vapor Deposition Using $[(\text{CH}_3)_2\text{N}]_3\text{SiN}_3$ ", Japanese Journal of Applied Physics, 33, 12B, (1994), pp.7076-7079.

Knox J. H., Molecular Thermodynamics, (Wiley-Interscience, 1971), pp. 95-136.

Kriegsmann, H. and Förster, W. "Das Schwingungsspektrum des Trisilylamins", Z. Anorg. Allgem. Chem., 298, (1959), pp.212-222.

Kubaschewski, O., Alcock, C.B and Spencer P.J., Materials Thermochemistry, Sixth Edition, (Pergamon, 1993), pp.174-176.

Kuo, Y. "PECVD Silicon Nitride as a Gate Dielectric for Amorphous Silicon Thin Film Transistor", J. Electrochem. Soc., 142, 1, (1995), pp.186-190.

Lanford, W.A. Trautvetter, H.P. Zeigler, J.F. and Keller, J. "New Precision Technique for Measuring the Concentration Versus Depth of Hydrogen in Solids", Appl. Phys. Lett., 28(9), (1976), pp.566-568.

Leahy, M.F. and Kaganowicz, G. "Magnetically Enhanced Plasma Deposition and Etching", Solid State Tech., 30, 4, (1987), pp.99-104.

Leclerc, S., Lecours, A., Caron, M., Richard, E., Turcotte, G. and Currie, J.F. "Electron Cyclotron Resonance Plasma Chemical Vapor Deposited Silicon Nitride for Micromechanical Applications", J. Vac. Sci. Tech. A16, (2), (1998), pp.881-884.

Lee, J.Y-M. Sooriakumar, K and Dange, M.M "The Preparation, Characterisation and Application of Plasma-Enhanced Chemically Vapour Deposited Silicon Nitride Films Deposited at Low Temperatures", Thin Solid Films, 203, (1991), pp.275-287.

Lee, K.R., Sundaram, K.B. and Malocha, D.C. "Deposition Parameters Studies of Silicon Nitride Films Prepared by Plasma-Enhanced CVD Process Using Silane-Ammonia", J. Mater. Science: Materials in Electronics, 4, (1993), pp.283-287.

Lide, D. A., Handbook of Chemistry and Physics, 74th edition, (CRC Press, 1993).

Ling, C.H. Kwok, C.Y. and Prasad, K. "Plasma-Enhanced Chemical Vapor Deposition SiN Films: Some Electrical Properties", J. Vac. Sci, Tech., A5 (4), (1987), pp.1874-1878.

Livant, P., McKee, M.L. and Worley, S.D. "Photoelectron Spectroscopic and Theoretical Study of Tris(trimethylsilyl)amine and Related Silylamines. Real and Hypothetical Planar Tertiary Amines", Inorg. Chem, 22, (1983), pp. 895-901.

Livengood, R.E. and Hess, D.W. "Plasma Enhanced Chemical Vapour Deposition of Fluorinated Silicon Nitride using SiH₄-NH₃-NF₃ Mixtures", Appl. Phys. Lett., 50(10), 9 Mar, (1987), pp.560-562.

Lucovsky, G. and Tsu, D.V. "Plasma Enhanced Chemical Vapour Deposition: Differences Between Direct and Remote Plasma Excitation", J. Vac. Sci. Tech., A5 (4), (1987), pp.2231-2238.

Lucovsky, G., Richard, P.D., Tsu, D.V., Lin, S.Y. and Markunas, R.J. "Deposition of Silicon Dioxide and Silicon Nitride by Remote Plasma Enhanced Chemical Vapour Deposition", J. Vac. Sci. Tech., A4 (3), (1986), pp.681-688.

Lucovsky, G., Yang, J., Chao, S.S., Tyler, J.E. and Czubytyj, W. "Nitrogen-Bonding Environments in Glow-Discharge-Deposited a-Si:H Films", Physical Review B, 28, 6, (1983), pp.3234-3240.

Madden, H.H. "AES Investigation of the Chemical Structure of Plasma-Deposited Silicon Nitride" J. Electrochem. Soc., 128, 3, (1981), pp.625-629.

Maeda, K. and Umezu, I. "Hydrogen Bonding Configurations in Silicon Nitride Films Prepared by Plasma-Enhanced Deposition", J. Appl. Phys., 70 (5), 1 September (1991), pp.2745-2754.

Maeda, M. and Nakamura, H. "Hydrogen Bonding Configurations in Silicon Nitride Films Prepared by Plasma-Enhanced Deposition", *J. Appl. Phys.*, 58 (1), (1985), pp.484-489.

Maeda, M. and Nakamura, H. "Insulation Degradation and Anomalous Etching Phenomena in Silicon Nitride Films Prepared by Plasma Enhanced Deposition", *Thin Solid Films*, 112, (1984), pp.279-288.

Martineau, P.M. and Davies, P.B. "PECVD - A Technique for New Technologies", *Chemistry in Britain*, October, (1989), pp.1018-1022.

Mazaev, V.A., Talanov, V.N., Il'in, M.M., Tsapuk, A.K., Miklin, L.S. and Domashenko, T.M. "Thermal Decomposition of Poly-N-Methylcyclosilazane", *Inorganic Materials*, 19, (1983), pp.1796-1799.

Meyer, O. and Scherber, W. "Analysis of Silicon Nitride Deposited from SiH_4 and N_2 on Silicon", *J. Phys. Chem. Solids*, 32, (1971), pp.1909-1915.

Meyyappan, M., Govindan, T.R. and Kreskovsky, J.P. "Plasma Modelling in Microelectronic Processing", *Proc. SPIE - Int. Soc. Opt. Eng.*, 1392, (1991), pp.67-76.

Miller, F.A., Perkins, J., Gibbon G.A. and Swisshelm, B.A. "Trisilylamine : Nitrogen Isotopic Effect in the Raman Spectrum and Planarity of the NSi_3 Skeleton", *J. Raman Spect.*, 2, (1974), pp. 93-100.

Miller, F.A. "Molecules We Have Recently Met", *Applied Spectroscopy*, 29, 6, (1975), pp. 461-469.

Miller, G.A. "Arsine and Phosphine Replacements for Semiconductor Processing", *Solid State Tech.*, August, (1989), pp. 59-60.

Miller, N.E. and Beinglass, I. "Hot-Wall CVD Tungsten for VLSI", *Solid State Tech.*, 23, Dec, (1980), pp.79-82.

Mito, H. and Sekiguchi, A. "Induction Heated Plasma Assisted Chemical Vapour Deposition of SiN", *J. Vac. Sci. Tech.*, A4 (3), (1986), pp.475-479.

Mitzel, N.W., Bissinger, P. and Schmidbaur, H. "Synthesis and Structure of (Hydridosilyl)hydrazines", *Chemische Berichte*, 126, (1993), pp.345-350.

Moriwaki, T. and Matsumoto, O. "Formation of Silicon Nitride Film by Plasma Decomposition of Methylsilazane", *J. Am. Ceram. Soc.*, 78, 5, (1995), pp. 1420-1422.

Morosanu, C.-E. and Soltuz, V. "Thin Film Preparation by Plasma and Low Pressure CVD in a Horizontal Reactor", *Vacuum*, 31, 7, (1981), pp.309-319.

Morosanu, C.-E. "The Preparation, Characterisation and Applications of Silicon Nitride Thin Films", *Thin Solid Films*, 65, (1980), pp.171-208.

Morosanu, C.-E. "A Bibliography on Silicon Nitride Films", *Microelectron. Reliab.*, 20, (1980), pp.357-370.

Murley, D., French, I., Deane, S. and Gibson, R. "The Effect of Hydrogen Dilution on the Aminosilane Plasma Regime used to Deposit Nitrogen-Rich Amorphous Silicon Nitride", *J. Non-Crystalline Solids*, 200, Pt.2, (1996), pp.1058-1062.

Nallapati, G. and Ajmera, P.K. "Process Characterization of Plasma Enhanced Chemical Vapor Deposition of Silicon Nitride Films with Disilane as Silicon Source", *J. Vac. Sci. Tech. B*16, (3), (1998), pp.1077-1081.

Narikawa, S., Kojima, Y. and Ehara, S "Investigations of N-H and Si-N Bonding Configurations in Hydrogenated Amorphous Silicon Nitride Films by Infrared Absorption Spectroscopy", *Japanese Journal of Applied Physics*, 24, 11, (1985), pp.L861-L863.

Nelson, N.J. "Silicon Nitride Films and Method of Deposition", US Patent, 4,158,717, (1979).

Newboe, B. "Toxic Gas: A Cause for Alarm", *Semiconductor International*, 14, 12, (1991), pp.68-72.

Nguyen, S.V. and Fridman, S. "Plasma Deposition and Characterisation of Thin Silicon-Rich Nitride Films", *J. Electrochem. Soc.*, 134, 9, (1987), pp.2324-2329.

Nguyen, S.V. "Plasma Deposition of Silicon Nitride and Silicon Oxynitride Using Inert Carrier Gases as Transport Agents", *Electrochem. Soc. Ext. Abs.*, 83-1, A136, (1983), pp.216-217.

Nishibayashi, Y. Imura, T. Osaka, Y. and Shizuma, K. "Properties of Amorphous Silicon Nitride Prepared at High Deposition Rate", *Jap. J. Appl. Phys.*, 24, 6, (1985), pp.L469-L471.

NIST Webbook URL - <http://webbook.nist.gov/chemistry/>

Noodleman, L. and Paddock, N.L. "Trimethylamine, Trisilylamine and Trigermylamine: A Comparative Study of Ionisation Energies, Charge Distribution and Bonding", *Inorganic Chemistry*, 18, 2, (1979), pp.354-360.

Olcaytug, F. Reidling, K and Fallman, W "A Low Temperature Process for the Reactive Formation of Si_3N_4 Layers on InSb", *Thin Solid Films*, 67, (1980), pp.321-324.

O.U. Course Team, ST 294 Principles of Chemical Processes Thermodynamics Parts 1 and 2, (Open University Press, 1975).

Osenbach, J.W., Zell, J.L., Knolle, W.R. and Howard, L.J. "Electrical, Physical and Chemical Characteristics of Plasma-Assisted Chemical-Vapor Deposited Semi-Insulating a-SiN:H and their Use as a Resistive Field Shield for High Voltage Integrated Circuits", *J. Appl. Phys.*, 67, 11, 1 June, (1990), pp.6830-6843.

Pai, C.S., Miner, J.F. and Foo, P.D. "Electron-Cyclotron Resonance Microwave-Discharge for Oxide Deposition using Tetramethylcyclotetrasiloxane", *J. Appl. Phys.*, 73, 7, (1993), pp.3531-3538.

Perkins, P.G. "The ($p \rightarrow d$) π -Bond in Trisilylamine", Chem. Comm., (1967) pp. 268-270.

Philipp, H.R. "Optical Properties of Silicon Nitride", J. Electrochem. Soc., 120, 2, (1973), pp.295-300.

Porritt, C.J. "Violent Reaction Between Silicon Fluoride and Lithium Nitride", Chemical Abstracts, 91: 221672, (1979), p.677.

Pradhan, M.M. and Arora, M. "Low Temperature Fourier Transform Infrared Spectroscopic Studies of Hydrogenated Amorphous Silicon Nitride Films", Japanese Journal of Applied Physics, 31, 2A, (1992), pp.176-180.

Rand, M.J. "Plasma Promoted Deposition of Thin Inorganic Films", J. Vac. Sci. Tech., 16 (2), (1979), pp.420-427.

Reimer, J.A. Vaughan, R.W. Knights, J.C. and Lujan, R.A. "Proton Magnetic Resonance Spectra of Plasma-Deposited Inorganic Thin Films", J. Vac. Sci. Tech., 19 (1), (1981), pp.53-56.

Reinberg, A.R. "Single Component Monomer for Silicon Nitride Deposition", US Patent, 4,200,666, (1980).

Reinberg, A.R. "Plasma Deposition of Inorganic Thin Films", Ann. Rev. Mater. Sci., 9, (1979a), pp.341-372.

Reinberg, A.R. "Plasma Deposition of Inorganic Silicon Containing Films", J. Electron. Mater., 8, 3, (1979b), pp.345-375.

Reinberg, A.R. "Radial Flow Reactor", US Patent, 3,757,733, (1973).

Retajczyk, T.F. and Sinha, A.K. "Elastic Stiffness and Thermal Expansion Coefficients of Various Refractory Silicides and Silicon Nitride Films", Thin Solid Films, 70, (1980), pp.241-247.

Robertson, J. "Defect and Impurity States in Silicon Nitride", J. Appl. Phys., 54, 8, August, (1983), pp.4490-4493.

Robinson, D. "The Vibrational Spectra of Trisilylamine and and Trisilylamine-*d*₉", J. Am. Chem. Soc., 80, (1958), pp.5924-5927.

Ron, Y., Raveh, A., Carmi, U., Inspektor, A. and Avni, R. "Deposition of Silicon Nitride from SiCl₄ and NH₃ in a Low Pressure R.F. Plasma", Thin Solid Films, 107, (1983), pp.181-189.

Rosler, R.S. and Engle, G.M. "Plasma Enhanced CVD in a Novel LPCVD Type System", Solid State Tech., 24, 4, (1981), pp.172-177.

Rosler, R.S., Benzing, W.C. and Baldo, J. "A Production Reactor for Low Temperature Plasma-Enhanced Silicon Nitride Deposition", Solid State Tech., June, (1976), pp.45-50.

Rosler, R.S. "The Evolution of Commercial Plasma Enhanced CVD Systems", Solid State Tech., 34, June, (1991), pp.67-71.

Sanjoh, A. Ikeda, N. Komaki, K. and Shintani, A. "Analysis of Interface States Between Plasma-CVD Silicon Nitride and Silicon-Substrate using Deep-Level Transient Spectroscopy", J. Electrochem. Soc., 137, 9, (1990), pp.2974-2979.

Scantlin, W.M and Norman, A.D "The Borane-Catalyzed Condensation of Trisilazane and N-Methyldisilazane" Inorganic Chemistry, 11, 12, (1972), pp.3082-3084.

Scarsbrook, G. Llewellyn, I.P. Ojha, S.M. and Heinecke, R.A. "Low Temperature Pulsed Plasma Deposition. Part 1 - A New Technique for Thin Film Deposition with Complete Gas Dissociation", Vacuum, 38, 8-10, (1988), pp.627-631.

Schlosser, T., Sladek, A., Hiller, W. and Schmidbaur, H. "New Mono- and Spirobicyclic aminosilanes: Synthesis, Structure and Properties", Z. fur Naturforschung, 49, (1994), pp.1247-1255.

Schlote, J., Tittelbachhelmrich, K., Tillack, B., Kuck, B. and Hunlich, T. "Systematic Classification of LPCVD Processes", *J. De Physique IV*, 5, C5, (1995), pp.283-290.

Schuh, H., Schlosser, T., Bissinger, P. and Schmidbaur, H. "Disilanyl-amines - Compounds Comprising the Structural Unit Si-Si-N, as Single Source Precursors for Plasma-Enhanced Chemical Vapour Deposition (PE-CVD) of Silicon Nitride", *Z. Anorg. Allg. Chem*, 619, (1993), pp.1347-1352.

Scott, B.A. Martinez-Duart, J.M. Beach, D.B. Nguyen, T.N. Estes, R.D. and Schad, R.G. "Preparation of Silicon Nitride with Good Interface Properties by Homogeneous Chemical Vapour Deposition", *Chemtronics*, 4, Dec, (1989), pp.230-234.

Sequeda, F. and Richardson Jr, R.E. "Summary Abstract: Silicon Nitride Deposition by Plasma Enhanced Low Pressure CVD Technique", *J. Vac. Sci. Tech.*, B8(2), (1981), pp.362-363.

Shams, Q.A. and Brown, W.D. "Effects of Nitrogen and Argon as Carrier Gases and Annealing Ambients on the Physical Properties of PECVD Silicon Nitride", *Microelect. Journal*, 20, 6, (1989a), pp.49-59.

Shams, Q.A. and Brown, W.D. "Effects of Post-Deposition Argon Implantation on the Memory Properties of Plasma Deposited Silicon Nitride Films", *J. Appl. Phys.*, 66 (7), (1989b), pp.3131-3135.

Sherman, A., *Chemical Vapor Deposition for Microelectronics* (Noyes, 1987).

Shiloh, M., Gayer, B. and Brinckman, F.E. "Preparation of Nitrides by Active Nitrogen. II. Si_3N_4 ", *J. Electrochem. Soc.*, 124, 2, (1977), pp.295-300.

Shitova, E.V. Vodzinskii, V.Y. and Kruze, T.A. "Mechanism of Synthesis of Silicon Nitride Films", *Inorganic Materials*, 11, (1975), pp.691-694.

Sidgwick, N.V., *The Chemical Elements and their Compounds*, Vol. 1 (Oxford Univ. Press, 1952).

Singer, P. "Trends in Liquid Sources", *Semicond. Int.*, June, (1993), pp.92-97.

Sinha, A.K. Levinstein, H.J. Smith, T.E. Quintana, G. and Hászko, S.E. "Reactive Plasma Deposited Si-N Films for MOS-LSI Passivation", *J. Electrochem. Soc.*, 125, 4, (1978a), pp.601-608.

Sinha, A.K. Levinstein, H.J. Smith, T.E. "Thermal Stresses and Cracking Resistance of Dielectric Films (SiN , Si_3N_4 , and SiO_2) on Si Substrates", *J. Appl. Phys.*, 49 (4), (1978b), pp.2423-2426.

Sinha, A.K. and Lugujo, E. "Lorentz-Lorentz Correlation for Reactively Plasma Deposited Si-N Films", *Appl. Phys. Lett.*, 32(4), (1978c), pp.245-246.

Smirnova, T.P. and Yakovkina, L.V. "The Mechanism of Dehydrogenation of $\text{SiN}_x\text{:H}$ Films", *Thin Solid Films*, 293, 1-2, (1997), pp.6-10.

Smith, D.L., Alimonda, A.S., Chen, C-C., Ready, S.E. and Wacker, B. "Mechanism of SiN_xH_y Deposition from $\text{NH}_3\text{-SiH}_4$ Plasma", *J. Electrochem. Soc.*, 137, 2 (1990a), pp.614-623.

Smith, D.L., Alimonda, A.S. and von Preissig, F.J. "Mechanism of SiN_xH_y Deposition from $\text{N}_2\text{-SiH}_4$ Plasma", *J. Vac. Sci. Tech.*, B8 (3), (1990b), pp.551-557.

Snow, W.R. "An Overview of PECVD Reactor System Capabilities for the Deposition of Electronic Materials", *Proceedings of the Tenth International Conference on Chemical Vapor Deposition 1987*, Honolulu, HI, Oct, 1987, pp.819-830.

Soldner, M., Riede, J., Schier, A. and Schmidbaur, H. "Isomeric Cyclic Disilanediyldimethylhydrazines", *Inorg. Chem.*, 37, 3, (1998a), pp.601-603.

Soldner, M., Schier, A. and Schmidbaur, H. "Binary Si/N-[4.4]-Spirocycles with Two SiH_2SiH_2 Loops", *Inorg. Chem.*, 37, 3, (1998b), pp.510-515.

Sterling, H.F. and Swann, R.C.G. "Chemical Vapour Deposition Promoted by r.f. Discharge", *Solid State Electronics*, 8, (1965), pp.653-654.

Stock, A. and Somieski, K. "Siliciumwasserstoffe, X.: Stickstoffhaltige Verbindungen", *Chemische Berichte*, 54, (1921), pp.740-758.

Sugiyama, K., Pac, S., Takahashi, Y. and Motojima, S. "Low Temperature Deposition of Metal Nitrides by Thermal Decomposition of Organometallic Compounds", *J. Electrochem. Soc.*, 122, 11 (1975), pp.1545-1549.

Sujishi, S. and Witz, S. "Effect of Replacement of Carbon by Silicon in Trimethylamine on the Stabilities of the Trimethyl-boron Addition Compounds. Estimation of the Resonance Energy for Silicon-Nitrogen Partial Double Bonds", *J. Am. Chem. Soc.*, 76, (1954), pp.4631-4636.

Suzuki, K. and Matsui, J. "SiN Membrane Masks for X-ray Lithography", *J. Vac. Sci. Tech.*, 20 (2), (1982), pp.191-194.

Sze, S.M. (Ed.), *VLSI Technology*, Second Edition, (McGraw-Hill, 1988).

Sze, S.M. (Ed.), *VLSI Technology*, (McGraw-Hill, 1983).

Tachibana, A. and Kurosaki, Y. "Direct Reaction Pathways for Silicon Nitride Bond Formation in the $\text{SiH}_4\text{-NH}_3$ Mixture in Gas Phase", *Acta Chimica Hungarica - MODELS IN CHEMISTRY*, 130 (1), (1993), pp.111-128.

Tachibana, A., Yamaguchi, K., Kawauchi, S., Kurosaki, Y. and Yamabe, T. " SiH_3 Radical Mechanism for Si-N Bond Formation", *J. Am. Chem. Soc.*, 114, (1992), pp.7504-7507.

Taylor, P.A. "Silicon Source Gases for Chemical Vapour Deposition", *Solid State Tech.*, May, (1989), pp.143-148.

Taylor, P.A. "Silane: Manufacture and Applications", *Solid State Tech.*, July, (1987), pp.53-59.

Thuraisingham, R.A. "Inclusion of Polarisation Functions in Molecular SCF Calculations", *Indian J. Chem.*, Vol. 18A, (1979), 509-511.

Trotman-Dickenson, A.F. (Exec. Ed.), *Comprehensive Inorganic Chemistry*, (Pergamon Press, 1973).

Tsu, D.V., Lucovsky, G. and Mantini, M.J. "Local Atomic Structure in Thin Films of Silicon Nitride and Silicon Diimide Produced by Remote Plasma-Enhanced Chemical-Vapour Deposition", *Physical Review B*, 33, 10, (1986a), pp.7069-7076.

Tsu, D.V. and Lucovsky, G. "Silicon Nitride and Silicon Diimide Grown by Remote Plasma Enhanced Chemical Vapour Deposition", *J. Vac. Sci. Tech.*, A4 (3), (1986b), pp.480-485.

Tucker, E.A. "Liquid Replacements for Arsine and Phosphine Gas", *European Semiconductor*, March, (1989), p.51.

Tucker, E.A. "Silane - Its Properties and Hazards", *Euro. Semicond. Des. & Prod.*, July, (1985), pp.27-29.

Turkdogan, E.T., Bills, P.M. and Tippett, V.A. "Silicon Nitrides: Some Physico-Chemical Properties", *J. Appl. Chem.*, 8, May, (1958), pp.296-302.

University of Maine, Department of Chemistry, CHY 551, Introduction to Molecular Modeling Course Notes.

Valco, G.J., Kapoor, V.J., Biedenbender, M.D. and Williams, W.D. "Plasma Deposited Silicon Nitride for Indium Phosphide Encapsulation", *J. Electrochem. Soc.*, 136, 1, (1989), pp.175-182.

Valco, G.J. and Kapoor, V.J. "Plasma Deposited Silicon Nitride for Gallium Arsenide Encapsulation", *J. Electrochem. Soc.*, 134, 3, (1987), pp.685-692.

Varma, R., MacDiarmid, A.G. and Miller, J.G. "Electric Dipole Moment of Trisilylamine", *J. Chem. Phys.*, 39, (1963), pp.3157-3158.

Voronkov, M.G., Sulimin, A.D., Iachmenev, V.V., Mirskov, R.G. and Chernova, V.G. "Production of Silicon-Nitride Films from Hexamethylcyclotrisilazane in a High Frequency Glow Discharge" *Doklady Akademii NAUK SSSR*, 259, 5, (1981), pp.1130-1132.

Wang, C.K., Ying, T.L., Wei, C.S. and Liu, L.M. "Investigation of a High Quality and Ultraviolet Light Transparent Plasma-Enhanced Chemical Vapor Deposition Silicon Nitride for Non-Volatile Memory Application", *Japanese Journal of Applied Physics*, 34, 9A, (1995), pp. 4736-4740.

Ward, L.G.L. "Bromosilane, Iodosilane, and Trisilylamine", *Inorganic Syntheses*, Volume XI, ed. Jolly, W.L. (McGraw-Hill, 1970), pp.159-170.

Watanabe, N., Yoshida, M., Jiang, Y-C., Nomoto, T. and Abiko, I. "Preparation of Plasma Chemical Vapor Deposition Silicon Nitride Films from SiH_2F_2 and NH_3 Source Gases" *Japanese Journal of Applied Physics*, 30, 4A, (1991), pp.L619-L621.

Weast, R.C., *Handbook of Chemistry and Physics*, 55th edition, (CRC Press, 1974).

Wells, R.L. and Schaeffer, R. "Studies of Silicon-Nitrogen Compounds. The Base-Catalysed Elimination of Silane from Trisilylamine", *J. Am. Chem. Soc.*, 88:1, Jan 5th, (1966), pp.37-42.

Wendel, J.A. and Goddard III, W.A. "The Hessian Biased Force Field for Silicon Nitride Ceramics: Predictions of Thermodynamic and Mechanical Properties for α - and β - Si_3N_4 ", *J. Chem. Phys.*, 97 (7), 1 October, (1992), pp.5048-5062.

Winderbaum, S., Yun, F. and Reinhold, O. " Application of Plasma Enhanced Chemical Vapor Deposition Silicon Nitride as a Double Layer Antireflection Coating and Passivation Layer for Polysilicon Solar Cells", J. Vac. Sci. Tech., A15, (3), (1997), pp. 1020-1025.

Yang, K.H. "An Optical Imaging Method for Wafer Warpage Measurements", J. Electrochem. Soc., 132, 5, (1985), pp.1214-1218.

Yasui, K., Otsuki, K. and Akahane, T. "Silicon Nitride Films Grown by Hydrogen Radical Enhanced Chemical Vapour Deposition Utilizing Trisdimethylaminosilane", J. Non-Crystalline Solids, 169, (1994), pp.301-305.

Yasui, K., Katoh, H., Komaki, K. and Kaneda, S. "Amorphous SiN Films Grown by Hot-Filament Chemical Vapor Deposition Using Monomethylamine", Appl. Phys. Lett., 56 (10), (1990a), pp.898-900.

Yasui, K., Nasu, M. and Kaneda, S. "Hydrogen-Radical-Assisted Chemical Vapor Deposition of SiN Films Using $\text{Si}(\text{CH}_3)_4$ and NH_2CH_3 ", Japanese Journal of Applied Physics, 29, 12, (1990b), pp.2822-2823.

Yeh, W.C., Ishihara, R., Morishita, S. and Matsumura, M. "Low Temperature Chemical Vapor Deposition of Silicon Nitride Film from Hexachlorodisilane and Hydrazine", Japanese Journal of Applied Physics, 35, 2B, (1996), pp.1509-L1512.

Yin, Z. and Smith, F.W. "Optical Dielectric Function and Infrared Absorption of Hydrogenated Amorphous Silicon Nitride Films: Experimental Results and Effective-Medium-Approximation Analysis", Physical Review B, 42, 6, (1990), pp.3666-3675.

Yoshimoto, M., Takubo, K., Ohtsuki, T., Komoda, M. and Matsunami, H. "Deposition Mechanism of Silicon Nitride in Direct Photoassisted Chemical Vapor Deposition Using a Low-Pressure Hg Lamp", J. Electrochem. Soc., 142, 6, (1995), pp.1976-1982.

Zarowin, C.B. "A Theory of Plasma-Assisted Chemical Vapor Transport Processes", J. Appl. Phys., 57, 3, 1 February, (1985), pp.929-942.

Zhang, X.M., Ding, K.B., Yang, A.L. and Shao, D.L. "Processing and Characterisation of PECVD Silicon Nitride Film", *Adv. Mater. For Optics and Electronics*, 6, 3, (1996), pp.147-150.

APPENDIX 1

THERMODYNAMIC VALUES FOR MOLECULES

Table A 1

Heat of Formation (ΔH_f°)

Compound	ΔH_f° (kJ mol ⁻¹)	Reference
N(SiH ₃) ₃	- 132.94	This work (1)
N(SiH ₃) ₃	- 131.0	Gmelin, 1989 (2)
N(SiH ₃) ₂ SiH ₂ NH ₂	- 224.90	This work (1)
N(SiH ₃) ₂ SiH ₂	- 37.67	This work (1)
Si(NH ₂) ₄	- 323.08	This work (1)
Si(NH ₂) ₃	- 225.98	This work (1)
SiH ₃ NH ₂	- 41.67	This work (1)
Si ₃ N ₄	- 743.5	Lide, 1993
SiO ₂	- 910.7	NIST Webbook, 1998
NH ₃	- 45.9	Lide, 1993
NH ₂	+ 109.37	NIST Webbook, 1998
N ₂ O	+ 82.05	NIST Webbook, 1998
SiH ₄	+ 34.3	Lide, 1993
SiH ₃	+ 210.97	Gmelin, 1982
H ₂	0	Lide, 1993
H	+ 218.0	NIST Webbook, 1998
N ₂	0	Lide, 1993
N	+ 472.7	NIST Webbook, 1998
Si	+ 450.0	NIST Webbook, 1998

(1) Mean value of MNDO/d, AM1 and PM3 semi-empirical calculations

(2) Converted from a mean reference value of - 31.3 kcal/mol using the factor 4.186

Table A 2
Standard Molar Entropy Of Formation (S°)

Compound	S° ($\text{J K}^{-1} \text{mol}^{-1}$)	Reference
$\text{N}(\text{SiH}_3)_3$	+ 286.8	This work
Si_3N_4	+ 101.3	Lide, 1993
SiO_2	+ 41.46	NIST Webbook, 1998
NH_3	+ 192.8	Lide, 1993
N_2O	+ 219.96	NIST Webbook, 1998
SiH_4	+ 204.6	Lide, 1993
H_2	+ 130.7	Lide, 1993
N_2	+ 191.5	NIST Webbook, 1998

APPENDIX 2

PARAMETERS USED IN SPARTAN SEMI-EMPIRICAL MO MODELS

# AM1 parameter file (sp, only)	# MNDO parameter file (sp, only)	# MNDO/d parameter file	# PM3 parameter file (sp, only)
#	#	#	#
# elements contained in this file:	# elements contained in this file (MNDO):	# elements contained in this file:	# elements contained in this file:
#	#	#	#
# Hydrogen	# Hydrogen	# Silicon [2]	# Hydrogen
# Boron	# Lithium	# Phosphorus [3]	# Lithium
# Carbon	# Beryllium	# Sulphur [3]	# Beryllium
# Nitrogen	# Boron	# Chlorine [1]	# Boron
# Oxygen	# Carbon	# Bromine [1]	# Carbon
# Fluorine	# Nitrogen	# Iodine [1]	# Nitrogen
# Aluminium	# Oxygen	#	# Oxygen
# Silicon	# Fluorine	atnum 14	# Fluorine
# Phosphorus	# Magnesium	n 3.0	# Magnesium
# Sulfur	# Aluminium	uss -36.0515290	# Aluminium
# Chlorine	# Silicon	upp -27.5356920	# Silicon
# Zinc	# Phosphorus	udd -14.6774390	# Phosphorus
# Germanium	# Sulfur	betas -8.2107340	# Sulfur
# Bromine	# Chlorine	betap -4.8846200	# Chlorine
# Tin	# Calcium	betad -2.6080110	# Calcium
# Iodine	# Zinc	zs 1.9156550	# Zinc
#	# Germanium	zp 1.6816110	# Gallium
atnum 1	# Bromine	zd 0.9667720	# Germanium
n 1.0	# Tin	alpha 1.6600690	# Arsenic
uss -11.3964270	# Iodine	#eisol -81.8118225	# Selenium
upp 0.0000000	# Mercury	gss 10.7416470	# Bromine
betas -6.1737870	# Lead	gsp 7.5606670	# Cadmium
betap 0.0000000	#	gpp 7.4364970	# Indium
zs 1.1880780	atnum 1	#gp2 6.5677543	# Tin
zp 0.0000000	n 1.0	gdd 7.0587500	# Antimony
alpha 2.8823240	uss -11.9062760	hsp 0.8775390	# Tellurium
eisol -11.3964270	upp 0.0000000	hform 108.3900000	# Iodine
gss 12.8480000	betas -6.9890640	zval 4.0000000	# Mercury
gsp 0.0000000	betap 0.0000000	atnum 15	# Thallium
gpp 0.0000000	zs 1.3319670	n 3.0	# Lead
gp2 0.0000000	zp 0.0000000	uss -47.0555310	# Bismuth
hsp 0.0000000	alpha 2.5441341	upp -38.0670590	#
k1 0.1227960	eisol -11.9062760	udd -23.6915970	# Gd*
k2 0.0050900	gss 12.8480000	betas -8.9021040	#
k3 -0.0183360	gsp 0.0000000	betap -9.3861100	atnum 1
k4 0.0000000	gpp 0.0000000	betad -2.0917010	n 1.0
l1 5.0000000	gp2 0.0000000	zs 2.2664630	uss -13.0733210
l2 5.0000000	hsp 0.0000000	zp 1.9400150	upp 0.0000000
l3 2.0000000	hform 52.1020000	zd 1.1001090	betas -5.6265210
l4 0.0000000	zval 1.0000000	alpha 1.8525510	betap 0.0000000
m1 1.2000000	atnum 3	gss 11.4797530	zs 0.9678070
m2 1.8000000	n 2.0	gsp 8.5575700	zp 0.0000000
m3 2.1000000	uss -5.1280000	gpp 8.2487230	alpha 3.3563860
m4 0.0000000	upp -2.7212000	gdd 7.5730170	eisol -13.0733210
hform 52.1020000	betas -1.3500400	hsp 2.1078040	gss 14.7942080
zval 1.0000000	betap -1.3500400	hform 75.5700000	gsp 0.0000000
atnum 5	zs 0.7023800	zval 5.0000000	gpp 0.0000000
n 2.0	zp 0.7023800	atnum 16	gp2 0.0000000
uss -34.4928700	alpha 1.2501400	n 3.0	hsp 0.0000000
upp -22.6315250	eisol -5.1280000	uss -56.8891300	a1 1.1287500
betas -9.5991140	gss 7.3000000	upp -47.2747460	a2 -1.0603290

betap	-6.2737570	gsp	5.4200000	udd	-25.0951180	b1	5.0962820
zs	1.6117090	gpp	5.0000000	betas	-10.9995450	b2	6.0037880
zp	1.5553850	gp2	4.5200000	betap	-12.2154370	c1	1.5374650
alpha	2.4469090	hsp	0.8300000	betad	-1.8806690	c2	1.5701890
eisol	-63.7172650	hform	38.4100000	zs	2.2258510	hform	52.1020000
gss	10.5900000	zval	1.0000000	zp	2.0997060	zval	1.0000000
gsp	9.5600000	atnum	4	zd	1.2314720	atnum	3
gpp	8.8600000	n	2.0	alpha	2.0230600	n	2.0
gp2	7.8600000	uss	-16.6023780	gss	12.1963010	uss	-5.3000000
hsp	1.8100000	upp	-10.7037710	gsp	8.8539010	upp	-3.4000000
k1	0.1826130	betas	-4.0170960	gpp	8.5402330	betas	-0.5500000
k2	0.1185870	betap	-4.0170960	gdd	7.9065710	betap	-1.5000000
k3	-0.0732800	zs	1.0042100	hsp	2.6463520	zs	0.6500000
k4	0.0000000	zp	1.0042100	hform	66.4000000	zp	0.7500000
l1	6.0000000	alpha	1.6694340	zval	6.0000000	alpha	1.2550000
l2	6.0000000	eisol	-24.2047560	atnum	17	eisol	-5.3000000
l3	5.0000000	gss	9.0000000	n	3.0	gss	4.5000000
l4	0.0000000	gsp	7.4300000	uss	-69.6229730	gsp	3.0000000
m1	0.7275920	gpp	6.9700000	upp	-59.1007290	gpp	5.2500000
m2	1.4666390	gp2	6.2200000	udd	-36.6745730	gp2	4.5000000
m3	1.5709750	hsp	1.2800000	betas	-6.0372920	hsp	0.1500000
m4	0.0000000	hform	76.9600000	betap	-19.1833850	a1	-0.4500000
hform	135.7000000	zval	2.0000000	betad	-1.8777820	a2	0.8000000
zval	3.0000000	atnum	5	zs	2.5616110	b1	5.0000000
atnum	6	n	2.0	zp	2.3893380	b2	6.5000000
n	2.0	uss	-34.5471300	zd	1.2513980	c1	1.0000000
uss	-52.0286580	upp	-23.1216900	alpha	2.1803000	c2	1.0000000
upp	-39.6142390	betas	-8.2520540	#eisol	-263.2984770	hform	38.4100000
betas	-15.7157830	betap	-8.2520540	gss	13.2111490	zval	1.0000000
betap	-7.7192830	zs	1.5068010	gsp	9.4194950	atnum	4
zs	1.8086650	zp	1.5068010	gpp	8.9962000	n	2.0
zp	1.6851160	alpha	2.1349930	#gp2	7.9452510	uss	-17.2647520
alpha	2.6482740	eisol	-64.3159500	gdd	8.5819920	upp	-11.3042430
eisol	-120.8157940	gss	10.5900000	hsp	3.0814990	betas	-3.9620530
gss	12.2300000	gsp	9.5600000	hform	28.9900000	betap	-2.7806840
gsp	11.4700000	gpp	8.8600000	zval	7.0000000	zs	0.8774390
gpp	11.0800000	gp2	7.8600000	atnum	35	zp	1.5087550
gp2	9.8400000	hsp	1.8100000	n	4.0	alpha	1.5935360
hsp	2.4300000	hform	135.7000000	uss	-65.4027780	eisol	-25.5166530
k1	0.0113550	zval	3.0000000	upp	-54.5537540	gss	9.0128510
k2	0.0459240	atnum	6	udd	-13.7280990	gsp	6.5761990
k3	-0.0200610	n	2.0	betas	-8.3149760	gpp	6.0571820
k4	-0.0012600	uss	-52.2797450	betap	-10.5070410	gp2	9.0052190
l1	5.0000000	upp	-39.2055580	betad	-0.9625990	hsp	0.5446790
l2	5.0000000	betas	-18.9850440	zs	2.5905410	a1	1.6315720
l3	5.0000000	betap	-7.9341220	zp	2.3308560	a2	-2.1109590
l4	5.0000000	zs	1.7875370	zd	1.3573610	b1	2.6729620
m1	1.6000000	zp	1.7875370	alpha	2.0910500	b2	1.9685940
m2	1.8500000	alpha	2.5463800	#eisol	-247.6408610	c1	1.7916860
m3	2.0500000	eisol	-120.5006060	gss	12.2223550	c2	1.7558710
m4	2.6500000	gss	12.2300000	gsp	8.2637200	hform	76.9600000
hform	170.8900000	gsp	11.4700000	gpp	8.5354640	zval	2.0000000
zval	4.0000000	gpp	11.0800000	#gp2	7.4821520	atnum	5
atnum	7	gp2	9.8400000	gdd	7.3109530	n	2.0
n	2.0	hsp	2.4300000	hsp	2.7495220	uss	-32.62381120
uss	-71.8600000	hform	170.8900000	hform	26.7400000	upp	-22.93367320
upp	-57.1675810	zval	4.0000000	zval	7.0000000	betas	-8.13742162
betas	-20.2991100	atnum	7	atnum	53	betap	-7.48788283
betap	-18.2386660	n	2.0	n	5.0	zs	1.22743088
zs	2.3154100	uss	-71.9321220	uss	-62.7653530	zp	1.53741122
zp	2.1579400	upp	-57.1723190	upp	-50.2921160	alpha	2.30404919
alpha	2.9472860	betas	-20.4957580	udd	-12.2483050	eisol	-62.79771668
eisol	-202.4077430	betap	-20.4957580	betas	-10.6994870	gss	9.50638613

gss	13.5900000	zs	2.2556140	betap	-4.9411780	gsp	8.22164867
gsp	12.6600000	zp	2.2556140	betad	-2.3504610	gpp	8.70903497
gpp	12.9800000	alpha	2.8613420	zs	2.7565430	gp2	8.44827081
gp2	11.5900000	eisol	-202.5662010	zp	2.2530800	hsp	.56610545
hsp	3.1400000	gss	13.5900000	zd	1.5023350	a1	.61297978
k1	0.0252510	gsp	12.6600000	alpha	1.9061740	b1	10.00000000
k2	0.0289530	gpp	12.9800000	#eisol	-229.6231990	c1	.83167600
k3	-0.0058060	gp2	11.5900000	gss	11.9807820	a2	-.47046442
k4	0.0000000	hsp	3.1400000	gsp	7.8559020	b2	6.00000000
l1	5.0000000	hform	113.0000000	gpp	7.7093720	c2	.80408766
l2	5.0000000	zval	5.0000000	#gp2	6.7185660	hform	135.7000000
l3	2.0000000	atnum	8	gdd	6.0972990	zval	3.0000000
l4	0.0000000	n	2.0	hsp	2.0714750	atnum	6
m1	1.5000000	uss	-99.6443090	hform	25.5170000	n	2.0
m2	2.1000000	upp	-77.7974720	zval	7.0000000	uss	-47.2703200
m3	2.4000000	betas	-32.6880820			upp	-36.2669180
m4	0.0000000	betap	-32.6880820			betas	-11.9100150
hform	113.0000000	zs	2.6999050			betap	-9.8027550
zval	5.0000000	zp	2.6999050			zs	1.5650850
atnum	8	alpha	3.1606040			zp	1.8423450
n	2.0	eisol	-317.8685060			alpha	2.7078070
uss	-97.8300000	gss	15.4200000			eisol	-111.2299170
upp	-78.2623800	gsp	14.4800000			gss	11.2007080
betas	-29.2727730	gpp	14.5200000			gsp	10.2650270
betap	-29.2727330	gp2	12.9800000			gpp	10.7962920
zs	3.1080320	hsp	3.9400000			gp2	9.0425660
zp	2.5240390	hform	59.5590000			hsp	2.2909800
alpha	4.4553710	zval	6.0000000			a1	0.0501070
eisol	-316.0995200	atnum	9			a2	0.0507330
gss	15.4200000	n	2.0			b1	6.0031650
gsp	14.4800000	uss	-131.0715480			b2	6.0029790
gpp	14.5200000	upp	-105.7821370			c1	1.6422140
gp2	12.9800000	betas	-48.2904660			c2	0.8924880
hsp	3.9400000	betap	-36.5085400			hform	170.8900000
k1	0.2809620	zs	2.8484870			zval	4.0000000
k2	0.0814300	zp	2.8484870			atnum	7
k3	0.0000000	alpha	3.4196606			n	2.0
k4	0.0000000	eisol	-476.6837810			uss	-49.3356720
l1	5.0000000	gss	16.9200000			upp	-47.5097360
l2	7.0000000	gsp	17.2500000			betas	-14.0625210
l3	0.0000000	gpp	16.7100000			betap	-20.0438480
l4	0.0000000	gp2	14.9100000			zs	2.0280940
m1	0.8479180	hsp	4.8300000			zp	2.3137280
m2	1.4450710	hform	18.8900000			alpha	2.8305450
m3	0.0000000	zval	7.0000000			eisol	-157.6137755
m4	0.0000000	#atnum	12			gss	11.9047870
hform	59.5590000	#n	3.0			gsp	7.3485650
zval	6.0000000	#uss	-15.04			gpp	11.7546720
atnum	9	#upp	-9.264			gp2	10.8072770
n	2.0	#betas	-2.586			hsp	1.1367130
uss	-136.1055790	#betap	-2.842			a1	1.5016740
upp	-104.8898850	#zs	1.049			a2	-1.5057720
betas	-69.5902770	#zp	0.889			b1	5.9011480
betap	-27.9223600	#alpha	1.813			b2	6.0046580
zs	3.7700820	#eisol	-22.69			c1	1.7107400
zp	2.4946700	#gss	7.39			c2	1.7161490
alpha	5.5178000	#gsp	6.57			hform	113.0000000
eisol	-482.2905830	#gpp	6.68			zval	5.0000000
gss	16.9200000	#gp2	5.90			atnum	8
gsp	17.2500000	#hsp	0.82			n	2.0
gpp	16.7100000	#hform	35.0			uss	-86.9930020
gp2	14.9100000	#zval	2.0			upp	-71.8795800
hsp	4.8300000	atnum	13			betas	-45.2026510

k1	0.2420790	n	3.0	betap	-24.7525150
k2	0.0036070	uss	-23.8070970	zs	3.7965440
k3	0.0000000	upp	-17.5198780	zp	2.3894020
k4	0.0000000	betas	-2.6702840	alpha	3.2171020
l1	4.8000000	betap	-2.6702840	eisol	-289.3422065
l2	4.6000000	zs	1.4441610	gss	15.7557600
l3	0.0000000	zp	1.4441610	gsp	10.6211600
l4	0.0000000	alpha	1.8688394	gpp	13.6540160
m1	0.9300000	eisol	-44.4840720	gp2	12.4060950
m2	1.6600000	gss	8.0900000	hsp	0.5938830
m3	0.0000000	gsp	6.6300000	a1	-1.1311280
m4	0.0000000	gpp	5.9800000	a2	1.1378910
hform	18.8900000	gp2	5.4000000	b1	6.0024770
zval	7.0000000	hsp	0.7000000	b2	5.9505120
atnum	13	hform	79.4900000	c1	1.6073110
n	3.0	zval	3.0000000	c2	1.5983950
uss	-24.3535850	atnum	14	hform	59.5590000
upp	-18.3636450	n	3.0	zval	6.0000000
betas	-3.8668220	uss	-37.0375330	atnum	9
betap	-2.3171460	upp	-27.7696780	n	2.0
zs	1.5165930	betas	-9.0868040	uss	-110.4353030
zp	1.3063470	betap	-1.0758270	upp	-105.6850470
alpha	1.9765860	zs	1.3159860	betas	-48.4059390
eisol	-46.4208150	zp	1.7099430	betap	-27.7446600
gss	8.0900000	alpha	2.2053160	zs	4.7085550
gsp	6.6300000	eisol	-82.8394220	zp	2.4911780
gpp	5.9800000	gss	9.8200000	alpha	3.3589210
gp2	5.4000000	gsp	8.3600000	eisol	-437.5171690
hsp	0.7000000	gpp	7.3100000	gss	10.4966670
k1	0.0900000	gp2	6.5400000	gsp	16.0736890
k2	0.0000000	hsp	1.3200000	gpp	14.8172560
k3	0.0000000	hform	108.3900000	gp2	14.4183930
k4	0.0000000	zval	4.0000000	hsp	0.7277630
l1	12.3924430	atnum	15	a1	-0.0121660
l2	0.0000000	n	3.0	a2	-0.0028520
l3	0.0000000	uss	-56.1433600	b1	6.0235740
l4	0.0000000	upp	-42.8510800	b2	6.0037170
m1	2.0503940	betas	-6.7916000	c1	1.8568590
m2	0.0000000	betap	-6.7916000	c2	2.6361580
m3	0.0000000	zs	2.1087200	hform	18.8900000
m4	0.0000000	zp	1.7858100	zval	7.0000000
hform	79.4900000	alpha	2.4152800	atnum	12
zval	3.0000000	eisol	-152.9599600	n	3.0
atnum	14	gss	11.5600000	uss	-14.6236880
n	3.0	gsp	10.0800000	upp	-14.1734600
uss	-33.9536220	gpp	8.6400000	betas	-2.0716910
upp	-28.9347490	gp2	7.6800000	betap	-0.5695810
betas	-3.7848520	hsp	1.9200000	zs	0.6985520
betap	-1.9681230	hform	75.5700000	zp	1.4834530
zs	1.8306970	zval	5.0000000	alpha	1.3291470
zp	1.2849530	atnum	16	eisol	-22.5530760
alpha	2.2578160	n	3.0	gss	6.6943000
eisol	-79.0017420	uss	-72.2422810	gsp	6.7939950
gss	9.8200000	upp	-56.9732070	gpp	6.9104460
gsp	8.3600000	betas	-10.7616700	gp2	7.0908230
gpp	7.3100000	betap	-10.1084330	hsp	0.5433000
gp2	6.5400000	zs	2.3129620	a1	2.1170500
hsp	1.3200000	zp	2.0091460	a2	-2.5477670
k1	0.2500000	alpha	2.4780260	b1	6.0094770
k2	0.0615130	eisol	-226.0123900	b2	4.3953700
k3	0.0207890	gss	12.8800000	c1	2.0844060
k4	0.0000000	gsp	11.2600000	c2	2.0636740
l1	9.0000000	gpp	9.9000000	hform	35.0000000

l2	5.0000000	gp2	8.8300000		zval	2.0000000
l3	5.0000000	hsp	2.2600000		atnum	13
l4	0.0000000	hform	66.4000000		n	3.0
m1	0.9114530	zval	6.0000000		uss	-24.8454040
m2	1.9955690	atnum	17		upp	-22.2641590
m3	2.9906100	n	3.0		betas	-0.5943010
m4	0.0000000	uss	-100.2271660		betap	-0.9565500
hform	108.3900000	upp	-77.3786670		zs	1.7028880
zval	4.0000000	betas	-14.2623200		zp	1.0736290
atnum	15	betap	-14.2623200		alpha	1.5217030
n	3.0	zs	3.7846450		eisol	-46.8647630
uss	-42.0298630	zp	2.0362630		gss	5.7767370
upp	-34.0307090	alpha	2.5422010		gsp	11.6598560
betas	-6.3537640	eisol	-353.1176670		gpp	6.3477900
betap	-6.5907090	gss	15.0300000		gp2	6.1210770
zs	1.9812800	gsp	13.1600000		hsp	4.0062450
zp	1.8751500	gpp	11.3000000		a1	-0.4730900
alpha	2.4553220	gp2	9.9700000		a2	-0.1540510
eisol	-124.4368355	hsp	2.4200000		b1	1.9158250
gss	11.5600050	hform	28.9900000		b2	6.0050860
gsp	5.2374490	zval	7.0000000		c1	1.4517280
gpp	7.8775890	atnum	20		c2	2.5199970
gp2	7.3076480	n	4.0		hform	79.4900000
hsp	0.7792380	uss	-11.870		zval	3.0000000
k1	-0.0318270	upp	-8.553		atnum	14
k2	0.0184700	betas	-2.307		n	3.0
k3	0.0332900	betap	-3.598		uss	-26.7634830
k4	0.0000000	zs	1.281		upp	-22.8136350
l1	6.0000000	zp	0.877		betas	-2.8621450
l2	7.0000000	alpha	1.940		betap	-3.9331480
l3	9.0000000	eisol	-17.980		zs	1.6350750
l4	0.0000000	gss	5.76		zp	1.3130880
m1	1.4743230	gsp	5.04		alpha	2.1358090
m2	1.7793540	gpp	4.32		eisol	-67.7882140
m3	3.0065760	gp2	4.00		gss	5.0471960
m4	0.0000000	hsp	0.52		gsp	5.9490570
hform	75.5700000	hform	42.6		gpp	6.7593670
zval	5.0000000	zval	2.0		gp2	5.1612970
atnum	16	atnum	30		hsp	0.9198320
n	3.0	n	4.0		a1	-0.3906000
uss	-56.6940560	uss	-20.8397160		a2	0.0572590
upp	-48.7170490	upp	-19.6252240		b1	6.0000540
betas	-3.9205660	betas	-1.0000000		b2	6.0071830
betap	-7.9052780	betap	-2.0000000		c1	0.6322620
zs	2.3665150	zs	2.0473590		c2	2.0199870
zp	1.6672630	zp	1.4609460		hform	108.3900000
alpha	2.4616480	alpha	1.5064570		zval	4.0000000
eisol	-191.7321930	eisol	-29.8794320		atnum	15
gss	11.7863290	gss	11.8000000		n	3.0
gsp	8.6631270	gsp	11.1820180		uss	-40.4130960
gpp	10.0393080	gpp	13.3000000		upp	-29.5930520
gp2	7.7816880	gp2	12.9305200		betas	-12.6158790
hsp	2.5321370	hsp	0.4846060		betap	-4.1600400
k1	-0.5091950	hform	31.1700000		zs	2.0175630
k2	-0.0118630	zval	2.0000000		zp	1.5047320
k3	0.0123340	atnum	32		alpha	1.9405340
k4	0.0000000	n	4.0		eisol	-117.9591740
l1	4.5936910	uss	-33.9493670		gss	7.8016150
l2	5.8657310	upp	-27.4251050		gsp	5.1869490
l3	13.5573360	betas	-4.5164790		gpp	6.6184780
l4	0.0000000	betap	-1.7555170		gp2	6.0620020
m1	0.7706650	zs	1.2931800		hsp	1.5428090
m2	1.5033130	zp	2.0205640		a1	-0.6114210

m3	2.0091730	alpha	1.9784980		a2	-0.0939350
m4	0.0000000	eisol	-76.2489440		b1	1.9972720
hform	66.4000000	gss	9.8000000		b2	1.9983600
zval	6.0000000	gsp	8.3000000		c1	0.7946240
atnum	17	gpp	7.3000000		c2	1.9106770
n	3.0	gp2	6.5000000		hform	75.5700000
uss	-111.6139480	hsp	1.3000000		zval	5.0000000
upp	-76.6401070	hform	89.5000000		atnum	16
betas	-24.5946700	zval	4.0000000		n	3.0
betap	-14.6372160	atnum	35		uss	-49.8953710
zs	3.6313760	n	4.0		upp	-44.3925830
zp	2.0767990	uss	-99.9864405		betas	-8.8274650
alpha	2.9193680	upp	-75.6713075		betap	-8.0914150
eisol	-372.1984310	betas	-8.9171070		zs	1.8911850
gss	15.0300000	betap	-9.9437400		zp	1.6589720
gsp	13.1600000	zs	3.8543019		alpha	2.2697060
gpp	11.3000000	zp	2.1992091		eisol	-183.4537395
gp2	9.9700000	alpha	2.4457051		gss	8.9646670
hsp	2.4200000	eisol	-346.6812500		gsp	6.7859360
k1	0.0942430	gss	15.03643948		gpp	9.9681640
k2	0.0271680	gsp	13.03468242		gp2	7.9702470
k3	0.0000000	gpp	11.27632539		hsp	4.0418360
k4	0.0000000	gp2	9.85442552		a1	-0.3991910
l1	4.0000000	hsp	2.45586832		a2	-0.0548990
l2	4.0000000	hform	26.7400000		b1	6.0006990
l3	0.0000000	zval	7.0000000		b2	6.0018450
l4	0.0000000	atnum	50		c1	0.9621230
m1	1.3000000	n	5.0		c2	1.5799440
m2	2.1000000	uss	-40.8518020		hform	66.4000000
m3	0.0000000	upp	-28.5602490		zval	6.0000000
m4	0.0000000	betas	-3.2351470		atnum	17
hform	28.9900000	betap	-4.2904160		n	3.0
zval	7.0000000	zs	2.0803800		uss	-100.6267470
atnum	30	zp	1.9371060		upp	-53.6143960
n	4.0	alpha	1.8008140		betas	-27.5285600
uss	-21.0400080	eisol	-92.3241020		betap	-11.5939220
upp	-17.6555740	gss	9.8000000		zs	2.2462100
betas	-1.9974290	gsp	8.3000000		zp	2.1510100
betap	-4.7581190	gpp	7.3000000		alpha	2.5172960
zs	1.9542990	gp2	6.5000000		eisol	-315.1949480
zp	1.3723650	hsp	1.3000000		gss	16.0136010
alpha	1.4845630	hform	72.2000000		gsp	8.0481150
eisol	-30.2800160	zval	4.0000000		gpp	7.5222150
gss	11.8000000	atnum	53		gp2	7.5041540
gsp	11.1820180	n	5.0		hsp	3.4811530
gpp	13.3000000	uss	-100.0030538		a1	-0.1715910
gp2	12.9305200	upp	-74.6114692		a2	-0.0134580
hsp	0.4846060	betas	-7.4144510		b1	6.0008020
hform	31.1700000	betap	-6.1967810		b2	1.9666180
zval	2.0000000	zs	2.2729610		c1	1.0875020
atnum	32	zp	2.1694980		c2	2.2928910
n	4.0	alpha	2.2073200		hform	28.9900000
uss	-34.1838890	eisol	-340.5983600		zval	7.0000000
upp	-28.6408110	gss	15.04044855		atnum	20
betas	-4.3566070	gsp	13.05655798		n	4.0
betap	-0.9910910	gpp	11.14778369		uss	-11.35010387
zs	1.2196310	gp2	9.91409071		upp	-10.34987587
zp	1.9827940	hsp	2.45638202		betas	-10.45737746
alpha	2.1364050	hform	25.5170000		betap	5.10954286
eisol	-78.7084810	zval	7.0000000		zs	.69567815
gss	10.1686050	atnum	80		zp	1.05125946
gsp	8.1444730	n	6.0		alpha	1.90107319
gpp	6.6719020	uss	-19.809574		eisol	-16.94020844

gp2	6.2697060	upp	-13.102530			gss	5.76
hsp	0.9370930	betas	-0.404525			gsp	5.04
hform	89.5000000	betap	-6.206683			gpp	4.32
zval	4.0000000	zs	2.218184			gp2	4.00
atnum	35	zp	2.065038			hsp	.52
n	4.0	alpha	1.335641			a1	.52766269
uss	-104.6560630	eisol	-28.819148			b1	10.0
upp	-74.9300520	gss	10.800000			c1	.51696708
betas	-19.3998800	gsp	9.300000			a2	-.00139269
betap	-8.9571950	gpp	14.300000			b2	6.0
zs	3.0641330	gp2	13.500000			c2	2.56686118
zp	2.0383330	hsp	1.300000			hform	42.6
alpha	2.5765460	hform	14.690000			zval	2.0000000
eisol	-352.3142087	zval	2.000000			atnum	30
gss	15.0364395	atnum	82			n	4.0
gsp	13.0346824	n	6.0			uss	-18.5321980
gpp	11.2763254	uss	-47.319692			upp	-11.0474090
gp2	9.8544255	upp	-28.847560			betas	-0.7155780
hsp	2.4558683	betas	-8.042387			betap	-6.3518640
k1	0.0666850	betap	-3.000000			zs	1.8199890
k2	0.0255680	zs	2.498286			zp	1.5069220
k3	0.0000000	zp	2.082071			alpha	1.3501260
k4	0.0000000	alpha	1.728333			eisol	-27.3872000
l1	4.0000000	eisol	-105.834504			gss	9.6771960
l2	4.0000000	gss	9.800000			gsp	7.7362040
l3	0.0000000	gsp	8.300000			gpp	4.9801740
l4	0.0000000	gpp	7.300000			gp2	4.6696560
m1	1.5000000	gp2	6.500000			hsp	0.6004130
m2	2.3000000	hsp	1.300000			a1	-0.1112340
m3	0.0000000	hform	46.627000			a2	-0.1323700
m4	0.0000000	zval	4.000000			b1	6.0014780
hform	26.7400000	#				b2	1.9958390
zval	7.0000000	# MNDOD parameters				c1	1.5160320
atnum	50	#				c2	2.5196420
n	5.0	atnum	30			hform	31.1700000
uss	-35.4967410	n	4.0			zval	2.0000000
upp	-28.0976360	uss	-18.0230010			atnum	31
betas	-3.2350000	upp	-12.2421660			n	4.0
betap	-2.5778900	betas	-5.0172610			uss	-29.8555930
zs	2.5993760	betap	-0.7120600			upp	-21.8753710
zp	1.6959620	zs	1.7315030			betas	-4.9456180
alpha	1.8369360	zp	1.3935830			betap	-0.4070530
eisol	-80.6887540	alpha	1.5176370			zs	1.8470400
gss	9.8000000	eisol	-27.4852740			zp	0.8394110
gsp	8.3000000	gss	8.5607280			alpha	1.6051150
gpp	7.3000000	gsp	7.4900360			eisol	-57.3280250
gp2	6.5000000	gpp	5.1396480			gss	8.4585540
hsp	1.3000000	gp2	4.5054030			gsp	8.9256190
hform	72.2000000	hsp	0.5329460			gpp	5.0868550
zval	4.0000000	hform	31.1700000			gp2	4.9830450
atnum	53	zval	2.0000000			hsp	2.0512600
n	5.0	atnum	48			a1	-0.5601790
uss	-103.5896630	n	5.0			a2	-0.2727310
upp	-74.4299970	uss	-16.9697000			b1	5.6232730
betas	-8.4433270	upp	-12.4009650			b2	1.9918430
betap	-6.3234050	betas	-2.7715440			c1	1.5317800
zs	2.1028580	betap	-1.8056500			c2	2.1838640
zp	2.1611530	zs	1.7488060			hform	65.4000000
alpha	2.2994240	zp	1.5632150			zval	3.0000000
eisol	-346.8642857	alpha	1.4246130			atnum	32
gss	15.0404486	eisol	-26.0349660			n	4.0
gsp	13.0565580	gss	7.9044340			uss	-35.4671955
gpp	11.1477837	gsp	7.5157070			upp	-31.5863583

gp2	9.9140907	gpp	7.4800000		betas	-5.3250024
hsp	2.4563820	gp2	6.5186640		betap	-2.2501567
k1	0.0043610	hsp	0.6367440		zs	2.2373526
k2	0.0157060	hform	26.7200000		zp	1.5924319
k3	0.0000000	zval	2.0000000		alpha	1.9723370
k4	0.0000000	atnum	80		eisol	-84.0156006
l1	2.3000000	n	6.0		gss	5.3769635
l2	3.0000000	uss	-18.8156490		gsp	10.2095293
l3	0.0000000	upp	-13.3971140		gpp	7.6718647
l4	0.0000000	betas	-2.2187220		gp2	6.9242663
m1	1.8000000	betap	-2.9097860		hsp	1.3370204
m2	2.2400000	zs	2.3331070		a1	0.9631726
m3	0.0000000	zp	1.7083110		a2	-0.9593891
m4	0.0000000	alpha	1.3822420		b1	6.0120134
hform	25.5170000	eisol	-29.3156490		b2	5.7491802
zval	7.0000000	gss	8.3156490		c1	2.1633655
		gsp	8.2121730		c2	2.1693724
		gpp	7.1152590		hform	89.5000000
		gp2	6.1712500		zval	4.0000000
		hsp	0.8359410		atnum	33
		hform	14.6900000		n	4.0
		zval	2.0000000		uss	-38.5074240
					upp	-35.1524150
					betas	-8.2321650
					betap	-5.0173860
					zs	2.6361770
					zp	1.7038890
					alpha	1.7944770
					eisol	-122.6326140
					gss	8.7890010
					gsp	5.3979830
					gpp	8.2872500
					gp2	8.2103460
					hsp	1.9510340
					a1	-0.4600950
					a2	-0.0889960
					b1	1.9831150
					b2	1.9929440
					c1	1.0867930
					c2	2.1400580
					hform	72.3000000
					zval	5.0000000
					atnum	34
					n	4.0
					uss	-55.3781350
					upp	-49.8230760
					betas	-6.1578220
					betap	-5.4930390
					zs	2.8280510
					zp	1.7325360
					alpha	3.0439570
					eisol	-192.7748115
					gss	7.4325910
					gsp	10.0604610
					gpp	9.5683260
					gp2	7.7242890
					hsp	4.0165580
					a1	0.0478730
					a2	0.1147200
					b1	6.0074000
					b2	6.0086720
					c1	2.0817170
					c2	1.5164230

			hform	54.3000000
			zval	6.0000000
			atnum	35
			n	4.0
			uss	-116.6193110
			upp	-74.2271290
			betas	-31.1713420
			betap	-6.8140130
			zs	5.3484570
			zp	2.1275900
			alpha	2.5118420
			eisol	-352.5398970
			gss	15.9434250
			gsp	16.0616800
			gpp	8.2827630
			gp2	7.8168490
			hsp	0.5788690
			a1	0.9604580
			a2	-0.9549160
			b1	5.9765080
			b2	5.9447030
			c1	2.3216540
			c2	2.3281420
			hform	26.7400000
			zval	7.0000000
			atnum	48
			n	5.0
			uss	-15.8285840
			upp	8.7497950
			betas	-8.5819440
			betap	-0.6010340
			zs	1.6793510
			zp	2.0664120
			alpha	1.5253820
			eisol	-22.4502080
			gss	9.2069600
			gsp	8.2315390
			gpp	4.9481040
			gp2	4.6696560
			hsp	1.6562340
			hform	26.7200000
			zval	2.0000000
			atnum	49
			n	5.0
			uss	-26.1762050
			upp	-20.0058220
			betas	-2.9933190
			betap	-1.8289080
			zs	2.0161160
			zp	1.4453500
			alpha	1.4183850
			eisol	-51.9750470
			gss	6.5549000
			gsp	8.2298730
			gpp	6.2992690
			gp2	4.9842110
			hsp	2.6314610
			a1	-0.3431380
			a2	-0.1095320
			b1	1.9940340
			b2	5.6832170
			c1	1.6255160
			c2	2.8670090

			hform	58.0000000
			zval	3.0000000
			atnum	50
			n	5.0
			uss	-34.5501920
			upp	-25.8944190
			betas	-2.7858020
			betap	-2.0059990
			zs	2.3733280
			zp	1.6382330
			alpha	1.6996500
			eisol	-78.8877790
			gss	10.1900330
			gsp	7.2353270
			gpp	5.6738100
			gp2	5.1822140
			hsp	1.0331570
			a1	-0.1503530
			a2	-0.0444170
			b1	6.0056940
			b2	2.2573810
			c1	1.7046420
			c2	2.4698690
			hform	72.2000000
			zval	4.0000000
			atnum	51
			n	5.0
			uss	-56.4321960
			upp	-29.4349540
			betas	-14.7942170
			betap	-2.8179480
			zs	2.3430390
			zp	1.8999920
			alpha	2.0343010
			eisol	-148.9382890
			gss	9.2382770
			gsp	5.2776800
			gpp	6.3500000
			gp2	6.2500000
			hsp	2.4244640
			a1	3.0020280
			a2	-0.0188920
			b1	6.0053420
			b2	6.0114780
			c1	0.8530600
			c2	2.7933110
			hform	63.2000000
			zval	5.0000000
			atnum	52
			n	5.0
			uss	-44.9380360
			upp	-46.3140990
			betas	-2.6651460
			betap	-3.8954300
			zs	4.1654920
			zp	1.6475550
			alpha	2.4850190
			eisol	-168.0945930
			gss	10.2550730
			gsp	8.1691450
			gpp	7.7775920
			gp2	7.7551210
			hsp	3.7724620

		a1	0.0333910
		a2	-1.9218670
		b1	5.9563790
		b2	4.9732190
		c1	2.2775750
		c2	0.5242430
		hform	47.0000000
		zval	6.0000000
		atnum	53
		n	5.0
		uss	-96.4540370
		upp	-61.0915820
		betas	-14.4942340
		betap	-5.8947030
		zs	7.0010130
		zp	2.4543540
		alpha	1.9901850
		eisol	-288.3160860
		gss	13.6319430
		gsp	14.9904060
		gpp	7.2883300
		gp2	5.9664070
		hsp	2.6300350
		a1	-0.1314810
		a2	-0.0368970
		b1	5.2064170
		b2	6.0101170
		c1	1.7488240
		c2	2.7103730
		hform	25.5170000
		zval	7.0000000
		atnum	80
		n	6.0
		uss	-17.762229
		upp	-18.330751
		betas	-3.101365
		betap	-3.464031
		zs	1.476885
		zp	2.479951
		alpha	1.529377
		eisol	-28.899738
		gss	6.624720
		gsp	10.639297
		gpp	14.709283
		gp2	16.000740
		hsp	2.036311
		a1	1.082720
		a2	-0.096553
		b1	6.496598
		b2	3.926281
		c1	1.195146
		c2	2.627160
		hform	14.690000
		zval	2.000000
		atnum	81
		n	6.0
		uss	-30.053170
		upp	-26.920637
		betas	-1.084495
		betap	-7.946799
		zs	6.867921
		zp	1.969445
		alpha	1.340951

			eisol	-56.649205
			gss	10.460412
			gsp	11.223883
			gpp	4.992785
			gp2	8.962727
			hsp	2.530406
			a1	-1.361399
			a2	-0.045401
			b1	3.557226
			b2	2.306995
			c1	1.092802
			c2	2.965029
			hform	43.550000
			zval	3.000000
			atnum	82
			n	6.0
			uss	-30.322756
			upp	-24.425834
			betas	-6.126024
			betap	-1.395430
			zs	3.141289
			zp	1.892418
			alpha	1.620045
			eisol	-73.4660775
			gss	7.011992
			gsp	6.793782
			gpp	5.183780
			gp2	5.045651
			hsp	1.566302
			a1	-0.122576
			a2	-0.056648
			b1	6.003062
			b2	4.743705
			c1	1.901597
			c2	2.861879
			hform	46.620000
			zval	4.0000000
			atnum	83
			n	6.0
			uss	-33.495938
			upp	-35.521026
			betas	-5.607283
			betap	-5.800152
			zs	4.916451
			zp	1.934935
			alpha	1.857431
			eisol	-109.277491
			gss	4.989480
			gsp	6.103308
			gpp	8.696007
			gp2	8.335447
			hsp	0.599122
			a1	2.581693
			a2	0.060320
			b1	5.094022
			b2	6.001538
			c1	0.499787
			c2	2.427970
			hform	50.100000
			zval	5.0000000

APPENDIX 3

EXAMPLE OF A HYPERCHEM LOG FILE FOR A SEMI-EMPIRICAL CALCULATION

HyperChem log start -- Fri Feb 27 08:39:16 1998.

Geometry optimization, SemiEmpirical, molecule = C:\MPHIL\HYPER\tsa_am1.hin.

AM1

PolakRibiere optimizer

Convergence limit = 0.0100000 Iteration limit = 100

Accelerate convergence = NO

Optimization algorithm = Polak-Ribiere

Criterion of RMS gradient = 0.1000 kcal/(A mol) Maximum cycles = 195

RHF Calculation:

Singlet state calculation

Number of electrons = 26

Number of Double Occupied Levels = 13

Charge on the System = 0

Total Orbitals = 25

Starting AM1 calculation with 25 orbitals

E=0.0000 Grad=0.000 Conv=NO(0 cycles 0 points) [Iter=1 Diff=3299.30425]

E=0.0000 Grad=0.000 Conv=NO(0 cycles 0 points) [Iter=2 Diff=28.27431]

E=0.0000 Grad=0.000 Conv=NO(0 cycles 0 points) [Iter=3 Diff=1.73400]

E=0.0000 Grad=0.000 Conv=NO(0 cycles 0 points) [Iter=4 Diff=0.01338]

E=0.0000 Grad=0.000 Conv=NO(0 cycles 0 points) [Iter=5 Diff=0.04314]

E=0.0000 Grad=0.000 Conv=NO(0 cycles 0 points) [Iter=6 Diff=0.01153]

E=0.0000 Grad=0.000 Conv=NO(0 cycles 0 points) [Iter=7 Diff=0.00334]

E=-905.0394 Grad=26.316 Conv=NO(0 cycles 1 points) [Iter=1 Diff=5.35203]

E=-905.0394 Grad=26.316 Conv=NO(0 cycles 1 points) [Iter=2 Diff=0.97395]

E=-905.0394 Grad=26.316 Conv=NO(0 cycles 1 points) [Iter=3 Diff=0.57083]

E=-905.0394 Grad=26.316 Conv=NO(0 cycles 1 points) [Iter=4 Diff=0.23323]

E=-905.0394 Grad=26.316 Conv=NO(0 cycles 1 points) [Iter=5 Diff=0.00391]

E=-923.8232 Grad=10.109 Conv=NO(0 cycles 2 points) [Iter=1 Diff=5.43031]

E=-923.8232 Grad=10.109 Conv=NO(0 cycles 2 points) [Iter=2 Diff=0.89891]

E=-923.8232 Grad=10.109 Conv=NO(0 cycles 2 points) [Iter=3 Diff=0.44902]

E=-923.8232 Grad=10.109 Conv=NO(0 cycles 2 points) [Iter=4 Diff=0.18467]

E=-923.8232 Grad=10.109 Conv=NO(0 cycles 2 points) [Iter=5 Diff=0.00194]

E=-920.8324 Grad=19.167 Conv=NO(0 cycles 3 points) [Iter=1 Diff=1.87868]
E=-920.8324 Grad=19.167 Conv=NO(0 cycles 3 points) [Iter=2 Diff=0.30982]
E=-920.8324 Grad=19.167 Conv=NO(0 cycles 3 points) [Iter=3 Diff=0.16660]
E=-920.8324 Grad=19.167 Conv=NO(0 cycles 3 points) [Iter=4 Diff=0.07398]
E=-920.8324 Grad=19.167 Conv=NO(0 cycles 3 points) [Iter=5 Diff=0.00065]
E=-925.6803 Grad=6.474 Conv=NO(1 cycles 4 points) [Iter=1 Diff=0.72174]
E=-925.6803 Grad=6.474 Conv=NO(1 cycles 4 points) [Iter=2 Diff=0.14729]
E=-925.6803 Grad=6.474 Conv=NO(1 cycles 4 points) [Iter=3 Diff=0.03784]
E=-925.6803 Grad=6.474 Conv=NO(1 cycles 4 points) [Iter=4 Diff=0.01103]
E=-925.6803 Grad=6.474 Conv=NO(1 cycles 4 points) [Iter=5 Diff=0.00351]
E=-927.8770 Grad=3.205 Conv=NO(1 cycles 5 points) [Iter=1 Diff=0.72815]
E=-927.8770 Grad=3.205 Conv=NO(1 cycles 5 points) [Iter=2 Diff=0.14694]
E=-927.8770 Grad=3.205 Conv=NO(1 cycles 5 points) [Iter=3 Diff=0.03704]
E=-927.8770 Grad=3.205 Conv=NO(1 cycles 5 points) [Iter=4 Diff=0.01054]
E=-927.8770 Grad=3.205 Conv=NO(1 cycles 5 points) [Iter=5 Diff=0.00327]
E=-928.0876 Grad=4.288 Conv=NO(1 cycles 6 points) [Iter=1 Diff=0.10434]
E=-928.0876 Grad=4.288 Conv=NO(1 cycles 6 points) [Iter=2 Diff=0.02016]
E=-928.0876 Grad=4.288 Conv=NO(1 cycles 6 points) [Iter=3 Diff=0.00489]
E=-928.2451 Grad=3.182 Conv=NO(2 cycles 7 points) [Iter=1 Diff=0.29531]
E=-928.2451 Grad=3.182 Conv=NO(2 cycles 7 points) [Iter=2 Diff=0.04627]
E=-928.2451 Grad=3.182 Conv=NO(2 cycles 7 points) [Iter=3 Diff=0.00863]
E=-929.3588 Grad=3.830 Conv=NO(2 cycles 8 points) [Iter=1 Diff=0.30410]
E=-929.3588 Grad=3.830 Conv=NO(2 cycles 8 points) [Iter=2 Diff=0.04864]
E=-929.3588 Grad=3.830 Conv=NO(2 cycles 8 points) [Iter=3 Diff=0.00921]
E=-929.8603 Grad=6.526 Conv=NO(2 cycles 9 points) [Iter=1 Diff=1.17418]
E=-929.8603 Grad=6.526 Conv=NO(2 cycles 9 points) [Iter=2 Diff=0.18854]
E=-929.8603 Grad=6.526 Conv=NO(2 cycles 9 points) [Iter=3 Diff=0.07979]
E=-929.8603 Grad=6.526 Conv=NO(2 cycles 9 points) [Iter=4 Diff=0.03499]
E=-929.8603 Grad=6.526 Conv=NO(2 cycles 9 points) [Iter=5 Diff=0.00011]
E=-929.1335 Grad=12.169 Conv=NO(2 cycles 10 points) [Iter=1 Diff=0.79810]
E=-929.1335 Grad=12.169 Conv=NO(2 cycles 10 points) [Iter=2 Diff=0.12684]
E=-929.1335 Grad=12.169 Conv=NO(2 cycles 10 points) [Iter=3 Diff=0.02374]
E=-929.1335 Grad=12.169 Conv=NO(2 cycles 10 points) [Iter=4 Diff=0.00481]
E=-929.8965 Grad=7.526 Conv=NO(3 cycles 11 points) [Iter=1 Diff=18.77525]
E=-929.8965 Grad=7.526 Conv=NO(3 cycles 11 points) [Iter=2 Diff=3.44760]
E=-929.8965 Grad=7.526 Conv=NO(3 cycles 11 points) [Iter=3 Diff=2.46781]
E=-929.8965 Grad=7.526 Conv=NO(3 cycles 11 points) [Iter=4 Diff=1.60331]
E=-929.8965 Grad=7.526 Conv=NO(3 cycles 11 points) [Iter=5 Diff=0.01907]
E=-929.8965 Grad=7.526 Conv=NO(3 cycles 11 points) [Iter=6 Diff=0.00637]
E=-928.6136 Grad=11.574 Conv=NO(3 cycles 12 points) [Iter=1 Diff=4.86184]

E=-928.6136 Grad=11.574 Conv=NO(3 cycles 12 points) [Iter=2 Diff=0.88718]
E=-928.6136 Grad=11.574 Conv=NO(3 cycles 12 points) [Iter=3 Diff=0.55818]
E=-928.6136 Grad=11.574 Conv=NO(3 cycles 12 points) [Iter=4 Diff=0.33103]
E=-928.6136 Grad=11.574 Conv=NO(3 cycles 12 points) [Iter=5 Diff=0.00200]
E=-933.2430 Grad=5.502 Conv=NO(4 cycles 13 points) [Iter=1 Diff=2.90684]
E=-933.2430 Grad=5.502 Conv=NO(4 cycles 13 points) [Iter=2 Diff=0.44949]
E=-933.2430 Grad=5.502 Conv=NO(4 cycles 13 points) [Iter=3 Diff=0.15427]
E=-933.2430 Grad=5.502 Conv=NO(4 cycles 13 points) [Iter=4 Diff=0.05640]
E=-933.2430 Grad=5.502 Conv=NO(4 cycles 13 points) [Iter=5 Diff=0.00020]
E=-934.7259 Grad=10.085 Conv=NO(4 cycles 14 points) [Iter=1 Diff=0.37858]
E=-934.7259 Grad=10.085 Conv=NO(4 cycles 14 points) [Iter=2 Diff=0.05871]
E=-934.7259 Grad=10.085 Conv=NO(4 cycles 14 points) [Iter=3 Diff=0.01040]
E=-934.7259 Grad=10.085 Conv=NO(4 cycles 14 points) [Iter=4 Diff=0.00198]
E=-935.4805 Grad=5.585 Conv=NO(5 cycles 15 points) [Iter=1 Diff=2.06305]
E=-935.4805 Grad=5.585 Conv=NO(5 cycles 15 points) [Iter=2 Diff=0.35455]
E=-935.4805 Grad=5.585 Conv=NO(5 cycles 15 points) [Iter=3 Diff=0.23975]
E=-935.4805 Grad=5.585 Conv=NO(5 cycles 15 points) [Iter=4 Diff=0.13921]
E=-935.4805 Grad=5.585 Conv=NO(5 cycles 15 points) [Iter=5 Diff=0.00105]
E=-932.9864 Grad=12.852 Conv=NO(5 cycles 16 points) [Iter=1 Diff=0.86948]
E=-932.9864 Grad=12.852 Conv=NO(5 cycles 16 points) [Iter=2 Diff=0.14879]
E=-932.9864 Grad=12.852 Conv=NO(5 cycles 16 points) [Iter=3 Diff=0.03116]
E=-932.9864 Grad=12.852 Conv=NO(5 cycles 16 points) [Iter=4 Diff=0.00756]
E=-936.4922 Grad=1.674 Conv=NO(6 cycles 17 points) [Iter=1 Diff=0.04366]
E=-936.4922 Grad=1.674 Conv=NO(6 cycles 17 points) [Iter=2 Diff=0.00734]
E=-936.7701 Grad=1.461 Conv=NO(6 cycles 18 points) [Iter=1 Diff=0.04793]
E=-936.7701 Grad=1.461 Conv=NO(6 cycles 18 points) [Iter=2 Diff=0.00816]
E=-936.9009 Grad=2.202 Conv=NO(6 cycles 19 points) [Iter=1 Diff=0.18476]
E=-936.9009 Grad=2.202 Conv=NO(6 cycles 19 points) [Iter=2 Diff=0.03144]
E=-936.9009 Grad=2.202 Conv=NO(6 cycles 19 points) [Iter=3 Diff=0.00602]
E=-936.7296 Grad=4.364 Conv=NO(6 cycles 20 points) [Iter=1 Diff=0.11045]
E=-936.7296 Grad=4.364 Conv=NO(6 cycles 20 points) [Iter=2 Diff=0.01844]
E=-936.7296 Grad=4.364 Conv=NO(6 cycles 20 points) [Iter=3 Diff=0.00348]
E=-936.9128 Grad=2.610 Conv=NO(7 cycles 21 points) [Iter=1 Diff=2.97837]
E=-936.9128 Grad=2.610 Conv=NO(7 cycles 21 points) [Iter=2 Diff=0.50122]
E=-936.9128 Grad=2.610 Conv=NO(7 cycles 21 points) [Iter=3 Diff=0.29334]
E=-936.9128 Grad=2.610 Conv=NO(7 cycles 21 points) [Iter=4 Diff=0.16585]
E=-936.9128 Grad=2.610 Conv=NO(7 cycles 21 points) [Iter=5 Diff=0.00097]
E=-934.9916 Grad=9.711 Conv=NO(7 cycles 22 points) [Iter=1 Diff=1.66830]
E=-934.9916 Grad=9.711 Conv=NO(7 cycles 22 points) [Iter=2 Diff=0.28079]
E=-934.9916 Grad=9.711 Conv=NO(7 cycles 22 points) [Iter=3 Diff=0.16403]

E=-934.9916 Grad=9.711 Conv=NO(7 cycles 22 points) [Iter=4 Diff=0.09287]
E=-934.9916 Grad=9.711 Conv=NO(7 cycles 22 points) [Iter=5 Diff=0.00055]
E=-937.1577 Grad=1.626 Conv=NO(8 cycles 23 points) [Iter=1 Diff=0.44196]
E=-937.1577 Grad=1.626 Conv=NO(8 cycles 23 points) [Iter=2 Diff=0.07353]
E=-937.1577 Grad=1.626 Conv=NO(8 cycles 23 points) [Iter=3 Diff=0.01454]
E=-937.1577 Grad=1.626 Conv=NO(8 cycles 23 points) [Iter=4 Diff=0.00315]
E=-937.3339 Grad=2.966 Conv=NO(8 cycles 24 points) [Iter=1 Diff=0.02469]
E=-937.3339 Grad=2.966 Conv=NO(8 cycles 24 points) [Iter=2 Diff=0.00400]
E=-937.3538 Grad=2.172 Conv=NO(9 cycles 25 points) [Iter=1 Diff=0.62184]
E=-937.3538 Grad=2.172 Conv=NO(9 cycles 25 points) [Iter=2 Diff=0.10367]
E=-937.3538 Grad=2.172 Conv=NO(9 cycles 25 points) [Iter=3 Diff=0.02003]
E=-937.3538 Grad=2.172 Conv=NO(9 cycles 25 points) [Iter=4 Diff=0.00423]
E=-937.0994 Grad=4.988 Conv=NO(9 cycles 26 points) [Iter=1 Diff=0.25312]
E=-937.0994 Grad=4.988 Conv=NO(9 cycles 26 points) [Iter=2 Diff=0.04198]
E=-937.0994 Grad=4.988 Conv=NO(9 cycles 26 points) [Iter=3 Diff=0.00806]
E=-937.4669 Grad=0.891 Conv=NO(10 cycles 27 points) [Iter=1 Diff=0.01964]
E=-937.4669 Grad=0.891 Conv=NO(10 cycles 27 points) [Iter=2 Diff=0.00349]
E=-937.4992 Grad=1.128 Conv=NO(10 cycles 28 points) [Iter=1 Diff=0.00047]
E=-937.5011 Grad=0.889 Conv=NO(11 cycles 29 points) [Iter=1 Diff=0.00684]
E=-937.5486 Grad=0.487 Conv=NO(11 cycles 30 points) [Iter=1 Diff=0.00850]
E=-937.5547 Grad=0.703 Conv=NO(11 cycles 31 points) [Iter=1 Diff=0.00038]
E=-937.5578 Grad=0.556 Conv=NO(12 cycles 32 points) [Iter=1 Diff=0.07277]
E=-937.5578 Grad=0.556 Conv=NO(12 cycles 32 points) [Iter=2 Diff=0.01182]
E=-937.5578 Grad=0.556 Conv=NO(12 cycles 32 points) [Iter=3 Diff=0.00237]
E=-937.5499 Grad=1.550 Conv=NO(12 cycles 33 points) [Iter=1 Diff=0.02110]
E=-937.5499 Grad=1.550 Conv=NO(12 cycles 33 points) [Iter=2 Diff=0.00334]
E=-937.5715 Grad=0.623 Conv=NO(13 cycles 34 points) [Iter=1 Diff=0.02110]
E=-937.5715 Grad=0.623 Conv=NO(13 cycles 34 points) [Iter=2 Diff=0.00366]
E=-937.5892 Grad=0.501 Conv=NO(13 cycles 35 points) [Iter=1 Diff=0.02399]
E=-937.5892 Grad=0.501 Conv=NO(13 cycles 35 points) [Iter=2 Diff=0.00432]
E=-937.5797 Grad=1.078 Conv=NO(13 cycles 36 points) [Iter=1 Diff=0.01565]
E=-937.5797 Grad=1.078 Conv=NO(13 cycles 36 points) [Iter=2 Diff=0.00269]
E=-937.5896 Grad=0.533 Conv=NO(14 cycles 37 points) [Iter=1 Diff=0.04926]
E=-937.5896 Grad=0.533 Conv=NO(14 cycles 37 points) [Iter=2 Diff=0.00811]
E=-937.5434 Grad=1.814 Conv=NO(14 cycles 38 points) [Iter=1 Diff=0.02483]
E=-937.5434 Grad=1.814 Conv=NO(14 cycles 38 points) [Iter=2 Diff=0.00405]
E=-937.5962 Grad=0.209 Conv=NO(15 cycles 39 points) [Iter=1 Diff=0.00050]
E=-937.5998 Grad=0.203 Conv=NO(15 cycles 40 points) [Iter=1 Diff=0.00070]
E=-937.6002 Grad=0.359 Conv=NO(15 cycles 41 points) [Iter=1 Diff=0.00004]
E=-937.6004 Grad=0.294 Conv=NO(16 cycles 42 points) [Iter=1 Diff=0.00415]

E=-937.5999 Grad=0.427 Conv=NO(16 cycles 43 points) [Iter=1 Diff=0.00080]
 E=-937.6035 Grad=0.144 Conv=NO(17 cycles 44 points) [Iter=1 Diff=0.00084]
 E=-937.6046 Grad=0.199 Conv=NO(17 cycles 45 points) [Iter=1 Diff=0.00000]
 E=-937.6046 Grad=0.182 Conv=NO(18 cycles 46 points) [Iter=1 Diff=0.00179]
 E=-937.6059 Grad=0.128 Conv=NO(18 cycles 47 points) [Iter=1 Diff=0.00001]
 E=-937.6060 Grad=0.111 Conv=NO(19 cycles 48 points) [Iter=1 Diff=0.00083]
 E=-937.6062 Grad=0.174 Conv=NO(19 cycles 49 points) [Iter=1 Diff=0.00010]
 E=-937.6064 Grad=0.082 Conv=YES(20 cycles 50 points) [Iter=1 Diff=0.00000]

ENERGIES AND GRADIENT

Total Energy = -13436.1610321 (kcal/mol)
 Total Energy = -21.411458026 (a.u.)
 Binding Energy = -937.6063741 (kcal/mol)
 Isolated Atomic Energy = -12498.5546580 (kcal/mol)
 Electronic Energy = -48948.1218499 (kcal/mol)
 Core-Core Interaction = 35511.9608178 (kcal/mol)
 Heat of Formation = -30.5183741 (kcal/mol)
 Gradient = 0.0831787 (kcal/mol/Ang)

MOLECULAR POINT GROUP

C3V

EIGENVALUES(eV)

Symmetry: 1 A1 1 E 1 E 2 A1 3 A1
 Eigenvalue: -31.929157 -17.372837 -17.372665 -15.321272 -14.588918

Symmetry: 2 E 2 E 3 E 3 E 4 E
 Eigenvalue: -14.104439 -14.104036 -12.046130 -12.045913 -11.820394

Symmetry: 4 E 1 A2 4 A1 5 E 5 E
 Eigenvalue: -11.820230 -11.479774 -9.887563 1.036464 1.036899

Symmetry: 5 A1 2 A2 6 E 6 E 7 E
 Eigenvalue: 1.461220 1.539539 1.546524 1.546643 1.867977

Symmetry: 7 E 6 A1 7 A1 8 E 8 E
 Eigenvalue: 1.868110 1.920007 2.115284 2.848690 2.848968

ATOMIC ORBITAL ELECTRON POPULATIONS

AO:	1 S N	1 Px N	1 Py N	1 Pz N	2 S Si
	1.568688	1.404521	1.339582	1.664252	0.822324
AO:	2 Px Si	2 Py Si	2 Pz Si	3 S Si	3 Px Si
	0.810222	0.664078	0.795029	0.822320	0.695285
AO:	3 Py Si	3 Pz Si	4 S Si	4 Px Si	4 Py Si
	0.779002	0.795023	0.822295	0.740201	0.779000
AO:	4 Pz Si	5 S H	6 S H	7 S H	8 S H
	0.750117	1.186653	1.209349	1.186661	1.186659
AO:	9 S H	10 S H	11 S H	12 S H	13 S H
	1.186666	1.209358	1.186667	1.209380	1.186666

NET CHARGES AND COORDINATES

Atom	Z	Charge	Coordinates(Angstrom)			Mass
			x	y	z	
1	7	-0.977044	-1.17183	0.59804	0.08100	14.00700
2	14	0.908346	-1.44602	2.22664	-0.39408	28.08600
3	14	0.908370	0.27223	-0.20334	-0.39408	28.08600
4	14	0.908387	-2.30505	-0.20330	1.09392	28.08600
5	1	-0.186653	-2.87653	2.54403	-0.51637	1.00800
6	1	-0.209349	-0.89233	3.19450	0.56499	1.00800
7	1	-0.186661	-0.83666	2.54404	-1.69405	1.00800
8	1	-0.186659	0.09459	-1.65782	-0.51633	1.00800
9	1	-0.186666	0.77456	0.26533	-1.69405	1.00800
10	1	-0.209358	1.36927	-0.00392	0.56497	1.00800
11	1	-0.186667	-2.32221	-1.65785	0.87900	1.00800
12	1	-0.209380	-2.02306	-0.00396	2.52361	1.00800
13	1	-0.186666	-3.68215	0.26534	0.87908	1.00800

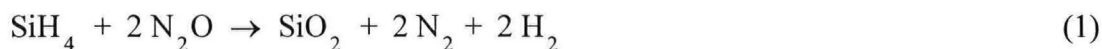
Dipole (Debyes)	x	y	z	Total
Point-Chg.	-0.191	-0.135	-0.333	0.407
sp Hybrid	0.000	0.000	0.000	0.000
pd Hybrid	0.000	0.000	0.000	0.000
Sum	-0.191	-0.135	-0.333	0.406

HyperChem log stop -- Fri Feb 27 08:41:04 1998.

APPENDIX 4

FORMATION OF SILICON DIOXIDE FILMS

Trisilylamine, like silane, reacts spontaneously with oxygen to form silicon dioxide. In the case of silane the commercial deposition of plasma enhanced CVD silicon dioxide films involves the reaction with nitrous oxide which minimises gas phase nucleation:



The standard molar enthalpy change for the reaction is given by:

$$\Delta H_m^\circ = \Delta H_f^\circ(\text{products}) - \Delta H_f^\circ(\text{reactants}) \quad (2)$$

If we consider the reaction for trisilylamine we can write an analogous equation:



Dividing by 2 and substituting values from Appendix 1 gives:

$$\begin{aligned} \Delta H_m^\circ &= 3 \Delta H_f^\circ(\text{SiO}_2) + 4\frac{1}{2} \Delta H_f^\circ(\text{H}_2) + 3\frac{1}{2} \Delta H_f^\circ(\text{N}_2) - \Delta H_f^\circ(\text{N}(\text{SiH}_3)_3) + 3 \Delta H_f^\circ(\text{N}_2\text{O}) \\ &= (-2732.1 + 0 + 0) - (-132.94 + 246.15) \\ &= -2845.31 \text{ kJ mol}^{-1} \end{aligned} \quad (4)$$

Applying the same calculation to silane and nitrous oxide we obtain a value for the standard molar enthalpy change of $\Delta H_m^\circ = -712.3 \text{ kJ mol}^{-1}$.

The standard molar entropy change (ΔS_m°) for the formation of silicon dioxide is given by the relationship:

$$\Delta S_m^\circ = \Delta S^\circ(\text{products}) - \Delta S^\circ(\text{reactants}) \quad (5)$$

For the reaction of trisilylamine and nitrous oxide substituting values from Appendix 1 gives:

$$\begin{aligned}
 \Delta S_m^\circ &= 3 \Delta S^\circ (\text{SiO}_2) + 4\frac{1}{2} \Delta S^\circ (\text{H}_2) + 3\frac{1}{2} \Delta S^\circ (\text{N}_2) - \Delta S^\circ (\text{N}(\text{SiH}_3)_3) + 3 \Delta S^\circ (\text{N}_2\text{O}) \\
 &= (124.38 + 588.15 + 670.6) - (286.8 + 659.88) \\
 &= + 436.45 \text{ J K}^{-1} \text{ mol}^{-1}
 \end{aligned}
 \tag{6}$$

For the reaction of silane and nitrous oxide substituting values from Appendix 1 gives a value for the standard molar entropy change of $\Delta S_m^\circ = + 41.54 \text{ J K}^{-1} \text{ mol}^{-1}$.

We can calculate the Gibbs free energy change (ΔS_m°) for the reaction of trisilylamine and nitrous oxide from the equation:

$$\Delta G_m^\circ = \Delta H_m^\circ - T\Delta S_m^\circ \tag{7}$$

Substituting into this equation and setting T equal to 298.15 K the value of ΔG_m° obtained for the formation of silicon dioxide from the trisilylamine and nitrous oxide reaction gives:

$$\begin{aligned}
 \Delta G_m^\circ &= - 2845.31 - (298.15 \times 0.43645) \\
 &= - 2845.31 - 130.13 \\
 &= - 2975.44 \text{ kJ mol}^{-1}
 \end{aligned}
 \tag{8}$$

Repeating the calculation for the silane and nitrous oxide:

$$\begin{aligned}
 \Delta G_m^\circ &= - 712.3 - (298.15 \times 0.04154) \\
 &= - 712.3 - 12.39 \\
 &= - 724.69 \text{ kJ mol}^{-1}
 \end{aligned}
 \tag{9}$$

It is evident from the Gibbs free energy values that both the reactions of trisilylamine and silane with nitrous oxide are thermodynamically feasible and it is reasonable to assume that the reaction of trisilylamine and nitrous oxide to form silicon dioxide has the potential for commercial exploitation for deposition of silicon dioxide films.